The Disruption of iASPP Binding to PP-1cα via Small Molecules Sourced from Marine Organisms

by

Melissa M. McLellan

A thesis submitted in partial fulfillment of the requirements for the degree of

Master in Science

Department of Biochemistry
University of Alberta

Abstract

Protein Phosphatase-1 (PP-1c) is a broad specificity Ser/Thr phosphatase catalytic subunit responsible for a variety protein dephosphorylation events in eukaryotic cells. The specificity and activity of PP-1c is largely controlled by over 200 regulatory subunits, including the Apoptotic Stimulating Proteins of p53 (ASPP). ASPP1 and ASPP2 are two members of the ASPP family that are responsible for promoting the pro-apoptotic activity of the tumour suppressor p53, while an inhibitory ASPP (termed iASPP) is responsible for inhibiting p53 activity. PP-1c, iASPP, and p53 form a protein complex which promotes the dephosphorylation of p53, and in turn, inhibits its pro-apoptotic activity.

iASPP is over-expressed in two thirds of all human cancers containing wild-type p53. The purpose of this Masters thesis project was to identify small molecules that may disrupt iASPP•PP-1c binding as a necessary first step to hindering dephosphorylation of p53 by PP-1c. The principal hypothesis was that the iASPP•PP-1c protein complex could be targeted for disruption with bioactive marine compounds. Such compounds may have the potential to be novel anti-cancer drugs in cancer types that over-express iASPP. This project was determined to be feasible because preliminary data by Dr. Tamara Arnold demonstrated that two marine compounds, Sokotrasterol Sulfate and Suvanine, disrupt iASPP•PP-1cα binding.

The results of this thesis show that iASPP•PP-1c binding can be targeted for disruption. Through the use of a novel protein-protein binding assay, I identified two novel iASPP disruptors, called Halistanol Sulfate and Coscinamide B. The potency and specificity of Halistanol Sulfate, Sokotrasterol Sulfate, and Suvanine were further characterized and all three demonstrated specificity towards the ASPP family vs. other PP-1c regulatory subunits, such as TIMAP (TGF-β-Inhibited Membrane-Associated Protein). Additionally, Suvanine preferentially disrupted iASPP binding to PP-1cα vs.

ASPP2; therefore, Suvanine is the most promising candidate for specific iASPP•PP-1c disruption.

Finally, during this investigation for PP-1c disruptors, I was also able to identify marine compounds that inhibit PP-1c activity. I discovered an abundant new source of the small molecule, Motuporin, as well, I discovered a novel bromophenol compound that potently inhibits the activity of PP-1c.

Acknowledgements

As there is so many people I must thank for helping me throughout the last two years, I will try to keep it short and sweet.

Firstly, I would like to thank Dr. Charles Holmes. Without his continual encouragement and guidance, I would not be were I am today. Secondly, to all my colleagues, I would like to thank them for the great memories and for the help in overcoming the daily ups and downs of graduate student life. To Dr. Tamara Arnold, for her support both inside and outside of the lab, it has been a pleasure to be her friend. To my lab associate, Ply Pasarj, for always being available whenever I needed it and for the great friendship that arose. As well, to the friends I have made throughout the department; Robyn Millott, Jen Wang, Gareth Armanious, Joe Primeau, Jessi Bak, Hector Vega, and M'Lynn Fisher, for all the laughs that kept my spirits high. It has been a privilege to know you all.

Last, but not least, I must give a huge thanks to my family. To both my brother, Ian, and my sister, Janie, whom I consider to be some of my best friends. And of course, to my parents. Without their unconditional love and support, I would not be the person I am today. I owe them everything.

Contents

List of Figures

List of Tables

Acronyms

ADDA	(2S, 3S, 8S, 9S)-3-amino-9-methoxy-2,6,8-trimethyl-10-phenyldeca-4,6-dienoic Acid
ADP	Adenosine Diphosphate
Ank	Ankyrin Repeats
ASPP	Apoptotic Stimulating Proteins of p53
ATP	Adenosine Triphosphate
CaN	Calcineurin
DNAPK	DNA-Dependent Protein Kinase
iASPP	Inhibitory Apoptotic Stimulation Proteins of p53
I2	Inhibitor-2
KiR	Ki67 and Repoman Protein Phosphatase-1c Binding Motif
MDM2	Mouse Double Min-2 Homolog
MyPhoNE	Myosin Phosphatase N-terminal Element
MYPT	Myosin Phosphatase Targeting Subunit Family
NFκB	Nuclear Factor Kappa-Light-Chain-Enhancer of Activated B Cells
Pi	Inorganic Phosphate
pNPP	para-Nitrophenyl Phosphate
PP-1	Protein Phosphatase-1
PP-1c	Protein Phosphatase-1 Catalytic Subunit
PxxP	Proline-rich SH3 Domain-Binding Motif
R-subunit	Regulatory Subunit of PP-1c
RVxF	Tetrapeptide PP-1c Binding Motif
SH3	Scr-homology 3
SILK	Tetrapeptide PP-1c Binding Motif
SLiMs	Short Linear Motifs
SpiDoC	Spinophilin Docking Site for the C-terminal Groove
TIMAP	TGF-β-Inhibited Membrane-Associated Protein

Standard Amino Acid Code

Alanine	Ala	A
Arginine	Arg	R
Asparagine	Asn	N
Aspartate	Asp	D
Cysteine	Cys	C
Glutamate	Glu	E
Glutamine	Gln	Q
Glycine	Gly	G
Histidine	His	H
Isoleucine	Ile	I
Leucine	Leu	K
Lysine	Lys	L
Methionine	Met	M
Phenylalanine	Phe	F
Proline	Pro	P
Serine	Ser	S
Threonine	Thr	T
Tryptophan	Trp	W
Tyrosine	Tyr	Y
Valine	Val	V

Chapter 1

Introduction

1.1 Reversible Protein Phosphorylation

Reversible protein phosphorylation is a vital process in cellular signalling used for an array of processes that includes cell adhesion, gene regulation, etc. [5]. Phosphorylation involves the addition of a phosphate group onto proteins substrates. Protein kinases are responsible for transferring the phosphate group from the energy molecule, adenosine triphosphate (ATP) and covalently attaching it to protein substrates via a monoester bond. This is followed by the removal of the phosphate group from the protein substrates by protein phosphatases, a process termed dephosphorylation. Protein phosphatases will bind the phosphorylation group and cleave the monoester bond, releasing the free inorganic phosphate (Pi) (see Figure 1.1). The first evidence of these protein phosphorylation events was seen in 1956, by the phosphorylation of a protein known as phosphorylase b, which resulted in a change in phosphorylase activity [74]. Recently, phosphoproteomic studies have established that phosphorylation occurs on over 70 % of all eukaryotic proteins [120, 121, 123].
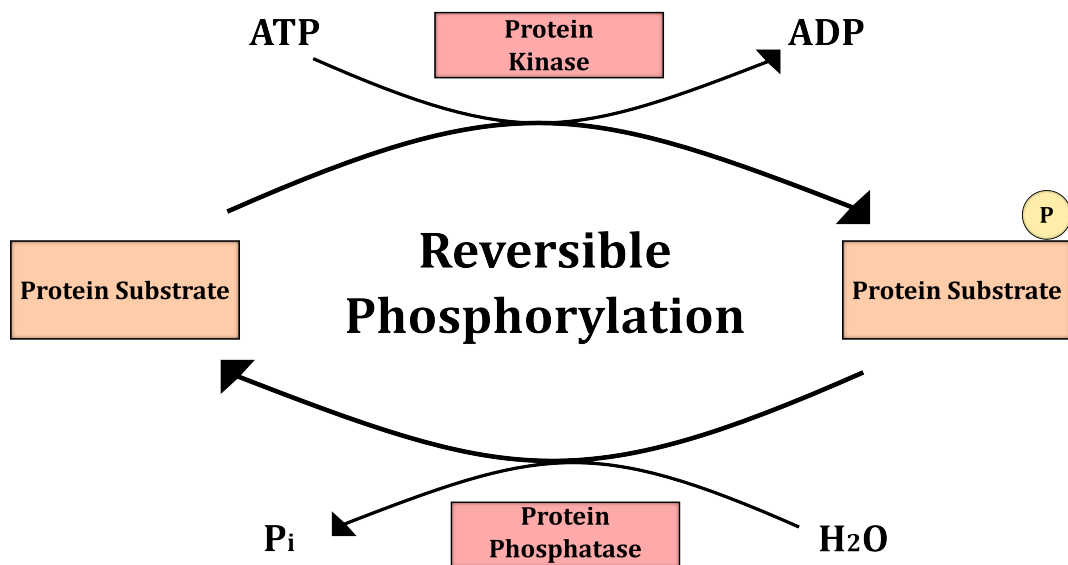
Figure 1.1: **The General Process of Reversible Phosphorylation.** Protein kinases transfer a phosphate group from ATP to a protein substrate, releasing ADP. Protein phosphatases remove phosphate groups from their protein substrates with the help of a water molecule, releasing a free inorganic phosphate.

1.2 The Phosphatase Families Responsible for Protein De-phosphorylation

There are nine different amino acids that can undergo phosphorylation: serine, threonine, tyrosine, histidine, cysteine, arginine, lysine, aspartate, and glutamate [113]. However, in humans, serine, threonine, and tyrosine are the targets for the majority of the protein phosphorylation events at rates of approximately 86 % on serine, 12 % on threonine, and less than 2 % on tyrosine [120, 133].

Human protein phosphatases can be classified into four distinct protein phosphatase families: 1) the Phosphoprotein Phosphatases, 2) the Metal-dependent Protein Phosphatases, 3) the Aspartate-based Phosphatases, and 4) Protein Tyrosine Phosphatases [5, 113]. The Phosphoprotein, Metal-dependent, Aspartate-based protein phosphatases carry out dephosphorylation solely on serine and threonine residues, and thus, are known as Protein Ser/Thr Phosphatases. Approximately 3 % of the human genome is com-

posed of protein kinases and protein phosphatases [5, 56, 100]. Despite the large dedicated portion of our genome to reversible phosphorylation, only ~ 40 genes encode for Ser/Thr phosphatases, in contrast to the more than 400 genes encoding for Ser/Thr kinases [114]. The Aspartate-based phosphatases employ an aspartate-based mechanism for dephosphorylation, whereas the Ser/Thr phosphates employ a metallo-dependent mechanism (described in detail in Section 1.2.2) [113, 133]. The protein tyrosine phosphatases comprises of two subfamilies; the Tyrosine-specific phosphatases and the Dual-specificity phosphatases. They largely only dephosphorylate tyrosine residues, however, dual-specificity phosphatase can also dephosphorylates serine and threonine residues.

The phosphoprotein phosphatases are the largest subfamily of the Ser/Thr phosphatase and consists of the members Protein Phosphatase-1 (PP-1), PP-2A, PP-2B/PP-3 (more commonly known as Calcineurin, CaN), PP-4, PP-5, PP-6, and PP-7 [123, 150]. While differing in many aspects, each member has an extremely uniform catalytic core [5, 50]. One of the most well studied members of the Phosphoprotein Phosphatase family is Protein Phosphatase-1 (PP-1), due its integral role in cellular dephosphorylation. PP-1c and PP-2A are responsible for the vast majority of protein dephosphorylation in eukaryotic cells [14, 50]. As well, PP-1 is a highly conserved enzyme, indicated by the more than 80 % sequence identity between human PP-1 and yeast Glc7p [42]. Both of which are huge indicators of how important PP-1c is to cellular function.

1.2.1   The Three-Dimensional Structure of Protein Phosphatase-1

In human cells, PP-1 has three encoded isoforms called alpha (α), beta (β), and gamma (γ), the γ isoform having two known splice variants, γ_1 and γ_2. All three isoforms are expressed ubiquitously in human tissue; except for the γ_2 isoform, which is solely found in the testis [2]. Figure 1.2 shows the sequence alignment of human PP-1 α, β, and γ and illustrates the fact that they share a high sequence identity (83 % between all three). The catalytic domain of PP-1 (PP-1c) is highly conserved and the three isoforms differ largely between their N-terminus and their C-terminal tails [43, 123]. The catalytic domain of this ~ 37 kDa enzyme resides over residues 7 to 300 and forms

three distinct grooves termed the hydrophobic groove, the C-terminal groove, and the acidic groove. These three grooves align to form a Y-shaped cleft (shown in Panel B of Figure 1.3, in red lines). The α/β fold is located near the acidic groove and is formed by a β sandwich at the top of the cleft, present between two α-helical domains [113]. The β12-β13 loop of PP-1c which connects the C-terminal groove to the acidic groove at the top of the catalytic cleft, is critical for the binding of many PP-1c toxins (described in detail in Section 1.3). The centre of the Y-shaped cleft houses the PP-1c active site and is pinpointed by the presence of two Mn^{2+} metal ions (see Panel A of Figure 1.3). These metal ions are required for the catalytic activity of the enzyme rather than its structure.

There are multiple interaction sites on PP-1c where secondary proteins may bind. A principal example is the PP-1c hydrophobic RVxF-binding groove located 20 $\mathring{A}$ away from its active site. This groove is used for the binding of regulatory subunits that contain a RVxF motif (explained further in Section 1.4) [30, 43]. The final 25 to 30 residues of PP-1 forms the C-terminal tail and accounts for the highest diversity between the three isoforms. Consequently, the C-terminal tail is thought to be where most PP-1c isoform specificity arises [29]. The tail is an extremely flexible and disordered region, until bound by a secondary protein, in which it becomes stabilized and structured [145]. The C-terminal tail also contains a short motif know as the PxxP motif. This motif is used to bind proteins that contain a Scr-homology 3 (SH3) domain (further discussed in Section 1.4).

1.2.2 The Mechanism of Catalytic Action by Protein Phosphatase-1c

In order to remove a phosphate group from a serine or threonine side chain, PP-1c requires its two metal ions to initiate a nucleophilic attack on the monoester bond of the phosphate group. As seen in Figure 1.4, the two metal ions coordinate with two adjacent water molecules and conserved PP-1c residues within the active site to keep the metal ions stable. Specifically, the first metal ion interacts with the two water molecules plus the three PP-1c residues His66, Asp92, and Asp64. The second metal ion shares

```
PP1α    1 MSDSEKLNLDSIIGRLLEVQGSRPGKNVQLTENEIRGLCLKSREIFLSQPILLELEAPLK
PP1β    1 MADGELNVDSLITRLLEVRGCRPGKIVQMTEAEVRGLCIKSREIFLSQPILLELEAPLK
PP1γ    1 MADLDKLNIDSIIQRLLEVRGSKPGKNVQLQENEIRGLCLKSREIFLSQPILLELEAPLK


PP1α   61 ICGDIHGQYYDLLRLFEYGGFPPESNYLFLGDYVDRGKQSLETICLLLAYKIKYPENFFL
PP1β   60 ICGDIHGQYTDLLRLFEYGGFPPEANYLFLGDYVDRGKQSLETICLLLAYKIKYPENFFL
PP1γ   61 ICGDIHGQYYDLLRLFEYGGFPPESNYLFLGDYVDRGKQSLETICLLLAYKIKYPENFFL


PP1α  121 LRGNHECASINRIYGFYDECKRRYNIKLWKTFTDCFNCLPIAAIVDEKIFCCHGGLSPDL
PP1β  120 LRGNHECASINRIYGFYDECKRRFNIKLWKTFTDCFNCLPIAAIVDEKIFCCHGGLSPDL
PP1γ  121 LRGNHECASINRIYGFYDECKRRYNIKLWKTFTDCFNCLPIAAIVDEKIFCCHGGLSPDL


PP1α  181 QSMEQIRRIMRPTDVPDQGLLCDLLWSDPDKDVQGWGENDRGVSFTFGAEVVAKFLHKHD
PP1β  180 QSMEQIRRIMRPTDVPDTGLLCDLLWSDPDKDVQGWGENDRGVSFTFGADVVSKFLNRHD
PP1γ  181 QSMEQIRRIMRPTDVPDQGLLCDLLWSDPDKDVLGWGENDRGVSFTFGAEVVAKFLHKHD


PP1α  241 LDLICRAHQVVEDGYEFFAKRQLVTLFSAPNYCGEFDNAGAMMSVDETLMCSFQILKPAD
PP1β  240 LDLICRAHQVVEDGYEFFAKRQLVTLFSAPNYCGEFDNAGGMMSVDETLMCSFQILKPSE
PP1γ  241 LDLICRAHQVVEDGYEFFAKRQLVTLFSAPNYCGEFDNAGAMMSVDETLMCSFQILKPAE


PP1α  301 KNKGKYGQFSGLNPGGRPITPPRNS--AKAK-K
PP1β  300 KKA-KY-QYGGLN-SGRPVTPPRTA--NPPKKR
PP1γ  301 KKK--------PN-ATRPVTPPRGMITKQAK-K
```

Figure 1.2: **The Sequence Alignment of the α, β, and γ Isoforms Human Protein Phosphatase-1c.** The alignment depicts the high sequence identity (83 %) between the three PP-1 isoforms, α, β, and γ. They largely differ in their N-terminus and C-terminal tails. This alignment was produced using *Uniport*. Accession Numbers for α, β, and γ: P62136, P62140, and P36873, respectively.
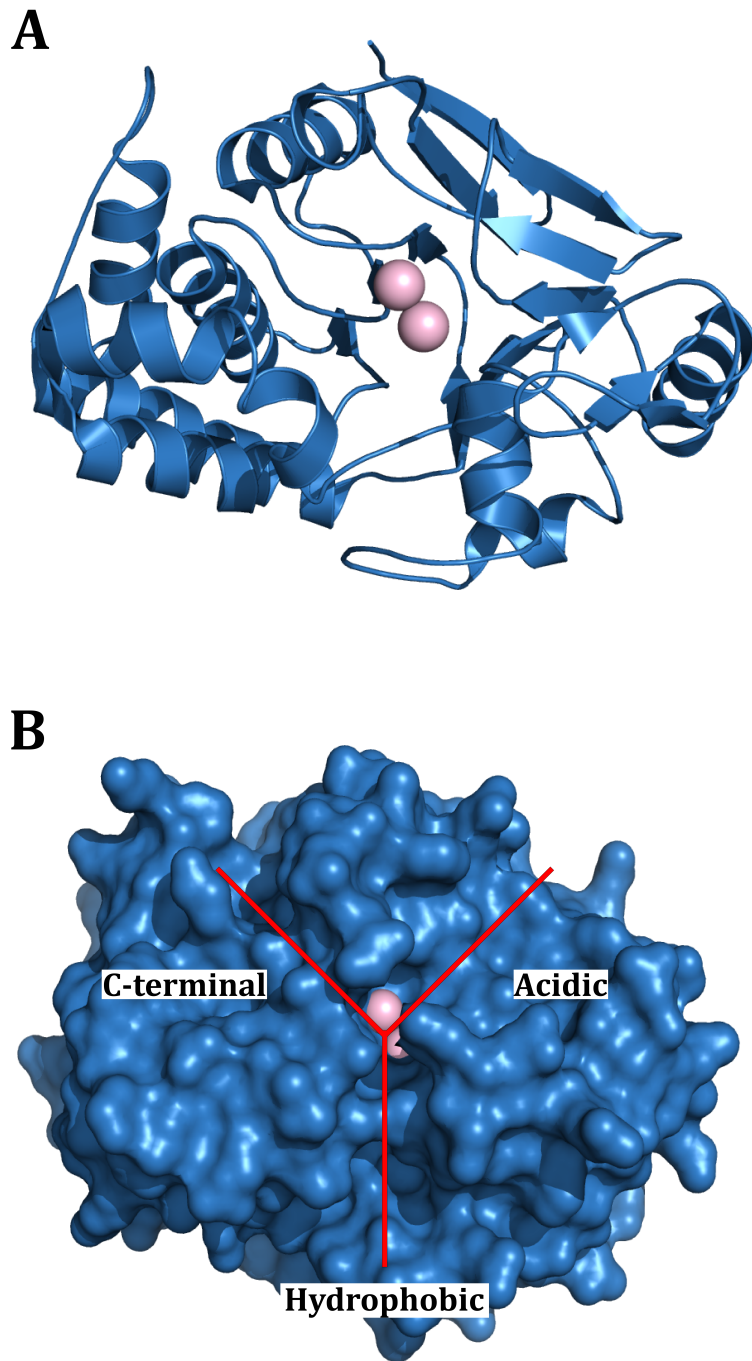
Figure 1.3: **The Three-Dimensional Crystal Structure of Mammalian Protein Phosphatase-1c.** (A) The cartoon structure of PP-1cα is represented in blue and the two Mn^{2+} are depicted as pink spheres. The two metal ions are housed in the centre of the PP-1c active site. The $\beta12$-$\beta13$ loop is seen above, connecting the C-terminal and acidic grooves. A β-sandwich is seen at the top, between two α-helical domains. (B) The surface model of PP-1c is shown in blue and the two Mn^2 are depicted as pink spheres. The location of the Y-shaped cleft is identified in red with labels describing the C-terminal, acidic, and hydrophobic grooves. These lines lay over the cleft and the three grooves surrounding it are labelled. This figure was produced with *PyMOL*. [PDB 1FJM] [43].

binding to one of the water molecules and Asp92 with the first. The second metal ion also coordinates with three amino acids: His173, His248, and Asn124. The two metal ions and the two arginines, Arg96 and Arg221, together create a positive surface within the PP-1c active site. This allows for the negatively charged phosphate group of the protein substrate to bind within the PP-1c active site long enough to undergo dephosphorylation. The phosphate group of the substrate interacts with the two metal ions of PP-1c via two water molecules inciting a nucleophilic attack on the phosphorous atom of the substrate and yielding a free inorganic phosphate [30, 43, 133].

Notably, a threonine residue located within the PP-1c C-terminal tail is conserved in all 3 isoforms of PP-1c (Thr320, Thr317, Thr311 in PP-1c α, β, and γ, respecitively). This residue can be phosphorylated by cyclin-dependent kinases resulting in the auto-inhibition mechanism of PP-1c at the G_1/S phase transition of the cell cycle [29]. When phosphorylated, the flexible C-terminal tail of PP-1 is thought to fold into its own active site and cause auto-inhibition by blocking substrate binding [43]. PP-1c can be reactivated by autodephosphorylation of this Thr residue, resulting in the release of the C-terminal tail from the active site and substrate dephosphorylation can be resumed [53].

1.2.3 Recombinant Protein Phosphatase-1c has a Different Specific Activity from Native Protein Phosphatase-1c

Between recombinant and native PP-1c, there are some important differences in their structure that affect their specific activity. PP-1c expressed by bacteria tends to be bound to Mn^{2+} ions, even though the active site of native PP-1c is likely to contain either Fe^{2+} or Zn^{2+} ions [14]. It was shown using glycogen-phosphatase and para-nitrophenylphosphate (pNPP) phosphatase activity assays that bacterially expressed human PP-1c had decreased specific activity compared to native rabbit PP-1c [51]. Recombinant PP-1c was capable of dephosphorylating substrates that resemble tyrosine residues, rather than only dephosphorylating serine or threonine residues, for example, pNPP (structure shown in Figure 1.5), while the native PP-1c is less able [30].
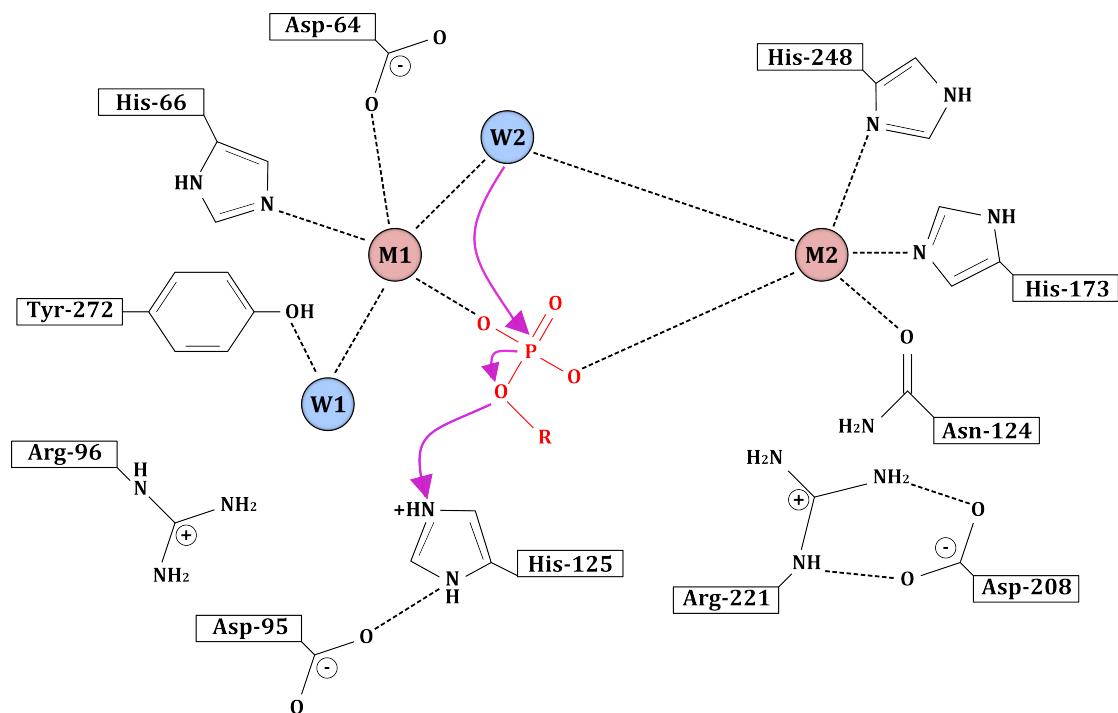
Figure 1.4: **The Catalytic Mechanism of Protein Phosphatase-1c Dephospho-rylation.** The active site of PP-1c house two metal ions (represented as a pink circle, labelled M1 and M2). M1 is stabilized by binding to Asp64 and His66 residues of PP-1c and two water molecules (represented as blue circles, labelled W1 and W2). M2 shares binding to W2 with M1 and is additionally stabilized by binding to Asn124, His172, and His248 residues of PP-1c. The purple arrows represent the nucleophilic attack on the phosphate group of the protein substrate (the phosphate group is represented in red). This figure was modified from [3, 30, 43].
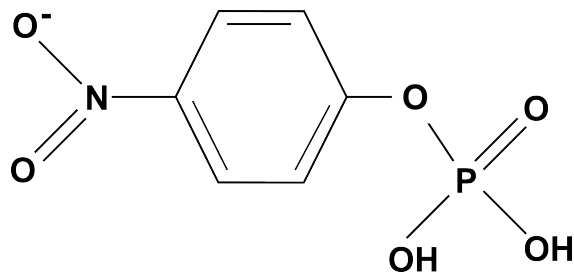
Figure 1.5: **The Chemical Structure of para-Nitrophenyl Phosphate.** The structure of pNPP contains a benzene ring with a phosphate group on position 1 and a nitrogen on position 3. This is more structurally related to tyrosine than serine or threonine residues, which have a methyl and hydroxyl groups and are significantly smaller.

Bacterially expressed Calcineurin exclusively incorporates Fe/Zn metal ions similar to native PP-1c and crystal structures of Calcineurin show that these metal ions occupy a larger region of the active site than Mn^{2+}. It is suggested that these Fe/Zn are large enough to block tyrosine residues from interacting within the active site of native PP-1c [96, 106, 123]. It has also been hypothesized that eukaryotes have chaperones that bind to PP-1c and ensure the correct metal ions are incorporated. When Mn^{2+} is present in solution, eukaryotic PP-1c does not associate with them. The highly specific PP-1c inhibitor, Inhibitor-2 (I2), is one protein that has the potential to be a PP-1c chaperone protein. Evidence shows that recombinant PP-1c loses its ability to dephosphorylate tyrosine residues after interacting with I2, suggesting that I2 helps PP-1c fold into its native conformation [15, 95, 150].

1.3 Natural Toxins Inhibit Protein Phosphatase-1c Activity

The importance of PP-1c activity has been exhibited by the fact that nature has developed many potent and specific inhibitors of PP-1c. Among the most well-known inhibitors are Microcystin (IC_{50} = 0.1 nM) [94], Okadaic Acid (IC_{50} = 10 nM) [104], Calyculin A (IC_{50} = 0.7 nM) [107], and Nodularin (IC_{50} = 0.3 nM) [68].

One of the first crystal structures elucidated of a natural toxin bound to PP-1c of Microcystin-LR bound to PP-1cα. The Microcystin class of toxins were identified in 1990 as a potent and specific inhibitors of both PP-1 and PP-2A and are cyclic heptapeptides produced by cyanobacteria (blue-green algae). The Microcystin structure has two variable residue positions and Microcystin-LR is the most common of the nine known variants of Microcystin, containing a leucine and an arginine at these positions (Panel A of Figure 1.6) [94]. Figure 1.7 depicts the crystal structure of Microcystin-LR bound to the active site of PP-1cα and demonstrates that Microcystin has three points of interaction with PP-1c: 1) to the metal ions, 2) to the hydrophobic groove, and 3) to the edge of the C-terminal groove. The long, hydrophobic amino acid (2S, 3S, 8S, 9S)-3-amino-9-methoxy-2,6,8-trimethyl-10-phenyldeca-4,6-dienoic acid of Microcystin, also known as ADDA, binds within the hydrophobic groove of PP-1c. As well, Microcystin was found to coordinate with the metal ions via two water molecules that interact with carboxylate and carbonyl groups of Microcystin. Lastly, a leucine residue on Microcystin interacts with the PP-1c β12-β13 loop that connects the C-terminal groove to the acidic groove. This leucine naturally covalently links to the conserved Cys273 on PP-1cα. While mutagenesis of the PP-1c Cys273 disrupts the covalent binding to Microcystin and results in decreased PP-1c inhibition, the toxin can still bind and inhibit PP-1c activity [43, 96, 111]. Initial PP-1c inhibition by Microcystin occurs when it binds the PP-1c active site, but the covalent binding requires a few hours to form.

Over the years, Okadaic Acid has become a crucial research tool due to its cell permeablity and ability to potently inhibit both PP-1 and PP-2A. Thus, Okadaic Acid is used frequently in biological studies to inhibit both PP-1c and PP-2A in cells [24, 33]. Panel B of Figure 1.6 depicts the chemical structure of Okadaic Acid and Figure 1.7 shows the crystal structure of Okadaic Acid bound to PP-1cγ [104]. When bound to PP-1cγ, the hydrophobic tail of Okadaic Acid rests along the hydrophobic groove in a similar manner to the ADDA residue of Microcystin. As well, Okadaic Acid interacts with the same β12-β13 loop of PP-1c as Microcystin; however, unlike Microcystin, Okadaic Acid binds in a non-covalent manner.

The crystal structure of Calyculin A bound to PP-1cγ (Figure 1.7) depicts the toxin interacting with both the hydrophobic and acidic groove of PP-1c. Uniquely, Calyculin A has a phosphate group (Panel C of Figure 1.6) that is used to coordinate with the metals ions of the PP-1c active site [72].

Lastly, Nodularin-R is a toxin that like Microcystin has an ADDA residue and it also lays across the hydrophobic groove in cleft of PP-1c (Panel D of Figure 1.6 and Figure 1.7). The Nodularin-R•PP-1cγcrystal structure also demonstrates interactions within the active site and non-covalent binding to the β12-β13 loop [68].

Figure 1.7 depicts the crystal structure of Microcystin-LR, Okadaic Acid, Calyculin A, and Nodularin-R bound to the PP-1c active site. It clearly shows that the majority of PP-1c toxins bind across the PP-1c catalytic subunit, in a similar fashion. By means of these structures, three key interaction sites have been identified for binding the PP-1c active site by these toxin: the hydrophobic groove, the active site metal ions, and the β12-β13 loop. The hydrophobic groove of the PP-1c cleft is critical because all of these toxins have demonstrated binding to this groove. Secondly, at the active site of PP-1c, there is typically coordination between the toxins and the two metal ions. Lastly, the interaction to the β12-β13 loop has been demonstrated to be crucial, but the covalent binding, present in Microcystin binding, has been determined to not be critical for PP-1c inhibition [68].

A

B

C

D
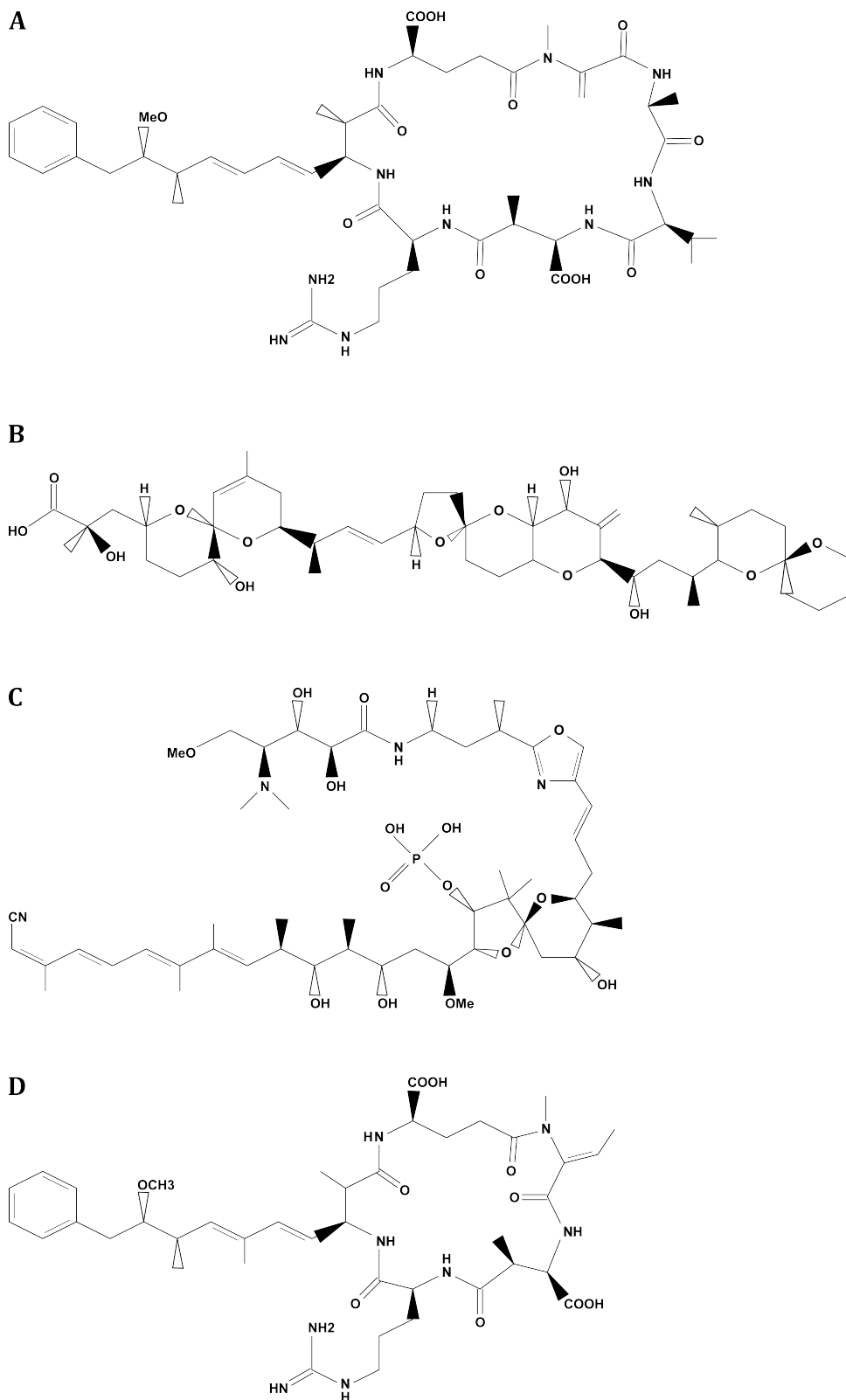
Figure 1.6: **The Chemical Structures of Natural Toxins Microcystin-LR, Okadaic Acid, Calyculin A, and Nodularin.** (A) Microcystin-LR, (B) Okadaic Acid, (C) Calyculin A, and (D) Nodularin-R.
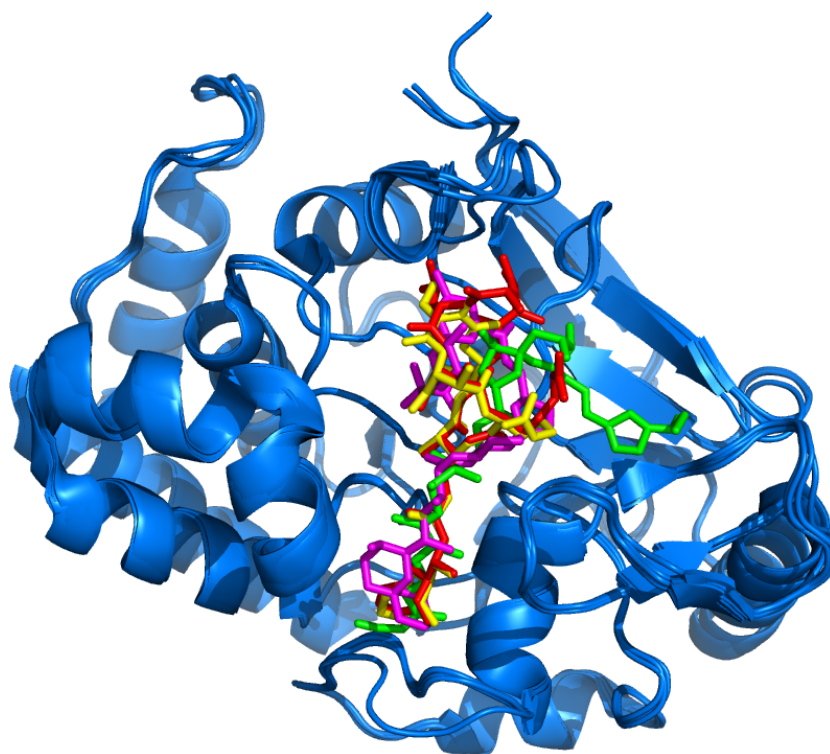
Figure 1.7: **Alignment of the Three-Dimensional Crystal Structures of Protein Phosphatase-1c Bound to Natural Toxins Microcystin-LR, Okadaic Acid, Calyculin A, and Nodularin-R.** The crystal structure of PP-1c bound to natural toxins Microcystin-LR (represented in red), Okadaic Acid (represented in magenta), Calyculin A (represented in green), and Nodularin-R (represented in yellow) were aligned to demonstrate the toxin binding to PP-1c. This demonstrated the overlap and vary similar fashion in which these toxins bind PP-1c. All four compounds interact with $\beta12$-$\beta12$ loop, the hydrophobic groove, and the metal ions within the active site of PP-1c. This figure was produced with *PyMOL*. Microcystin-LR [PDB 1FJM] [94]. Okadaic Acid [PDB 1JK7] [104]. Calyculin A [PDB 1IT6] [107]. Nodularin-R [PDB 3E7A] [68].

1.4 Regulatory Subunit Control of Protein Phosphatase-1c Activity

Genomic studies have demonstrated that eukaryotes encode for over 400 Ser/Thr kinase genes, but only $\sim$ 40 Ser/Thr phosphatase genes [114]. In addition, kinase activity is mainly controlled through a large number of consensus sequences that create highly specific enzyme-substrate interactions, whereas, PP-1c struggles to recognize the sequences of short peptides based on its own physiological substrates [14]. In the past, this had lead many to believe that PP-1c has a general, non-specific, activity that functions only to counteract that of kinases. In recent years, we have become increasingly aware of how specific PP-1c dephosphorylation activity is obtained through hundreds of regulatory subunits (R-subunits). *In vitro*, PP-1c has a broad specificity and can dephosphorylate an array of substrates with ease. Evidence shows that when PP-1c is bound by small peptides, preventing the interaction of PP-1c R-subunits, PP-1c substrates are hypo-dephosphorylated and this misregulation leads to cell death [21]. However, *in vivo*, when in contact with its R-subunits, the actions of PP-1c are precise and controlled [15]. PP-1 actually functions as a holoenzyme, where PP-1c binds to R-subunits that are required for substrate specificity.

PP-1c is often expressed at a consistent level in the cell, while the amounts of R-subunits available are often present in excess of PP-1c [29, 50, 92, 150]. Therefore, PP-1c is almost constantly bound to one or more of its R-subunits, preventing uncontrolled dephosphorylation. As well, a large number of these R-subunits function by inhibiting PP-1c activity and the holoenzyme is predominately inactive at basal conditions [49, 150]. As a result, PP-1c activity is extremely dependent on the levels of R-subunits present. The levels of R-subunits available for PP-1c regulation can have a major impact on PP-1c activity and specificity. If the levels of a single R-subunit are too high or too low, it could lead to PP-1c activity to be too tightly restricted or result in the loss of a specific activity. Therefore, the available levels of R-subunits and their binding to PP-1c needs to be tightly regulated and the cell controls this in multiple ways, such as,

competition for PP-1c binding, R-subunit proteolysis, and modifying R-subunit binding affinity for PP-1c by post-translational modifications [14, 49, 50, 150]. The tight regulation of R-subunit binding to PP-1c by the cell allows for strict control of PP-1c specific activity.

PP-1c R-subunits are responsible for the increased specific activity of PP-1c towards its substrates in mainly two manners; the first is through subcellular localization of PP-1c and the second is through the alteration of PP-1c activity towards its substrates [19]. The different subcellular localizations of PP-1c isoforms was indicative of the existence of R-subunits. The PP-1c localization suggested that there must be a targeting protein present to differentiate between recruitment of PP-1c to different regions of the cell [2, 25, 55]. Many R-subunits including Spinophilin, Repoman, and Myosin Phosphatase Targeting Protein (MYPT) family, are known to recruit PP-1c to different subcellular locals [150]. For example, Spinophilin is able to recruit PP-1cγ_1 to F-actin-rich regions, but is unable to recruit PP-1cβ [17]. In addition, R-subunits can provide docking sites which creates scaffolds and targets PP-1c to specific cellular areas. The local concentration of PP-1c increases or PP-1c is escorted within proximity of its substrates, and ultimately, increasing substrate dephosphorylation [14, 50, 158]. Secondly, substrates are often weak affinity binders of PP-1c on their own, but become better PP-1c targets when in the presence of R-subunits. The PP-1c R-subunits can function either by bringing PP-1c and its substrate into proximity by binding both PP-1c and the PP-1c substrate or by increasing PP-1c specificity a substrate that is a typically weak binder [54, 150]. For example, MYPT1 binds PP-1c and increases the length of the PP-1c acidic groove in the PP-1c cleft. This elongation allows for better binding of the PP-1c target, myosin [64, 145].

Currently, there are over 200 known R-subunits which are largely structurally unrelated, even though PP-1c itself only has a small number of binding domains [13, 14, 49, 50]. This leads to competition between R-subunits for binding of the same docking sites. These parameters result in hundreds of possible holoenzyme combinations [50]. On average, R-subunits occupy a large region of over 400 $\mathring{A}^2$ of PP-1c surface area and binding

often does not lead to change in the conformation of PP-1c [14, 57, 123, 145]. Figure 1.8 shows the R-subunits I2, Spinophilin, and MYPT1 binding to PP-1c and demonstrates the large surface area occupied by each R-subunit. R-subunits often achieve this large interface interaction by binding PP-1c via short linear motifs or SLiMs and binding domains [150]. Currently, there are a handful of known PP-1c SLiMs, which have a variety of roles in regards to function. Despite small number of known SLiMs, the R-subunits can bind many different surface areas of PP-1c. Figure 1.8 depicts the three R-subunits MYPT1, I2, and Spinophilin, that occupy largely different areas of PP-1c due to their differing SLiMs.

The majority of R-subunits bind PP-1c via a SLiM termed the RVxF-motif, a primary PP-1c docking motif mentioned previously. The RVxF motif ([K/R][X0][1][V/I/L][x][F/W], where x can be any amino acid except proline) is typically present as an unstructured loop [14, 19, 31] and binds the RVxF-hydrophobic binding pocket of PP-1c located ~ 20 Å away from the active site (Figure 1.8). A second PP-1c binding motif is the SILK motif ([G/L][I][L][R/K]). This SLiM is typically located N-terminal to the RVxF motif and binds a hydrophobic pocket opposite of the PP-1c active site. The SILK motif has been identified in R-subunits, such as Inhibitor-2 (I2) [14, 49, 57, 154]. Thirdly, Scr Homology 3 (SH3) domain mediates protein-protein interactions and binds proline-rich regions of target protein. The SH3 domain of the Apoptotic Stimulating Proteins of p53 (ASPP) family can bind to the traditional SH3 PxxP binding motif on PP-1c, where x is any amino acid [86, 112, 138]. The RVxF and SILK SLiMs and the SH3 domain all function as PP-1c anchors for secondary binding sites or proteins [154].

Another SLiM called the myosin phosphatase N-terminal element (MyPhoNE) has the consensus sequence of [R][x][x][Q][V/I/L][K/R][x][Y/W] that is used by the MYPT family member MYPT1 and other R-subunits. The MyPhoNE SLiM has a substrates selection functions that is not well-understood [14, 49, 50, 132]. The SLiM known as SpiDoC, short for Spinophilin docking site for the C-terminal groove, is also used for substrate selection and functions blocking substrate binding sites. As the name suggests, the neuron protein Spinophilin, remains unstructured until bound to the C-
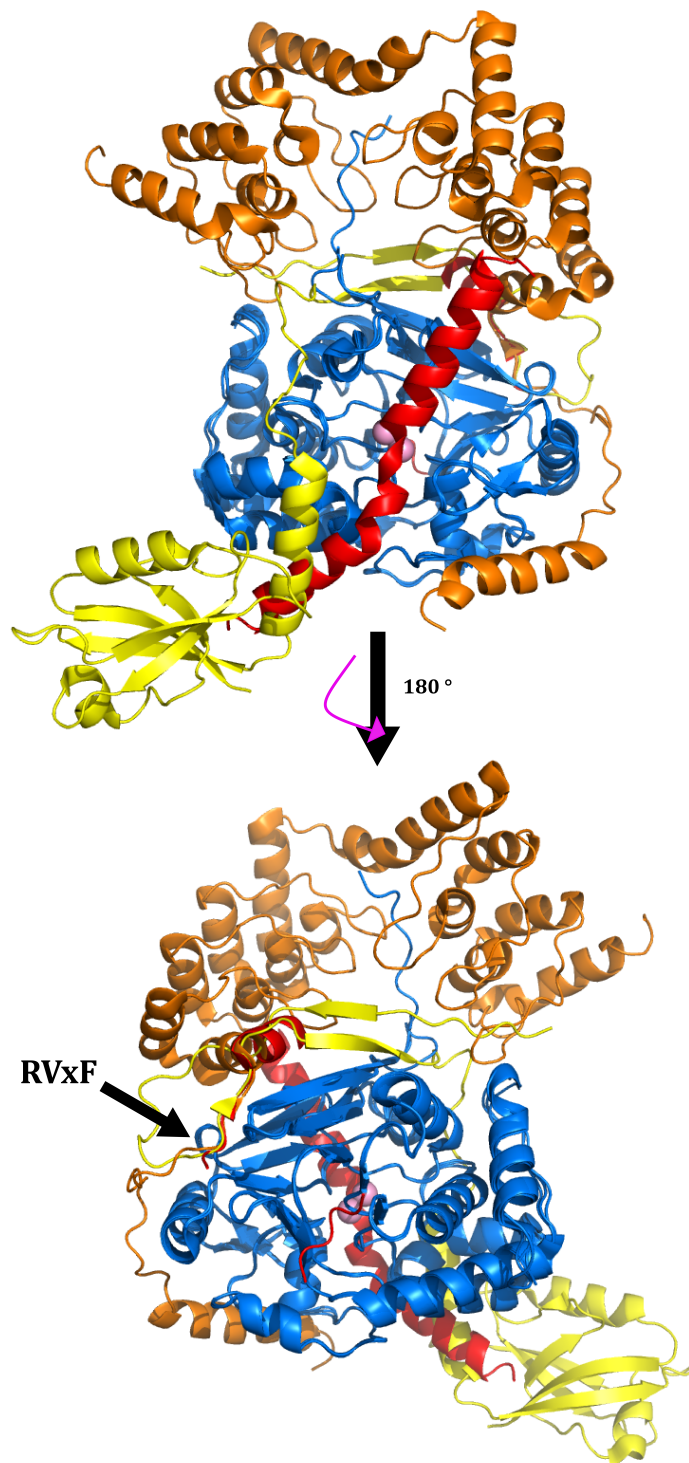
Figure 1.8: **Alignment of the Three-Dimensional Crystal Structures of Protein Phosphatase-1c Bound to Regulatory Subunits Inhibitor-2, Spinophilin, and MYPT1.** The binding of the regulatory subunits Inhibitor-2 (red), Spinophilin (yellow), and MYPT1 (orange) demonstrate how the regulatory subunits bind PP-1c (blue) over a large surface area and that they can bind in to many different areas. All three contain an RVxF motif, which is pointed out and bound to the back side of PP-1c at the hydrophobic-binding pocket. This figure was produced with *PyMOL*. Inhibitior-2 [PDB 2O8A] [57]. Spinophilin [PDB 3EGG] [125]. MYPT1 [PDB 1S70] [145].

17

terminal groove of PP-1c through its SpiDoC motif. This occupation sterically blocks the binding of PP-1c substrates without inhibiting the activity of PP-1c [125]. Both the MyPhoNe and SpiDoC SLiMs have a substrate selection function.

Ankyrin (Ank) repeats are responsible for isoform specificity of PP-1c and are present in R-subunits, such as, MYPT and other families. The Ank repeats bind the disordered C-terminal tail of PP-1c [49]. As described earlier, the key differences between the PP-1c isoforms are in their C-terminal tails. As well, there is also evidence that the binding of MYPT1 via its Ank repeats may extends the hydrophobic groove of the PP-1 catalytic subunit and allows for the binding of other substrates [14, 145]. A novel SLiM was recently discovered on nuclear proteins Ki67 and RepoMan, termed KiR, occupies a novel PP-1c binding pocket [150]. The KiR SLiM allows for isoform specificity of the R-subunits via the binding of a single amino acid rather than the C-terminal tail as typically seen. Ki67 and RepoMan can bind Arg20, present in PP-1cγ and PP-1cβ, but the corresponding residue, Gln20, on PP-1cα, prevents these R-subunits from binding [14, 75].

Lastly, pseudosubstrate SLiMs can block substrate binding and inhibit PP-1c activity when the SLiM is phosphorylated. For example, Inhibitor-1 is phosphorylated by protein kinase A at Thr35 which then occupies the PP-1c active site and prevents further substrate dephosphorylation [32, 36]. The summary of these binding motifs or SLiMs along with examples of R-subunits that use them, can be found in Table 1.1.

SLiMs	SLiM Function	R-subunit Examples
RVxF	Anchor	G-subunit, ASPP, MYPT
SILK	Anchor	I2 , MYPT
SH3 domain	Anchor	ASPP
MyPhoNE	Substrate Selection	MYPT1
SpiDoC	Substrate Selection	Spinophillin
Ank Repeats	Isoform Specificity	MYPT, ASPP
KiR	Isoform Specificity	Ki67, RepoMan
Pseudosubstrate	Substrate Blocking	Inhibitor-1, MYPT1

Table 1.1: **The Short Linear Motifs of Regulatory Subunits.** List of known SLiMs, their functions, and examples of R-subunits that use them.

In summary, R-subunit binding has been described using five key words: specific, universal, degenerate, non-exclusive, dynamic [50]. These terms describe what has become known as the *PP1 binding code.* PP-1c binding is described as specific because most R-subunits do not bind other members of the Phosphoprotein Phosphatse subfamily (for example, PP2A, CaN). It is universal because PP-1c binding is evolutionarily conserved. It is degenerate because different R-subunits have different binding affinities with similar motifs which allows for flexibility in PP-1c binding (ex: the RVxF motif) [14]. Also, it is non-exclusive because multiple R-subunits can bind PP-1c at the same time (see Section 1.6 for examples). Lastly, it is dynamic because R-subunits can compete with one another for binding [50].

1.5 The Structure and Role of the Myosin Phosphatase Targeting Protein Family of Regulatory Subunits of Protein Phosphatase-1c

The Myosin Phosphatase Targeting Protein (MYPT) family is a regulatory subunit family of PP-1c that contains five isoforms in mammalian cells: MYPT1 [136], MYPT2 [37], MYPT3 [139], MBS85 [144], and TGF-β-inhibited membrane-associated protein (TIMAP) [16]. The MYPT protein is a regulatory subunit of the trimeric holoenzyme known as the Myosin phosphatase that is formed by PP-1c, a MYPT protein and a 20 kDa subunit known as M20. The Myosin phosphatase is responsible for the dephosphorylation of the myosin subunit, myosin light chain, which leads to the relaxation of smooth muscle [59, 140, 141]. The role of the MYPT family in this holoenzyme is to target and regulate the actions of PP-1c and has preferential binding for the PP-1cβ isoform [25, 46, 132].

MYPT1 is the most well-studied of the five isoforms and MYPT1•PP-1cβ binding complex was the first structure of a PP-1c holoenzyme solved (the 2.7 $\mathring{A}$ resolution crystal structure shown in Figure 1.9). MYTP1 binds PP-1cβ via its RVxF motif (present as KVKF$_{35\text{-}38}$), its six Ank repeats and a novel MyPhoNE motif, a motif seen for the first

time [25, 145]. Although it was previously thought the isoform specificity of MYPT1 solely resulted from the Ank repeat binding around the C-terminal of PP-1c, the crystal structure shows that the central region of PP-1cβ causes isoform specificity of MYPT1 at the key residues Thr197, Ser232, Asn236, and Arg237 [132]. The crystal structure was also able to demonstrate that MYPT1 binding leads to elongation of the acidic groove of the catalytic cleft of PP-1cβ which is likely responsible for PP-1cβ specificity for myosin [145]. In addition, MYPT1 has a pseudosubstrate docking mechanism for PP-1c. When phosphorylated at Thr696 and Thr853, MYPT1 interacts with the PP-1c active site causing autoinhibition of the myosin phosphatase [69]. Lastly, MYPT1 can bind to myosin, merlin [61], and moesin proteins which are all actin-binding proteins and PP-1c substrates.

The most recently discovered member of the MYPT family, TIMAP, was identified in 2002 [16]. The 64 kDa protein shares 13 % sequence identity with MYPT1. TIMAP contains five Ank repeats, an RVxF motif (present as $KVSF_{63-66}$), and a C-terminal CAAX box that is used for anchoring proteins to the plasma membrane [16]. As its name suggest, TIMAP is regulated by TGF-β-1 and is predicted to bind PP-1cβ in a similar manner to MYPT1 [16, 137, 157].
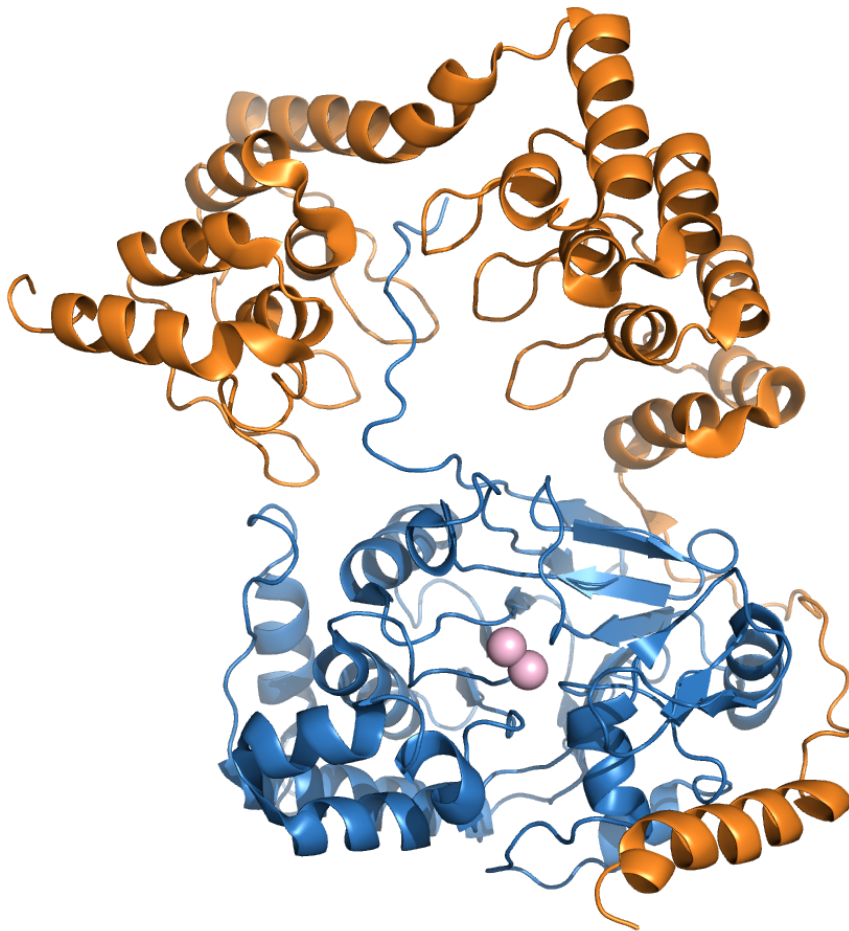
Figure 1.9: **The Three-Dimensional Crystal Structure of MYPT1 Bound to PP-1cβ.** The regulatory subunit MYPT1 (orange) bind PP-1cβ (blue) via Ank repeats around the C-terminal tail of PP-1cβ and by its RVxF motif. The two Mn^{2+} are in the active site of PP-1cβ (represented by pink spheres). This figure was produced with *PyMOL*. [PDB 1S70] [145].

1.6 The Structure and Role of the Apoptotic Stimulating Proteins of p53

The Apoptotic Stimulating Proteins of p53 (ASPP) family are proteins responsible, in part, for the regulation of the tumour suppressor, p53. The first member of the ASPP family was originally identified as p53 Binding Protein 2 (53BP2) for its ability to bind p53 in a yeast two-hybrid experiment in 1994 [60]. 53BP2 contains two major domain types; four Ank repeats followed by an SH3 domain [60]. Years later, 53BP2 was discovered to be the C-terminus of a larger protein which was termed, ASPP2 [130]. In 1996, the first 2.2 $\mathring{A}$ structure was produced between the DNA-binding domain of p53 and 53BP2, which shows the Ank repeats and the PxxP ligand binding region of the SH3 domain of 53BP2 bound to a region of p53 that overlaps with its DNA-binding domain (Figure 1.11) [45, 127].

The full-length ASPP1 and ASPP2 proteins were discovered in 2001 because of their ability to bind to p53 and induce apoptosis, but not cell-cycle arrest [6, 130]. ASPP1/2 both contain an α-helical domain within their N-terminus, a Proline-rich domain, followed by Ank repeats and an SH3 within the C-terminus (shown in Figure 1.10). This is where the second name of the ASPP family stems from; the Ankyrin repeat, SH3 domain, and Proline-rich-region containing Protein family. The N-terminus of ASPP2 also contains a nuclear localization signal and a potential Ras-associating domain (although some key residues are not conserved) [58, 129, 147]. The inhibitory ASPP (iASPP) was first discovered in 1999 as a RelA-associated inhibitor [156]. This protein was determined to be an ASPP family member in 2003 by its ability to inhibit p53 activity and its sequence similarity to ASPP1/2 [7, 80]. iASPP is the only ASPP family member homolog present in *Caenorhabditis elegans* making it the most evolutionarily conserved family member [7]. iASPP does not contain the pro-apoptotic region on its N-terminus that ASPP1/2 do, but all three share highly conserved C-terminal ends (Figure 1.10) [143].

Samuels-Lev *et. al.* showed that ASPP1/2 expression was inhibited when bound by

anti-sense RNA, resulting in decreased p53-induced apoptosis. As well, that ASPP1/2 both function to enhance the pro-apoptotic activity of p53 through specifically enhancing the DNA binding and transactivation of p53 [130]. ASPP1/2 both bind p53 through its central, DNA-binding domain and it is thought that ASPP1/2 binding results in a conformational change in p53, allowing it to better bind its promoter regions [130, 143]. ASPP1/2 were also the first activators found to stimulate activity of all three of the structurally-related tumour suppressors; p53, p63, p73 and it was thought to be a result of all three proteins sharing over 60 % sequence identity in their DNA-binding domain [6]. Like ASPP1/2, iASPP can bind the DNA-binding domain of p53 via its Ank repeats and SH3 domain, but uniquely, iASPP has been shown to have a drastic decrease in p53 binding when the proline-rich region of p53 was deleted [8]. Overall, there is conflicting evidence in how the ASPP proteins regulated p53 activity.

Over the years, ASPP1/2 has been shown to be down-regulated and iASPP is up-regulated in many cancers expressing wild-type p53, including breast, lung, and leukemia sarcomas [1, 7, 85, 115, 116, 126, 130]. Furthermore, ASPP2 down-regulation has been linked with poor prognosis in breast cancers, lymphomas, and leukemias [23, 88, 161]. Mice studies of ASPP2 demonstrated both homozygous ASPP2 knock-out and ASPP2/p53 knock-out mutations were lethal. As well, the heterozygous mice had a higher incidence of tumour formation [66, 152]. This highlights the obvious importance the ASPP family has on regulating the pro-apoptotic functions of p53 and how their misregulation can lead to vast uncontrolled cell growth.

Although, the regulation of ASPP activity is not completely understood, there is evidence that the ASPP family can be regulated by both gene silencing/protein levels and autoinhibitory mechanisms [143]. ASPP1/2 levels have been linked to control mechanisms, such as, methylation, levels of transcription factors like E2F1, and proteasome degradation [1, 22, 35, 52, 84, 142, 163]. iASPP protein levels have been shown to down-regulated by microRNAs [48, 79]. Recently, it has also been shown that ASPP2 can undergo an autoinhibitory process where the intrinsically disordered Proline-rich region can bind its first Ank repeat and the SH3 domain to prevent its own binding

to other proteins, such as, p53 and NFκB (nuclear factor kappa-light-chain-enhancer of activated B cells) [127, 128]. iASPP has been shown to undergo dimerization between its N- and C-terminal leading to autoinhibition [90].

The ASPP family has also recently been found to be regulatory subunits of PP-1c [86, 112]. Both ASPP1/2 contain the primary PP-1c binding motif, RVxF [31], that binds within the hydrophobic binding pocket of PP-1c. As discussed in Section 1.4 this is a major PP-1c binding motif, which interact ~ 20 $\mathring{A}$ away from the PP-1c active site. In ASPP1, the RVxF motif is present in the form of RVRF$_{883\text{-}886}$ and in ASPP2 it is in form of RVKF$_{921\text{-}924}$. Originally thought to not be able to bind PP-1c, iASPP binds PP-1c via a non-canonical RVxF motif (RARL$_{622\text{-}625}$). Recently it has been found that all isoforms of PP-1c contain an SH3 PxxP binding motif, that is essential for ASPP binding to PP-1c. The PxxP motif is present as PITPPR$_{318\text{-}323}$, PVTPPR$_{313\text{-}319}$, and PVTPPR$_{308\text{-}313}$ in the α, β, and γ isoforms of PP-1c, respectively. This motif binds the SH3 domains of the ASPP proteins located on their C-termini. All three isoforms have preferential binding to α isoform of PP-1c. Lastly, there has been predicted binding between one or more of the ASPP Ank repeats to PP-1c, in a similar manner to the MYPT protein (Figure 1.9) [138].

In recent years, there has been evidence that the ASPP family can form trimeric complexes with PP-1c substrates. For example, ASPP1/2 mediates binding of PP-1c to YAP/TAZ (yes-associated protein/transcriptional coactivator with PDZ-binding motif) allowing for their dephosphorylation and activation of the Hippo pathway [91, 151, 159]. Also, ASPP1/2 have been shown to promote binding between PP-1cα and the centrosome linker protein, C-Nap1 (centrosomal Nek2-associated protein 1) [162].
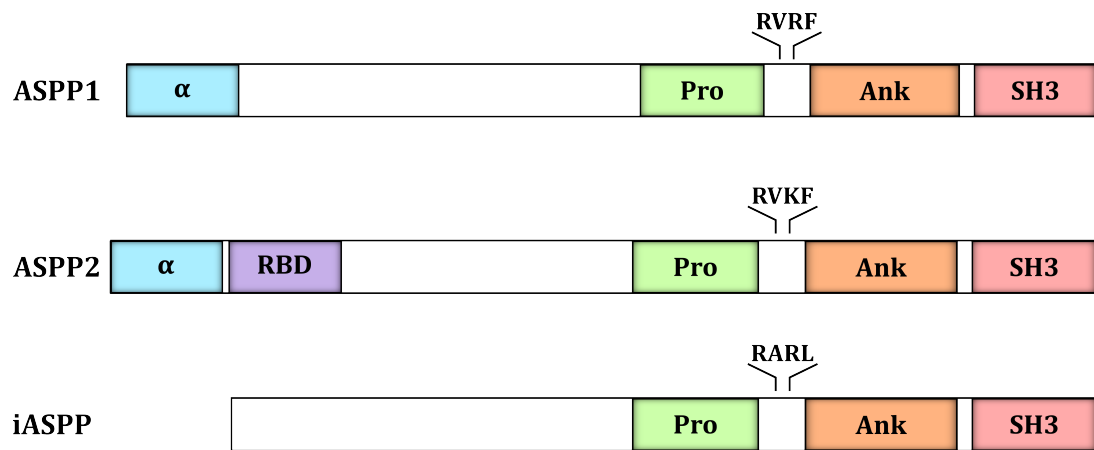
Figure 1.10: **The Domains Found within the ASPP Family of Proteins.** All three ASPP family members contain a proline-rich domain, Ank repeats, an SH3 domain and an RVxF motif at their C-terminus. The ASPP1/2 also have an α-helical domain. Only ASPP2 has evidence of a potential Ras-associated domain.
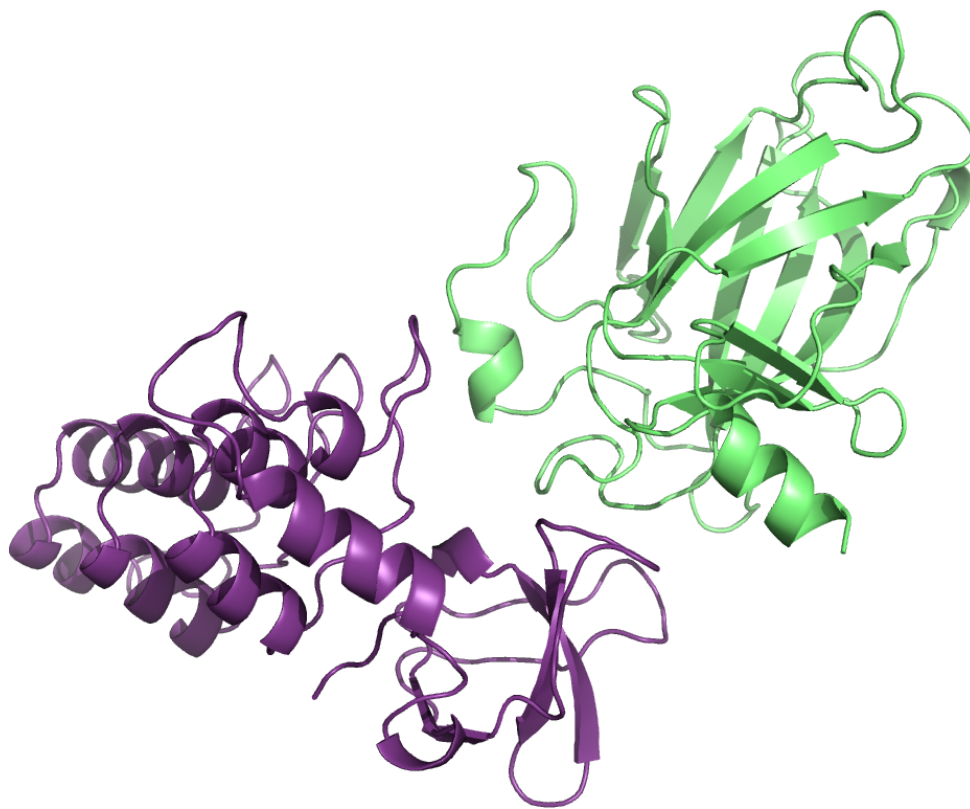
Figure 1.11: **The Three-Dimensional Crystal Structure of the DNA-binding Domain of p53 Bound to 53BP2.** The DNA-binding domain of p53 (lime) was shown to bind to the SH3 domain and Ank repeats of 53BP2 (violet purple). This figure was produced with *PyMOL*. [PDB 1YCS] [45].

1.7 The Pro-Apoptotic Activity of p53 Regulated via Reversible Phosphorylation

p53 has often been called the *guardian of the genome* due to its crucial role in cell apoptosis and its activation in response to cell damage or stress [153]. Under such conditions, p53 will transactivate damage response genes, which enact an array of functions including DNA repair, cell-cycle arrest, or apoptosis [44]. p53 was the first tumour suppressor gene to be identified in 1979 [153] and is known to have two structurally-related proteins, p63 [155] and p73 [65]. The importance of p53 was quickly realized by the fact that p53 is mutated in over 50 % of human cancers [34, 40, 109], while its counterparts, p63 and p73, are rarely mutated [6]. These mutations often lead to the inhibition of the transactivation activity of p53 response genes; therefore, leading decreased damage response, such as, cell-cycle arrest and apoptosis. Overall, this contributes to uncontrolled cell growth within tumours [160].

The four major functional domains of p53 are depicted in Figure 1.12. p53 contains two N-terminal transactivation domain, a proline-rich domain, a DNA-binding domain/core domain, and an oligomerizatoin domain [63]. There is over 60 % sequence homology in the DNA-binding domain shared between p53 and the structurally-related proteins, p63 and p73 [6].

The activity of p53 can be regulated through multiple post-translational modifications, such as phosphorylation, acetylation, ubiquitination, glycosylation, proyl isomerization, etc. [11, 76, 82]. For example, several residues on p53 are phosphorylated in response to cellular stress or DNA damage. One study found that 17 different sites were phosphorylated after exposure to UV irradiation. These phosphorylation sites are largely located in the transactivation domain and include serine 6, 9, 15, 20, 33, 37, 46, as well as, threonine 18 [11, 134, 146].

Phosphorylation events can affect binding of p53 regulatory proteins, such as the mouse double min-2 homolog (MDM2). MDM2 is a major negative regulator of p53 that

functions as an E3 ubiquitin-protein ligase. The N-terminal transactivation domain of MDM2 binds the transactivation domain of p53 (shown in Figure 1.13), promotes p53 degradation by ubiquitination and decreases p53 stability and activity [40]. As a result of p53 phosphorylation, MDM2 is prevented from binding. Consequently, the stability and transactivation of p53 increases, which leads to cell apoptosis [82, 134]. MDM2 is also a transcriptional target of p53. Expression of MDM2 in the absence of cellular stress is responsible for maintaining the levels of p53 through an autoinhibitory feed-back loop [81, 108].

Figure 1.12: **The Domains Found within the p53 Protein.** The p53 protein contains four major domain types: N-terminal transactivation domain (TAD1 and TAD2), proline-rich domain (Pro), DNA-binding/core domain (DBD), and oligomerization domain (Olig).

1.7.1   Regulation of p53 by Protein Phosphatase-1c

It is well-established that Ser15 and Ser37 are key p53 phosphorylation sites in regards p53 regulation. Their phosphorylation has been linked to the promotion of transactivation, as well as, cell-cycle arrest by p53 [28, 89]. But only recently, has it been known how these sites are dephosphorylated. Li *et. al.* found that one way PP-1c promotes cell survival is through the dephosphorylation of p53. Specifically, the Ser15 and Ser37 residues of p53 are hyper-phosphorylated when the activity of PP-1c is inhibited by the natural toxins, Okadaic Acid and Calyculin A [82]. Dephosphorylation of these sites could allow MDM2 to bind p53 and perform its negative regulation by inhibiting the transactivation activity of p53 and exporting p53 from the nucleus. Additionally, Robyn Millott, a fellow lab member, has also been able to show that PP-1cα is able to dephosphorylate Thr18 residue on p53 and has indirect evidence of Ser46 dephosphorylation (Masters Thesis, 2017). Despite this, PP-1c has been shown to not bind directly to p53 [82, 138].
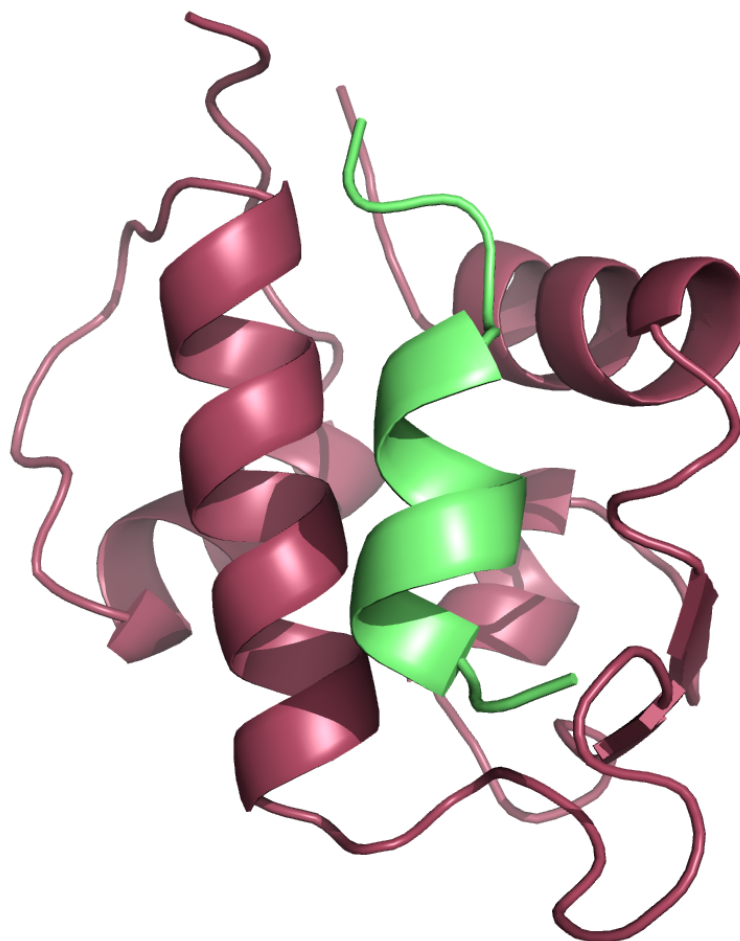
Figure 1.13: **The Three-Dimensional Crystal Structure of the N-terminal of MDM2 Bound to the Transactivation Domain of p53**. The N-terminus of MDM2 (residues 12-126, shown in raspberry) is bound to the unphosphorylated transactivation domain of p53 (residues 25-29, shown in lime). This figure was produced with *PyMOL*. [PDB 1YCR] [77].

1.7.2   Regulation of p53 by the Apoptotic Stimulating Proteins of p53

As mentioned earlier in Section 1.6, the ASPP family has an important role in the regulation of p53 activity. Studies of ASPP1/2 have extensively shown that they promote the pro-apoptotic activity of p53 [130], while the inhibitory member, iASPP, prevents p53 transcriptional activation [7]. The DNA-binding domain is both a highly conserved and highly mutated region of p53 and ASPP1, ASPP2, and iASPP directly bind it via their Ank repeats and SH3 domains [8, 130, 143]. These regions of the ASPP2 C-terminus were confirmed to bind the DNA-binding domain in the 1996 crystal structure (Figure 1.11) [45]. It has been suggested that the ASPP proteins may function by binding and changing the p53 conformation, so that p53 may better bind DNA. Due to their similarity in structure, ASPP1/2 likely compete for binding of p53 with iASPP [143]. But, only iASPP has demonstrated preferential binding to the proline-rich region of p53 over the DNA-binding domain and it has been proposed to be part of the reason of why iASPP may inhibit p53 activity and ASPP1/2 do not. Although, the complete reason why ASPP1/2 are p53 stimulators and iASPP is an inactivator is still unclear [8].

1.7.3   PP-1c, iASPP, and p53 Form a Multimeric Binding Complex

Until recently, it remained very unclear how PP-1c and the ASPP family members were responsible for p53 regulation, until it was proposed that perhaps these three proteins formed a mulitmeric complex with one another. In a recent study, Skene-Arnold *et. al.* were able to show evidence of this complex via gel filtration experiment and demonstrated that PP-1cα, iASPP, and p53 form a protein binding complex in solution [138]. The formation of this binding complex would allow PP-1c to be in proximity of p53, resuling in p53 dephosphorylation and further explain how the ASPP family is able to regulate p53 activity. Recent unpublished work by lab member Robyn Millott, demonstrated that the formation of this multimeric complex leads to increased dephosphorylation of Ser15, Ser37, and Thr18. This suggests that this protein complex

does promote p53 dephosphorylation by PP-1cα. This complex would further explain how both PP-1c and iASPP regulate the pro-apoptotic activity of p53, which was poorly understood.

1.8 Therapeutic Drugs that are Known Protein-Protein Antagonists

Drug discovery can be a very difficult process and attempting to find small molecules that are specific, potent, and cell permeable are just some of the challenges. To treat disease, many therapeutic drugs attempt to target the function of misregulated proteins. This is largely done by preventing proteins from being localized to their functional area of the cell, inhibiting their mode of action or that of a down-stream target. These types of drugs are often small peptides that tend to be expensive and difficult to make cell permeable. As well, targeting the activity of enzymes tend to be problematic because it may inhibit the entire function of the enzyme and can be difficult to make the drug specific.

Antagonizing protein-protein interaction is a new promising method for drug design, but can also be particularly challenging. Typically proteins have large surface areas of interaction and preventing this binding with a small molecule, often less than 500 Da, can be difficult. As well, there are very few crystal structures of protein binding complexes. Less than 0.5 % of the PDB submissions are of protein-protein complexes [119]. If these key binding interactions between proteins remain unknown, it can be difficult to know where to target your small molecule. Therefore, there are few protein-protein antagonists currently on the market. But, despite the difficulties, this mechanism of drug action can be very rewarding. The inhibition of misregulated proteins by targeting their binding partners, increases the likelihood of only affecting a single activity of the misregulated protein, rather than attenuating all of a targets proteins activity. As well, if the key interaction sites between the proteins are well-understood, this allows for even more specific targeting. In other words, a small molecule that antagonizes the binding of

31

a target protein and its regulator at key interaction sites can increase a drugs specificity, while remaining small enough to potentially be cell permeable.

One prominent example of a class of FDA-approved drugs that are designed to disrupt protein complexes are the Nutlins. First identified in 2004, the Nutlin class of small molecule, specifically Nutlin-3, a synthetic cis-imidazoline molecule, were selected for their ability to prevent the p53•MDM2 binding complex analyzed by surface plasmon resonance at the nM range. The same study also show inhibition of tumour growth in mice treated with the MDM2 antagonist [149].

Also, Lenalidomide and Venetroclax are both examples of protein-protein disruptors that are FDA approved. Lenalidomide is a drug approved in 2006 based on its ability to treat haematological malignancies, but its specific function was only discovered in 2012. It was found to target the E3 ligase cereblon that lead to the disruption of cereblon binding to the DNA damage binding protein-1 [87].

Venetroclax is an anti-tumour drug approved for use by the FDA in 2016. Venetroclax was identified by NMR-based compound discovery to bind to the B-cell lymphoma 2 family members, Bcl-2-associated X protein and Bcl-2 homologous killer. This disruptor prevents complex formation with BH3 proteins and the subsequent anti-apoptotic activity [122]. The discovery of this type of drug is at the forefront of the field.

1.9 Marine Organisms as a Source of Potential Novel Therapeutic Compounds

Currently MarinLit, a database for marine natural products, has over 30,000 published articles on the structures and activities of the small molecules currently known [101]. In 2015 alone, there were 1340 novel marine compounds identified [10]. The ocean covers over 70 % percent of the Earth's surface and has proven to be an immense source of bioactive compounds much more diverse than those seen in plants or animals. Now, more than ever, we have better access to this resource due to technological advance-

ments, in SCUBA and deep sea diving [41].

These bioactive compounds are produced by marine organisms largely for chemical defence and chemical signalling, as a result of being unable to move from one location to another or have a proper immune system like animals [9]. As well, some of this diversity stems from the ability to incorporate a different range of elements (eg. bromine) that terrestrial compounds cannot [47]. Additionally, many marine organism co-exist with epibiotic organisms that also produce an array of bacterial metabolites creating a secondary source of natural compounds and diversity. These bacterial organisms tend to be easier to culture in a lab than compared to marine sponges [73].

Many marine compounds discovered have demonstrated a range of therapeutic functions, including antiviral, antitumour, antidiabetic, and antifungal properties [9, 117, 131]. These compounds have great potential as novel therapeutic drugs because they have a structural uniqueness that is difficult to obtain through synthetic peptide development. Currently, over 60 % of new anti-cancer drugs are naturally derived [98]. Several examples include Cytarabine, approved by the FDA in 1969 to treat leukaemia, Trabectedin, an anti-neoplastic drug approved by the FDA in 2015, and Eribulin mesylate, approved by the FDA in 2010 to treat advance stages of breast cancer [83]. These advances prove that the marine organisms are a fantastic source of novel bioactive compounds for anyone with the resources to search for them.

1.10 iASPP•PP-1cα Disruptors Found in Marine Extracts by Dr. Tamara Arnold

Sokotrasterol Sulfate that was first identified as an iASPP•PP-1c by Dr. Tamara Arnold in marine extract PNG08-035 (Papa New Guinea, year 2008, marine extract number 35) via an assay-guided purification in collaboration with the Dr. Ray Anderson lab at UBC similar to the one discussed in Section 2.7 [3]. The fractionation process (shown in Figure 1.15) was modified from her thesis and the compound was identified

in fraction BuOH-C [3]. Sokotrasterol Sulfate is a sterol compound with sulfate groups at C-2, C-3 and C-6, as well as, a 10-carbon aliphatic side chain with an unsaturated double bond at position C-17 (Figure 1.14).

It was first discovered near the coast of Sokotra Island, in 1983, in the sponge *Halichondriiae sponge* by Makarieve *et. al.* who determined its structure through NMR analysis [97]. The authors selected Sokotrasterol Sulfate because of its moderate cytotoxic properties and was discovered to have a novel sterol side chain that contains two extra methyl groups at C-26 and one additional methyl group at C-25 [97]. Years later, Sokotrasterol Sulfate was rediscovered by Dr. Rob va Soest in the marine sponge *Topsentia ophirhaphidites* collected off the coast of Prince Rupert Bay in the Commonwealth of Dominica, in 1997. They were searching for small molecules with the ability to stimulate blood vessel growth as a therapeutic for ischemia. Sokotrasterol Sulfate was found to promote endothelial sprouting both *in vitro* and *in vivo*. The authors were also able to show that while partially sulfated Sokotrasterol Sulfate maintained its ability to promote neovascularization, the desulfated steroid cannot. Further, evidence shows that Sokotrasterol Sulfate interacts with proteins associated with angiogenesis [67, 118].

Suvanine was the second marine natural compound identified that disrupts iASPP•PP-1cα binding by Dr. Tamara Arnold. The modified figure, Figure 1.17, represents the fractionation of Suvanine [3]. Marine extract PNG08-039 first underwent solvent partitioning and Suvanine was located in fractions EtOAc-C and EtOAc-D via the iASPP•PP-1cα disruption assay. The structure of Suvanine is shown in Figure 1.16 and is a sesterterpene compound due to its 25 carbons and 5 isoprene units. The C-3 of the furan ring is attached via a propyl group to the C-14 of the tetradecahydrophenanthrene. Although it is a steroid-like structure, the tetradecahydrophenanthrene lacks the 4th and only 5-membered ring. The ringed group of Suvanine also includes two methyl groups at C-4, as well as, a methyl group at both C-8 and C-10. Lastly, Suvanine also has a single sulfate group that is bound to C-13 through a methylene group.

The sponge *Cosinoderma sponge* has been widely studied as source of bioactive sulfated terpenoids. Maine *et. al.* determined the sponge produced Suvanine in 1983 and

identified its sulfated sesterterpene structure in 1988 [99]. Since then, Suvanine has been determined to have a multitude of activities including, anti-inflammatory [103], antibacterial against Gram-negative/positive bacteria [4], antiviral activity against the Hepatitis C virus [38], inhibitory activity against enzymes including serine proteases (thrombin, trypsin, and non structural protein 3 helicase) [38, 71], isocitrate lyase, $Na+/K+$-ATPase [4], acetyl cholinesterase [99], and cytotoxicity against numerous cancer cell lines, such as, colon, lung, leukemia, stomach, and prostate [4, 70, 78]. Furthermore, a study of cell interactome identificatied Heat Shock Protein 60 as a major cellular target of Suvanine, which is involved in anti-inflammatory response [18].
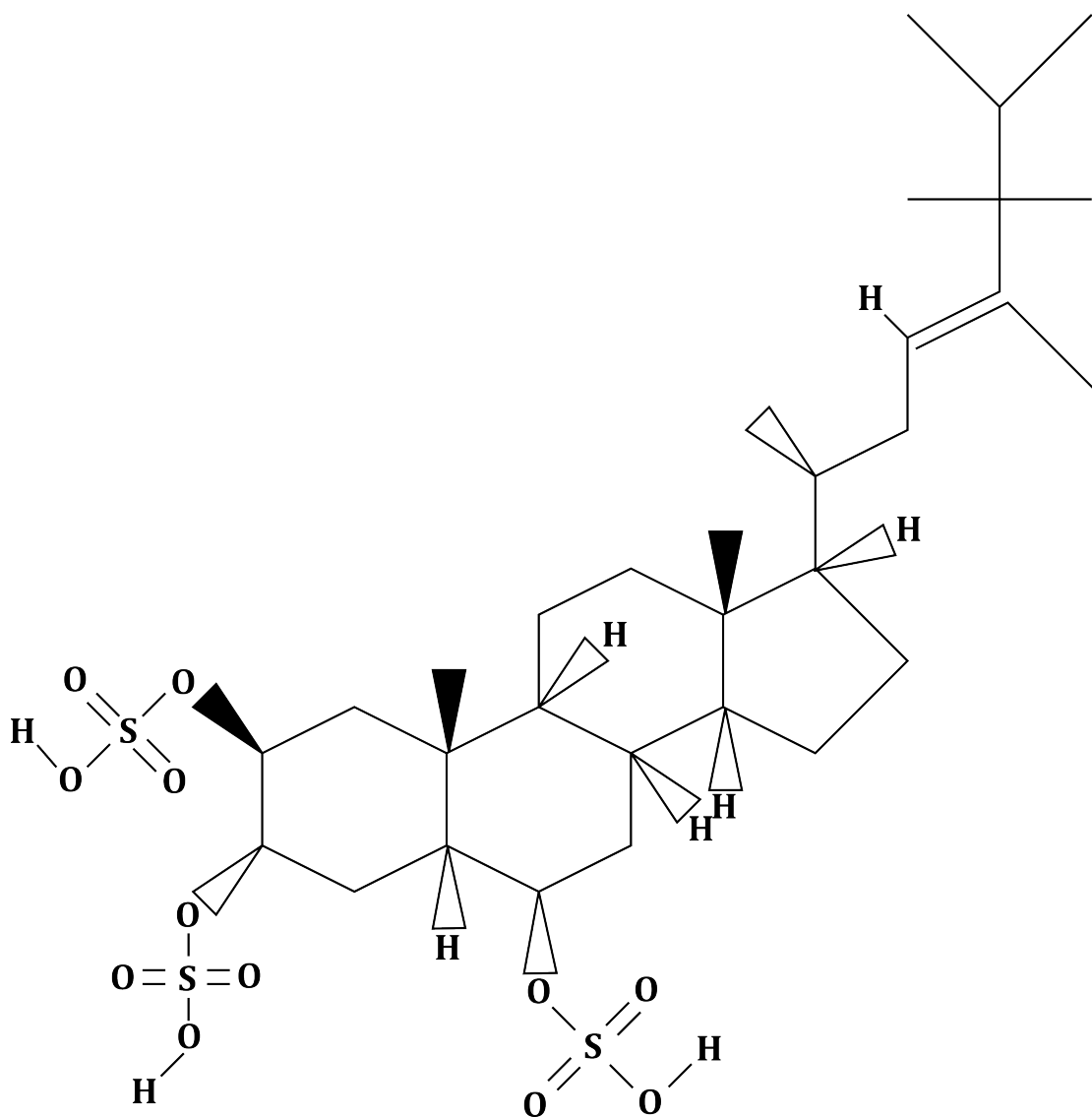
Figure 1.14: **The Chemical Structure of Sokotrasterol Sulfate (Marine Extract PNG08-035).** Sokotrasterol Sulfate is a trisulfated sterol with a long aliphatic chain at position 17 [124].
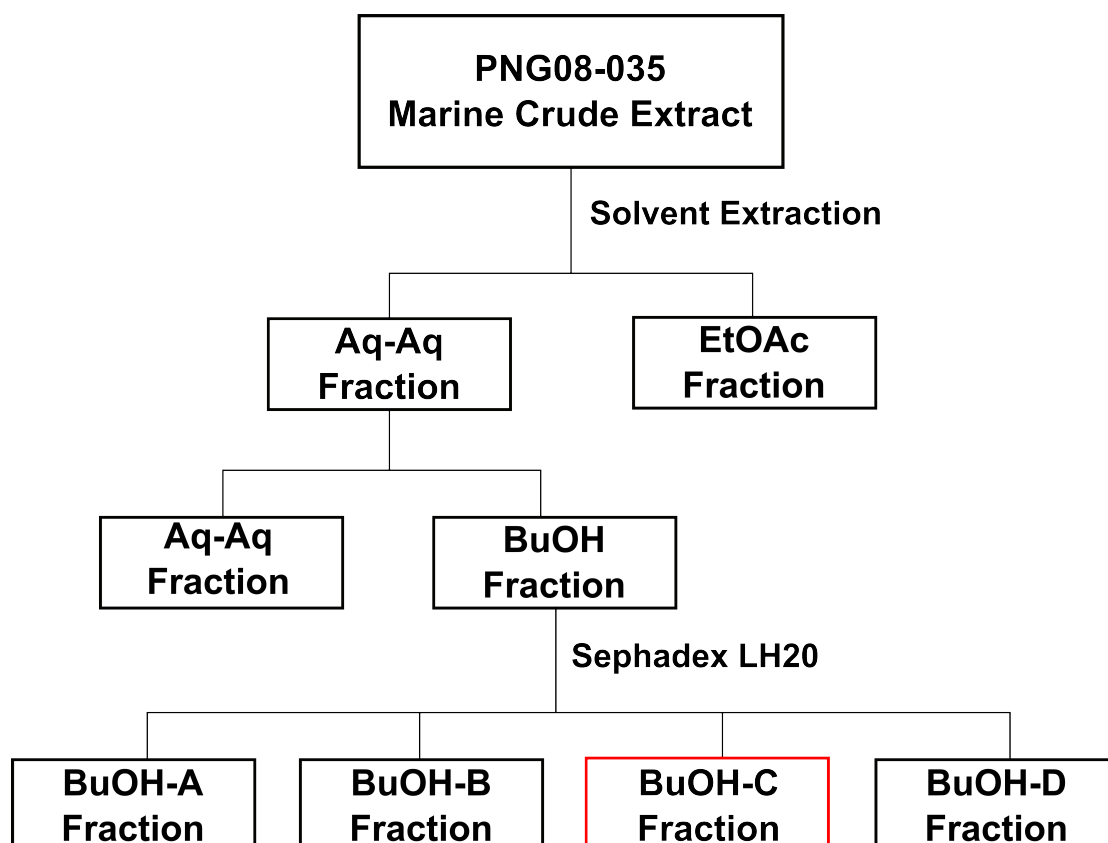
Figure 1.15: **Fractionation of Marine Extract PNG08-035.** The solvent and size fractionation of marine extract PNG08-035 that lead to the identification of the compound, Sokotrasterol Sulfate. The red box indicates the fraction that Sokotrasterol Sulfate was identified within, namely BuOH-C. *Modified from the PhD thesis of Dr. Tamara Arnold* [3].
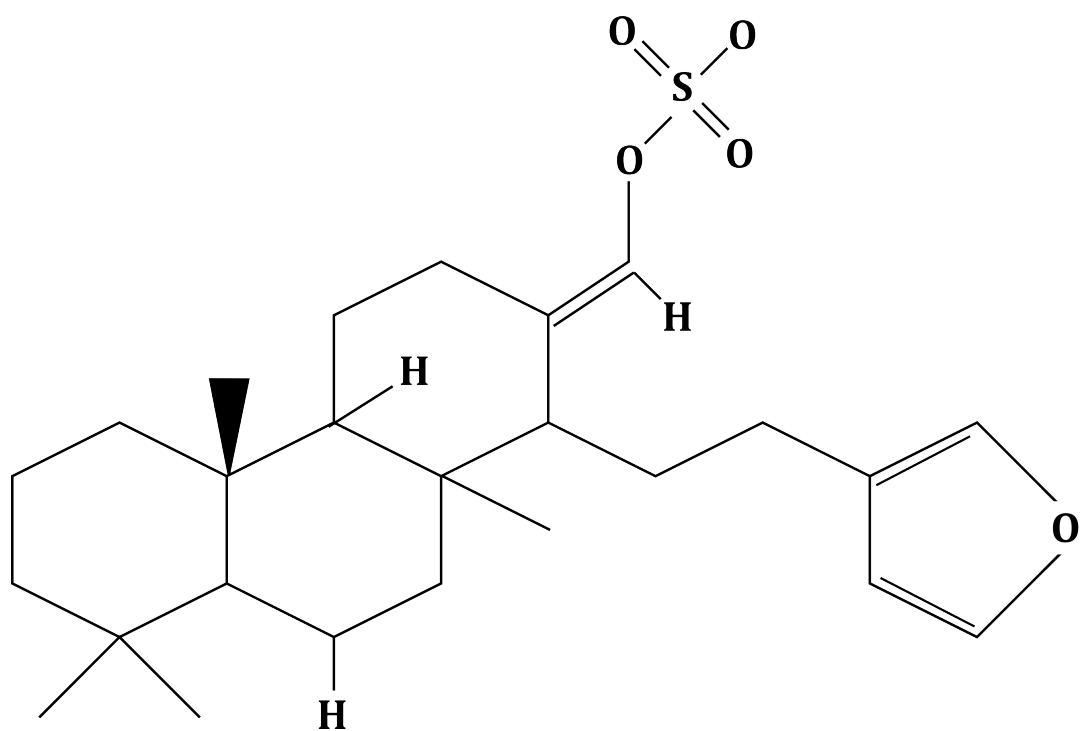
Figure 1.16: **The Chemical Structure of Suvanine (Marine Extract PNG08-039).** Suvanine is a sesterterpene and contains a furan ring attached to an alkyl chain. There is also one sulfate group present attached to C-13.
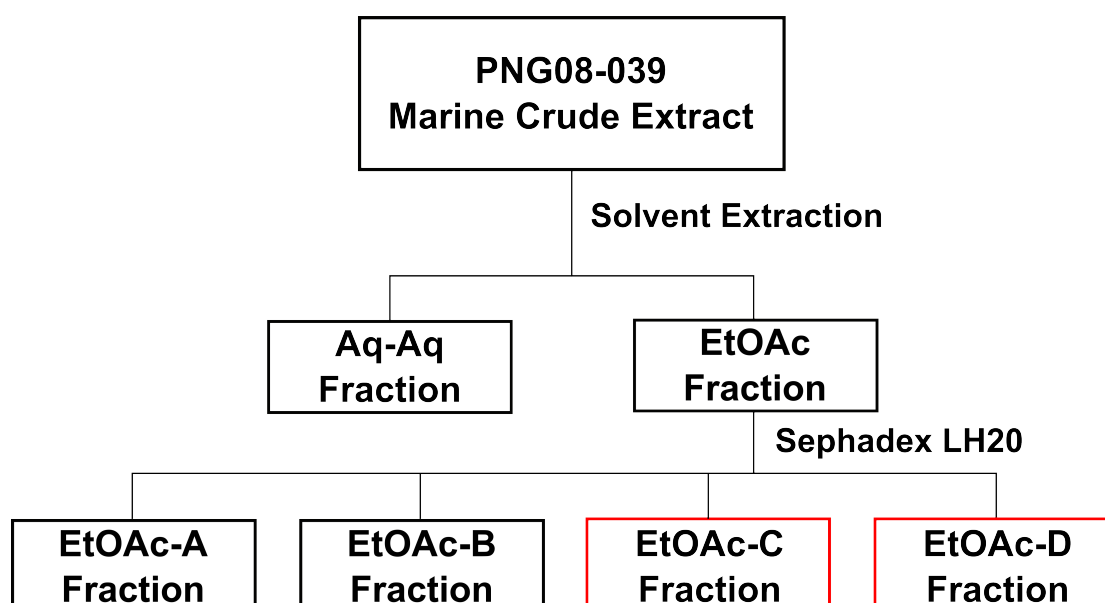
Figure 1.17: **Fractionation of Marine Extract PNG08-039.** The solvent and size fractionation marine extract PNG08-039 lead to the identification of the compound, Suvanine. The red boxes indicate the fractions that Suvanine was identified within, namely EtOAc-C and EtOAc-D. *Modified from the PhD thesis of Dr. Tamara Arnold* [3].

1.11 The Aims of the Thesis Project

With regards to cell regulation and druggable targets, the role of protein kinases have been extensively studied and well-established, but roles of the protein phosphatases have been vastly overlooked. In recent years, we have become increasingly aware that not only are protein kinases specific cell cycle regulators and targetable for anti-cancer drugs, but so are protein phosphatases and their regulatory subunits [135]. Based on our current knowledge, summarized above, I believe that the PP-1c$\alpha\bullet$iASPP binding complex is an excellent and druggable target for novel anti-cancer drugs.

It has been established that PP-1c dephosphorylates the key regulatory sites of p53, Ser15 and Ser37 [82]. When these sites are dephosphorylated, the E3 ubiquitin ligase, MDM2, can bind and target p53 for degradation, ultimately, leading to decrease p53 levels and inhibition of apoptosis [40]. The dephosphorylation of p53 by PP-1c is increased in the presence of its regulatory subunit, iASPP (Robyn Millott, Masters Thesis, 2017). iASPP levels are often up-regulated in many forms of cancer [161], which would result in the over-formation of the iASPP$\bullet$PP-1c$\bullet$p53 multimeric complex and increase inhibition of the pro-apoptotic activity of p53 (Figure 1.18). The iASPP$\bullet$PP-1cα binding interactions have been well characterized making it easier to target. iASPP binds PP-1cα via its SH3 domain and non-canonical RVxF motif, RARL [138].

My central hypothesis is that the PP-1c$\alpha\bullet$iASPP binding interaction could be targeted with small molecules, in order to prevent the dephosphorylation of p53 by PP-1c and allow p53 to remain active. Secondly, these small molecules could be potential novel anti-cancer drugs. As discussed in Section 1.9, the ocean is an excellent source of vast array novel small molecules. I propose that this source could be used for the discovery of a potentially valuable source of protein-protein disruptors.

Throughout my thesis project I have aimed to answer the following major questions on the role of the PP-1c$\alpha\bullet$iASPP$\bullet$p53 protein complex and its role on p53 regulation. Is it possible to for a small molecule to specifically inhibit the iASPP$\bullet$PP-1cα binding? Will the disruption of iASPP to PP-1cα impact the dephosphorylation of p53?
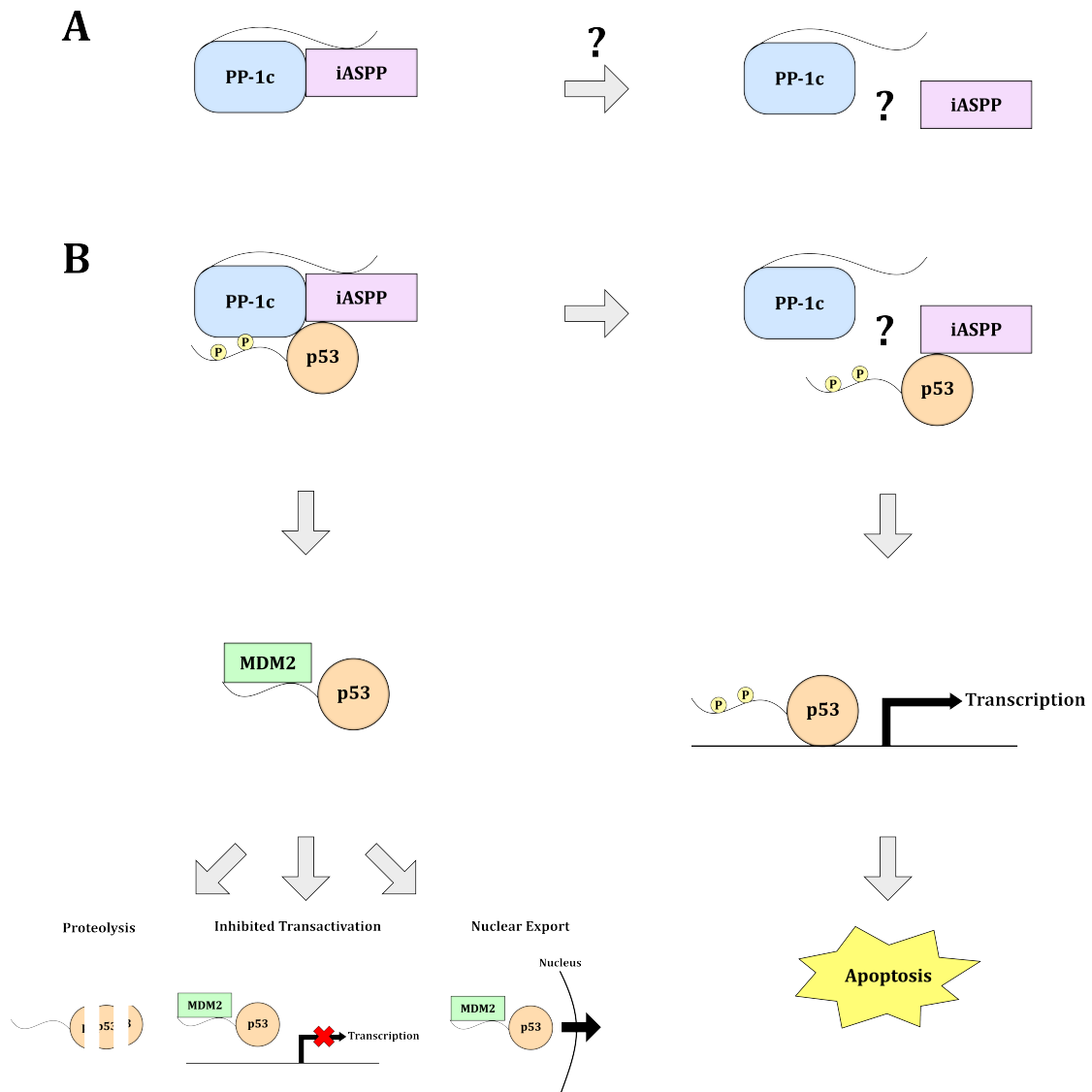
Figure 1.18: **The Potential Targeted Disruption of the iASPP•PP-1c Binding Complex and Aims to be Investigated during this Thesis Project.** (A) The activity of PP-1c is, in part, regulated by its regulatory subunit, iASPP. Can the binding of PP-1c and iASPP be targeted and disrupted? (B) The activity of p53 is in part regulated by its phosphorylation state. When dephosphorylated at key sites, the negative regulator of p53, MDM2 can bind p53. This interaction can lead to p53 inactivation in a few ways: proteolysis of p53, inhibition of the transactivation activity of p53, and exportation of p53 from the nucleus. Can disruption of iASPP and PP-1c binding prevent the formation of the mutlimeric complex between iASPP, PP-1c and p53? Will prevention of iASPP and PP-1c binding affect p53 dephosphorylation by PP-1c?

41

Chapter 2

Materials and Methods

2.1 Materials

ASPP2$_{905\text{-}1128}$ (0.4 mg/mL) and p53$_{2\text{-}293}$ (0.123 mg/mL) were supplied by Robyn Millott, a Masters student in the Holmes Lab. Marine extracts were supplied by Dr. Ray Andersen, Dr. David Williams, and Kalindi Morgan at the University of British Columbia. All other chemical and reagents were supplied by Sigma and Fisher unless otherwise stated.

2.2 Expression and Purification of Protein Phosphatase-1c Isoforms

Human PP-1cα and PP-1cγ were both prepared with the same method unless otherwise indicated. *Escherichia coli (E. coli)* DH5α cells prepared by Dr. Tamara Arnold [3] containing plasmid that has full length PP-1c and Ampicillin (Amp) resistance were plated onto 200 μg/mL Amp plates and incubated overnight at 37 °C. A single colony was used to inoculate into 400 mL of Luria Bertani (LB) media containing 200 μg/mL ampicillin (Amp) and 1 mM manganese (II) chloride (MnCl$_2$). The culture was incubated overnight at 37 °C with shaking and was then subcultured into 4L of LB media

containing 200 μg/mL Amp, 1 mM $MnCl_2$, and 0.01 % Vitamin B_1. Cultures were then incubated at 37 °C with shaking until the optical density at 600 nm (OD_{600}) was greater than 0.400 for PP-1cα or 0.600 for PP-1cγ. PP-1c expression was induced by the addition of isopropyl β-D-1-thiogalactopyranoside (IPTG, 0.3 mM for PP-1cα and 0.5 mM for PP-1cγ) and the culture was incubated overnight, with shaking, at 28 °C. Cells were collected by centrifugation at 6,000 g for 18 mins at 4 °C and the cell pellet was frozen at -80 °C until needed.

The frozen cell pellets were thawed and then dissolved in Buffer A (5 mM imidazole pH 7.5, 50 μM ethylenediaminetetraacetic acid (EDTA), 10 % glycerol, 0.5 M ethylene glycol-bis(β-aminoethyl ether)-N,N,N',N'-tetraacetic acid (EGTA), 100 mM sodium chloride (NaCl), 2 mM $MnCl_2$, 3 mM dithiothreitol (DTT), 2 mM benazmidine, and 0.4 mM phenylmethane sulfonyl fluoride (PMSF)) containing 2 protease SigmaFast tablets (2 mM 4-(2-aminoethyl)benzensulfonyl (ABESF), 0.3 μM Aprotinin, 130 μM Bestatin, 1 mM EDTA, 14 μM E-64, and 1 μM Leupeptin) and 2 μg/μL DNase A. Cells were then lysed with three passes through an Emulsiflex-C3 high-pressure homogenizer (Avestin). The lysate was centrifuged (Beckman GS-15R) at 13,000 g for 45 mins at 4 °C and the supernatant was loaded onto the Heparin-Sepharose CL-6B Column (GE Healthcare) via a superloop on a fast protein liquid chromatography (FPLC) instrument. PP-1c was eluted using a 400 mL gradient of 100 mM NaCl to 500 mM NaCl Buffer A, collecting 5 mL fractions. Fractions were analyzed by pNPP phosphatase activity (described in Section 2.4) and 12 % sodium dodecyl sulfate polyacrylamide gel electrophoresis (SDS-PAGE) monitoring for PP-1c. The fractions that contained the most PP-1c were identified and pooled together.

The pool was loaded onto the Human Inhibitor-2 (HI_2) column in Buffer B (5 mM imidazole pH 7.5, 50 μM EDTA, 20 % glycerol, 2 mM $MnCl_2$, 2 mM DTT, and 0.5 mM PMSF) via a superloop and PP-1c was eluted with a step-wise gradient of Buffer B containing 200 mM NaCl and Buffer B containing 1 M NaCl, collecting 2 mL fractions (60 mL each step in PP-1cα prep and 40 mL and 30 mL, respectively, in γ prep). Fractions were again analyzed by the pNPP assay and 12 % SDS-PAGE. The fractions containing

the most PP-1c were pooled together. Pools of PP-1c were concentrated in a 10 kDa (PP-1cα) or 30 kDa (PP-1cγ) cut-off Millipore tube by centrifugation at 4,000 g and exchanging the buffer to Buffer B containing 750 mM NaCl. PP-1cα was concentrated to 0.3-0.43 mg/mL (after addition of 50 % glycerol). PP-1cγ was concentrated to 0.2-1.0 mg/mL (after glycerol addition) (total 3.1 mg). The concentrated PP-1c was stored in 50 % glycerol and at -20 °C.

2.3   Expression and Purification of TGF-beta Inhibited Membrane-Associated Protein

Full length bovine TGF-β-inhibited membrane-associated protein (TIMAP) that was N-terminally linked with glutathione S-transferase (GST) affinity tag system was cloned into a pGEX-4T3 vector ampicillin resistant that was provided by Micheal Shopik. This vector was transformed into DH5α cells [137]. The cells were plated on 200 μg/mL AMP/34 μg/mL Chloramphenicol (Cam) plates and grown overnight at 37 °C. A single colony was used to inoculate 100 mL of LB media containing 200 μg/mL Amp and 34 μg/mL Cam and grown overnight with shaking, at 37 °C. The cell culture (20 mL) was subcultured into 2 L of LB media containing 200 μg/mL Amp and 34 μg/mL and grown at 37 °C with shaking until the OD$_{600}$ reached over 0.700. Expression was induced with 0.1 mM IPTG at 18 °C for 7 hrs. The cells were collected by centrifugation at 4,000 g for 25 mins at 4 °C. The pellets were frozen at -80 °C overnight.

The pellets were resuspended in 5 mL per g of cells of Buffer C (50 mM 4-(2-hydroxyethyl)-1-piperazineethanesulfonic acid (HEPES) pH 7.5, 5 mM EDTA, 5 mM EGTA, 2 mM Benzamidine, 1 mM PMSF, and 1 mM DTT) containing one protease SigmaFast tablet and 10 μg/μL DNase A. The cells were lysed with three passes through an Emulisflex-C3 high-pressure homogenizer at 2,000 psi and the lysate was centrifuged at 13,700 xg for 45 mins at 4 °C. The supernatant was combined with 5 mL of Gluathione Sepharose 4B (GS, GE Healthcare) in a column and incubated for 90 mins, end over end, at 4 °C with Buffer C. The beads are washed four times with 50 mL of Buffer D (50

mM HEPES pH 7.5, 5 mM EDTA, 5 mM EGTA, 1 mM DTT). TIMAP was eluted with 6 loads of 10 mL of Buffer E (50 mM Tris-HCl pH 8.0 and 30 mM reduced glutathione), collecting 1 mL fractions. The fractions were analyzed by 10 % SDS-PAGE and the fractions containing the most TIMAP were pooled together. The pooled protein was concentrated by centrifugation at 4,500 g with 50 KDa cut-off Millipore tubes and the buffer was exchanged for the Buffer F (50 mM Tris-HCl pH 7.5, 100 mM NaCl, and 1 mM DTT). TIMAP was concentrated to 0.24 mg/mL (after glycerol added, $\sim$ 4 mL total). Gel digests were performed with mass spectrometry identification (by Fahlman Lab, University of Alberta) to confirm TIMAP presence. Concentrated TIMAP was stored in a 50 % glycerol solution and at -2 °C.

2.4 Para-Nitrophenol Phosphatase Assay

The pNPP assay measures the activity of PP-1c by measuring the conversion of para-nitrophenyl phosphate (pNPP) to para-nitrophenol. Para-nitrophenyl phosphate is a colourless compound that, when dephosphorylated by PP-1c, becomes yellow. The activity of PP-1c can be quantified by measuring the absorbance at 405 nm, which measures the yellow wavelength. PP-1cα and marine extract/compound were incubated in Buffer G (50 mM Tris-Base pH 8.3, 0.1 mM EDTA, 34 mM magnesium chloride, 1 mg/mL bovine serum albumin (BSA), 0.5 mM MnCl$_2$, and 0.2 % β-mercaptoethanol (BME)) for 10 mins at 37 °C. pNPP (5 μM) was added to each well and the initial absorbance of the plate was measured using a kinetic microplate reader (Molecular Devices) at 405 nm. The plate was then incubated at 37 °C until the absorbance at 405 nm reached between 0.400 and 0.500. The final absorbance at 405 nm (Abs$_{\text{final}}$) of each sample was corrected against the initial absorbance (Abs$_{\text{initial}}$). This value was then standardized against the corrected control absorbance (Abs$_{\text{control}}$) value and was shown as a of percentage of the control. The equation is shown below.

$$Activity = \frac{Abs_{\text{final}} - Abs_{\text{initial}}}{Abs_{\text{control}}} \; x \; 100\% \tag{2.1}$$

2.5   Purification of Microcystin

The stock of unpurified MC collected from Little Beaver Lake, Alberta, was supplied and semi-purified by lab member Ply Pasarj. Crude Microcystin (500 μg) was diluted into 500 μL of Solvent A (0.1 % Trifluoroacetic acid (TFA) in ddH$_2$O) and centrifuged at 14,000 g for 10 mins at 4 °C. The crude Microcystin was analyzed with High Performance Liquid Chromatography (HPLC) (Beckman) by eluting for 5 mins at 100 % Solvent A, followed by an elution gradient of 0 % to 100 % Solvent B (0.1 % TFA in acetonitrile (ACN)) for 80 mins at a flowrate of 1 mL/min (absorbance at 214 nm). The MC was then eluted for an additional 5 mins at 100 % Solvent B and 5 mins at 100 % Solvent A. Fractions (1 mL) were collected throughout the entire elution process. The following fractions were pooled based on the variants of Microcystin eluted: fractions 42-46 (Microcystin-RR), fractions 47-52 (Microcystin-LR), fractions 53-58 (Microcysitn-LA), and fractions 59-61 (Microcystin-LL). Pooled fractions were dried down using a speed vac and stored at -20 °C.

2.6   Preparation of Microcystin-Sepharose

DMSO (5 mL) and 5 N NaOH (2 mL) were combined with ddH$_2$O (8 mL) and purged with N$_2$ gas. A 1 g/mL stock of aminoethanethiol (AET) was made by combining 1g of AET with purged ddH$_2$O. The AET stock was combined with 0.9 mg of Microcystin-LR (0.63 mg/mL), DMSO (2 mL), and 5 N NaOH (0.67 mL) were combined in ddH$_2$O (1.07 mL) and purged. The reaction was heated to 50 °C for 30 mins while purging with N$_2$ gas and the reaction was cooled to room temperature. Glacial acetic acid (6.5 mL) was added to quench the reaction. Solvent A (50 mL) was added and 100 % TFA used to bring the reaction's pH to 1.5 and washed with 10 mL of Solvent C (0.1 % TFA/10 % ACN). Microcystin-LR was eluted with 40 mL of Solvent B in 10 mL loads and 1 mL fractions were collected. The Microcystin-LR fractions were dried down using a SpeedVac (Savant SpeedVac SC100) and stored at -20 °C. Dried down fractions of Microcystin-LR were resuspended into 1.5 mL of Buffer H (50 mM sodium bicarbonate

(NaHCO$_3$) pH 9.2, 50 mM Tris-HCl, pH 8, 0.5 M NaCl, 50 mM sodium acetate (NaOAc) pH 4, and 1 mM HCl).

NHS-Activated Sepharose (NS, 6 mL) was centrifuged (Eppendorf) at 2500 rpm for 5 mins at 4 °C. The NS was then washed four times with 10 mL of 1 mM HCl and then centrifuged at 2,500 rpm for 5 mins at 4 °C. The resuspended Microcystin-LR was combined with the NS and 50 mM NaHCO$_3$ was used to bring the solution to pH 8.5. The solution was incubated end over end, for 4 hrs, at room temperature. The supernatant was removed and 10 mL of 50 mM Tris-HCl was then added to block the reaction. The solution was incubated over night at 4 °C, end over end. The beads were washed by alternating between 10 mL of Buffer I (50 mM Tris-HCl, 50 mM NaOAc, and 0.5 M NaCl) and 10 mL of NaCl with centrifugation for 7 mins, at 3,000 rpm, at 4 °C, five times. Lastly, the beads were washed three times with 20 % EtOH and the Microcystin-Sepharose (MC-S) beads are stored at 4 °C. A successful reaction was verified by analyzing the elution of the supernatant by HPLC. The elution time of the supernatant off the HPLC C-18 reverse-phase column was compared to the elution time of a Microcystin-LR standard to determine if any Microcystin-LR was unbound to the Sepharose and present in the supernatant.

2.7   Microcystin-Sepharose Disruption Assay

For each reaction, 20 μL of Microcystin-Sepharose beads (MC-S) were washed with 25 column volumes of ddH$_2$O and centrifuged at 3,500 rpm for 1.5 mins at room temperature. The MC-S beads were then washed twice with 25 column volumes of Buffer J (50 mM Tris-HCl pH 7.5, 0.1 mM EDTA, 0.5 mM MnCl$_2$, and 0.2 % BME) containing 150 mM NaCl. PP-1cα (2 μg) was added to each reaction and incubated for 1 hr at 4 °C, end over end. The MC-S beads were washed twice with 25 column volumes of Buffer J containing 150 mM NaCl. iASPP$_{608\text{-}828}$ (1 μg) was added to each reaction along with marine extract/compound to the PP-1cα bound MC-S beads and incubated for 1 hr at 4 °C, end over end. Lastly, the MC-S beads were washed four times with

25 column volumes of of Buffer J containing 300 mM NaCl. 1X SDS-PAGE Buffer was added to each sample and boiled for 5 mins at 37 °C. Samples were separated by a 12 % SDS-PAGE and the gel was stained with Coomassie Blue. The cartoon of testing iASPP•PP-1c binding in the presence of marine extract/bioactive compound using the MC-S disruption assay is depicted in Figure 2.1. A new term was developed termed the half maximal disruption concentration (DC_{50}) to establish relative potency between compound in this assay.
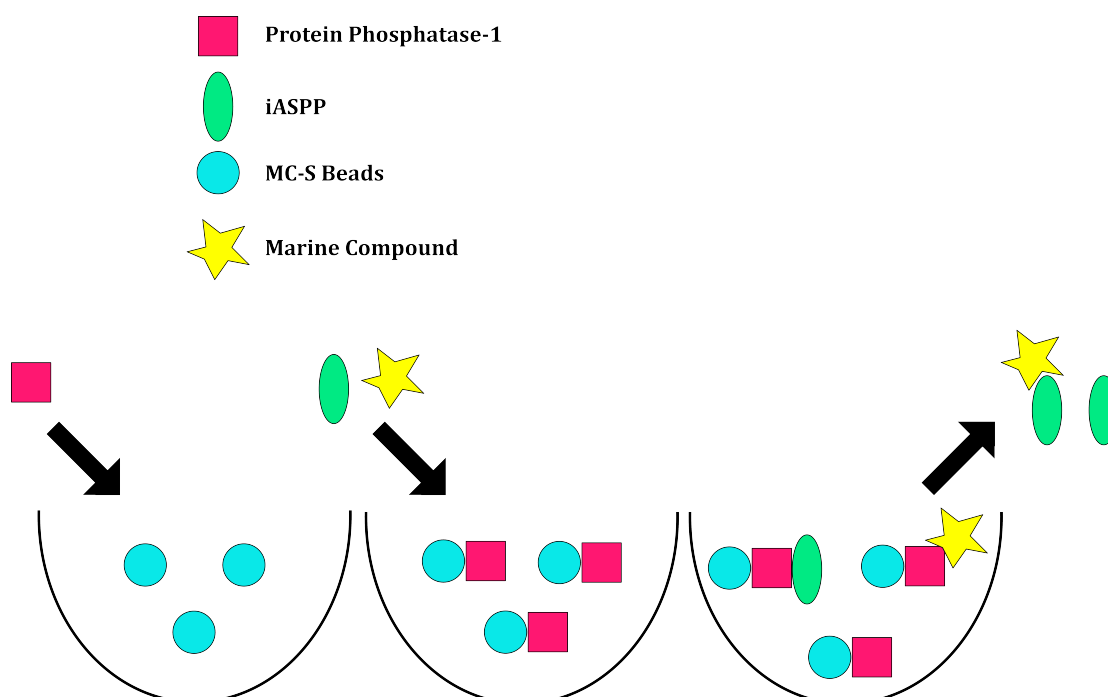
Figure 2.1: **The Cartoon Representation of the Microcystin-Sepharose Disruption Assay.** The Microcystin-Sepharose beads (represented as blue circles) are incubated with PP-1c (represented as red squares). The PP-1c bound Microcystin-Sepharose beads are incubated with iASPP (represented as green ovals) and marine extracts. Anything remaining unbound is then washed out. Marine compounds (represented as yellow stars) can disrupt iASPP and PP-1c binding in two ways: by binding to iASPP or by binding to PP-1c. If the compound does not affect the complex binding that both iASPP and PP-1c will remain bound to the beads.

2.8 Glutathione 4B Sepharose Disruption Assay

Due to the fact that full-length TIMAP bound to too much surface area of PP-1cγ resulted in PP-1cγ to be knocked off the MC-S beads, the proteins in the assay had to be bound in the reverse order compared to the MC-S disruption assay. The regulatory subunit, TIMAP, was first bound to Glutathione 4B Sepharose beads via its GST-tag followed by the binding of PP-1c.

Glutathione-4B Sepharose (GS, 20 μL) beads were washed with 25 column volumes of ddH$_2$O and centrifuged at 3,500 rpm for 1.5 mins at room temperature. The GS beads were washed twice with 25 column volumes of Buffer K (50 mM Tris-HCl, 0.1 mM EDTA, 0.5 mM MnCl$_2$, 0.2 % BME, and 0.1 % Tween) containing 150 mM NaCl. TIMAP (1.5 μg) was added to each reaction and incubated for 1 hr at 4 °C, end over end. The GS beads were washed twice with 25 column volumes of Buffer K containing 150 mM NaCl. PP-1cγ (1 μg) was added to each reaction along with marine extract/compound and was incubated for 1 hr at 4 °C, end over end. Lastly, the GS beads were washed four times with 25 columns of Buffer K containing 300 mM NaCl and 1X SDS-PAGE Buffer is added to each sample. The samples were boiled for 5 mins at 100 °C and loaded onto a 10 % SDS-PAGE and the gel was stained with Coomassie Blue.

2.9 Assay-guided Purification of the Crude Marine Extracts that Disrupt iASPP•PP-1cα Binding

Dr. David Williams from the Dr. Ray Andersen Lab from the University of British Columbia (UBC) aided in the isolation and purification of the compounds of interest through an assay-guided purification process. Crude marine extracts that disrupted the binding of iASPP to PP-1cα underwent the first step in the fractionation process, in which the evaporation-dried crude sample were solvent partitioned by resuspending them in the ethylacetate (EtOAc), followed by solvents of increasing polarity, typically using butanol (BuOH) followed with resuspension in water. At this point, the fractions

were dried down and sent to our lab for biochemical analysis. The samples were resuspended into methanol (MeOH) and were analyzed for disruption of iASPP binding to PP-1cα using the MC-S disruption assay (Section 2.7). After identification of fractions that contained the compound of interest, Dr. David Williams further partitioned the fractions by a Sephadex LH20 column chromatography; a size exclusion column that separates smaller organic compounds. Continual rounds of fractionation and analysis were performed until the compound of interest was purified synthetically for NMR analysis.

2.10 High Performance Liquid Chromatography of Marine Extract PNG11-279

The crude PNG11-279 marine extract was separated via C18 reverse phase column by High Performance Liquid Chromatography (HPLC). The sample (750 μg) was drieddown in an evaporation speed vacuum and resuspended in Solvent A. Chromatography was developed over 80 mins employing a gradient of 0 % to 100 % Solvent B for compound elution (1 mL/min), while collecting fractions (1 mL).

2.11 Dephosphorylation of Serine 15 on p53

The phosphorylation of p53 by DNAPK was set up by adding 1X Kinase Buffer (50 mM Tris-HCl, 10 mM MgCl, 2.2 mM EGTA, 10 mM NaCl, 0.0025 % Tween-20, and 2 mM DTT), together with 0.5 mM ATP, 1 mM $MnCl_2$, 75 mM KCl, 0.01 mg/mL CTDNA, 0.025 mg/mL p53, and 18.75 U/μL DNAPK (Promega). The reactions were incubated for 90 mins in a 30 °C water bath. The phosphorylation reaction was stopped after 90 mins by the addition of 1 mM LY249002 inhibitor and incubation for an additional 10 mins at room temperature.

The dephosphorylation reaction was set-up by pre-incubating PP-1cα (0.5 μg) and

iASPP$_{608\text{-}828}$ (0.5 μg) along with the marine compound, 1X Kinase Buffer, and ASPP Buffer (250 mM Imidazole, 0.5 % Tween-20, 125 mM NaCl, 6 mM NaH$_2$PO$_4$, and 10 mM of Na$_2$HPO$_4$). The samples were then incubated for 30 mins in a 30 °C water bath. The pre-incubation reaction (4.5 μL) was mixed with the phosphorylated p53 (5.5 μL) and were incubated for 30 mins in a 30 °C. The reaction was stopped with the addition of 1X SDS-PAGE Buffer. The samples were spun at 10,000 rpm, for 30 secs, at room temperature and boiled for 5 mins at 100 °C. Samples were loaded onto a 12 % SDS-PAGE.

The proteins were transferred to a nitrocellulose membrane (GE Healthcare) for 45 mins, at 75 V, at 4 °C in Transfer Buffer (25 mM Tris-HCl, 192 mM glycine, 3 μM SDS, and 20 % MeOH). The nitrocellulose membrane was stained with Pierce^{TM} Reversible Colourimetric Stain to visualize the proteins that transferred. The stain was removed with Pierce^{TM} Erase solution and the nitrocellulose membrane was incubated in Blocking Buffer (5 % w/v milk (Carnation)/TBST Buffer (50 mM Tris-HCl pH 7.6, 150 mM NaCl and 0.001 % Tween)) for 90 mins, with shaking, at room temperature. The nitrocellulose membrane was incubated in 1:15,000 Ser15 primary antibody (antibody:Blocking Buffer) containing 0.02 % NaNO$_3$ overnight at 4 °C, with rotation. The nitrocellulose membrane was washed three times in TBST Buffer for 10 mins, with shaking, at room temperature. Then it was incubated in 1:10,000 secondary Anti-mouse IgG (Cellular Signalling Technology) (antibody:Blocking Buffer) for 1 hr with shaking, at room temperature. The nitrocellulose membrane was washed again three times in TBST Buffer for 10 mins with shaking, at 4 °C. The nitrocellulose membrane was developed in 20 % enhanced chemiluminescence (ECL) solution (10 % enhancer solution and 10 % peroxide solution) for 1 min. The nitrocellulose membrane was exposed to film in a dark room for varying times to visualize the amounts of 2 ° antibody present.

Chapter 3

The Isolation and Identification of Compounds in Marine Extracts that Disrupt the Binding of iASPP to PP-1cα

3.1 Identification of Marine Extracts that Disrupt the Binding of iASPP$_{608\text{-}828}$ to PP-1cα

One of the objectives of this thesis project was to identify marine extracts that contain compounds that disrupt the iASPP•PP-1cα binding complex. The complex is a potential, druggable target due to the fact that the binding of iASPP to PP-1c is required for the regulation of p53 activity by PP-1c. Unpublished data by Robyn Millott, a fellow lab member, has demonstrated that *in vitro* there is increased dephosphorylation of p53 by PP-1c at key regulatory sites when iASPP is present. As well, the iASPP•PP-1cα binding interaction has been well-characterized making it easier to target [138]. Additionally, iASPP is vastly over-expressed in many cancers that have wild-type p53 [161].

The over-expression of iASPP leads to decreased p53 pro-apoptotic activity; therefore, targeting iASPP function with anti-cancer drugs has the potential to be very effective. Marine organisms make an excellent source of potential PP-1c$\alpha \bullet$iASPP antagonists. They contain a vast array of novel bioactive compounds that have been demonstrated numerous therapeutic effects. Thus, marine extracts collected by our collaborators in the Dr. Ray Andersen Lab at the University of British Columbia (UBC) were analyzed to identify compounds that disrupt the PP-1c$\bullet$iASPP binding complex.

3.1.1 Identification of Marine Extracts that Disrupt the iASPP$\bullet$PP-1cα Complex

A total of 73 marine extracts were analyzed for the ability to disrupt the iASPP$_{608\text{-}828}\bullet$PP-1cα binding complex via the MC-S disruption assay described in Section 2.7 and the results are shown in Figures 3.1 to 3.6. PP-1cα was first bound to the MC-S via the PP-1c active site. Microcystin binds to PP-1c at the two metal ions within its the active and at the hydrophobic groove. This gives iASPP$_{608\text{-}828}$ access to bind the RVxF-hydrophobic binding pocket located 20 $\mathring{A}$ away and the PxxP binding motif of PP-1c. The binding of iASPP$_{608\text{-}828}\bullet$PP-1cα in the presence of the marine extracts was interpreted from the amount of protein visualized on the corresponding SDS-PAGE. Decreased amounts of iASPP, relative to the amounts in the positive control and PP-1cα present, was indicative that the marine extract was able to prevent iASPP$_{608\text{-}828}$ from binding PP-1cα. Seven marine extracts were identified to antagonize iASPP$_{608\text{-}828}$ binding to PP-1cα and are listed in Table 3.1.
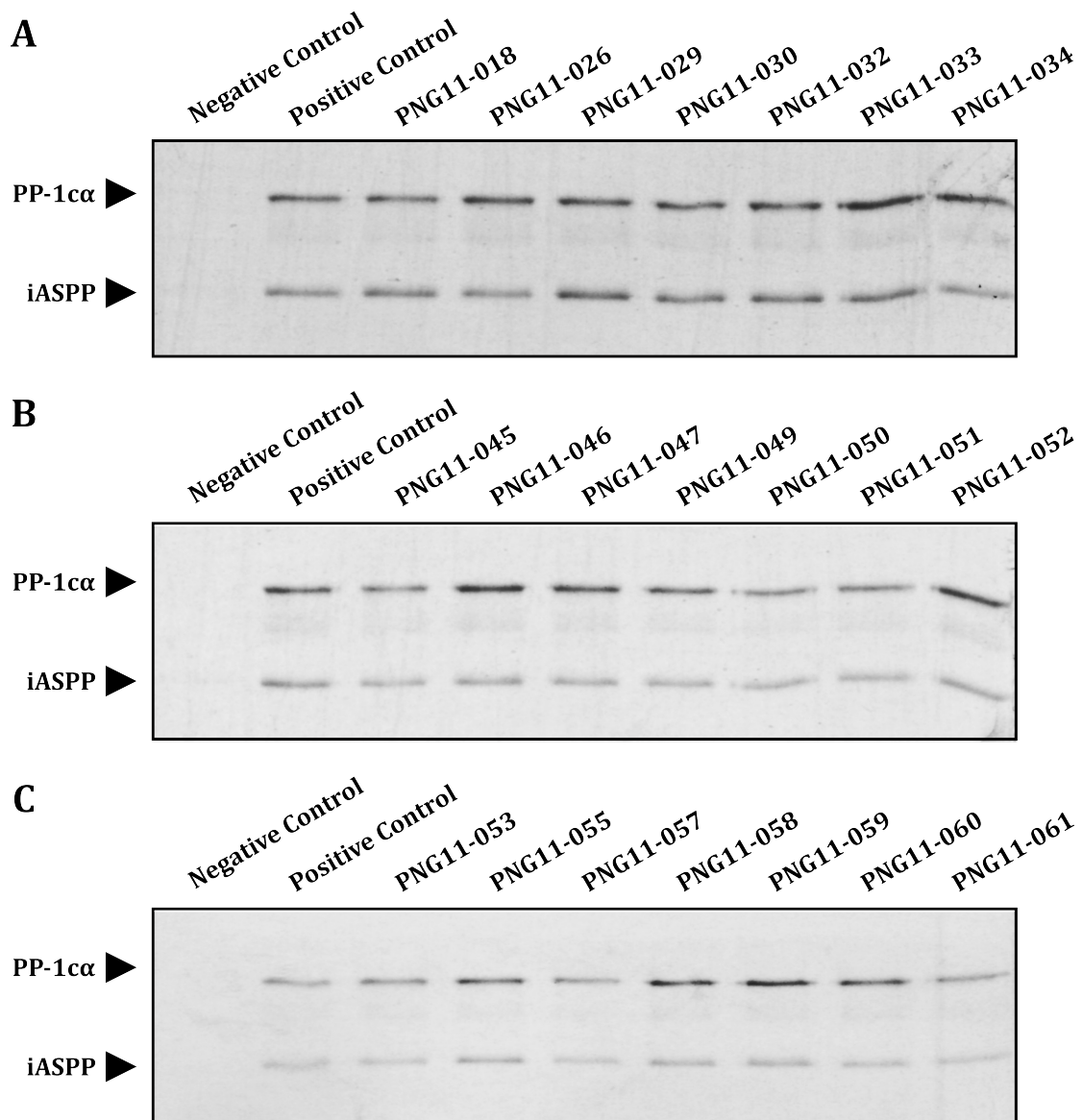
Figure 3.1: **Marine Extracts PNG11-018 to PNG11-061 do not Effect PP-1cα•iASPP$_{608\text{-}828}$ Binding.** MC-S (20 μL) was first washed with 25 column volumes of ddH$_2$O and centrifuged at 3,500 rpm for 1.5 mins at room temperature. The beads were then washed twice with 25 column volumes of Buffer J + 150 mM NaCl. PP-1cα (2 μg) was incubated with the MC-S for 1 hr at 4 °C, end over end and the beads were washed twice with 25 column volumes of Buffer J + 150 mM NaCl. iASPP$_{608\text{-}828}$ (1 μg) and marine extracts (100 μg) were incubated with the PP-1cα-bound MC-S for 1 hr at 4 °C, end over end. The beads were washed four times with 25 column volumes of Buffer J + 300 mM NaCl. 1X SDS-PAGE Buffer was added to each sample and boiled for 5 mins at 100 °C. Samples were separated by a 12 % SDS-PAGE and stained with Coomassie Blue. Each assay was carried out in duplicate with a representative figure is shown above.

Figure 3.2: **Marine Extracts PNG11-062 to PNG11-187 do not Effect PP-1c$\alpha\bullet$iASPP$_{608\text{-}828}$ Binding.** MC-S (20 μL) was first washed with 25 column volumes of ddH$_2$O and centrifuged at 3,500 rpm for 1.5 mins at room temperature. The beads were then washed twice with 25 column volumes of Buffer J + 150 mM NaCl. PP-1cα (2 μg) was incubated with the MC-S for 1 hr at 4 °C, end over end and the beads were washed twice with 25 column volumes of Buffer J + 150 mM NaCl. iASPP$_{608\text{-}828}$ (1 μg) and marine extracts (100 μg) were incubated with the PP-1cα-bound MC-S for 1 hr at 4 °C, end over end. The beads were washed four times with 25 column volumes of Buffer J + 300 mM NaCl. 1X SDS-PAGE Buffer was added to each sample and boiled for 5 mins at 100 °C. Samples were separated by a 12 % SDS-PAGE and stained with Coomassie Blue. Each assay was carried out in duplicate with a representative figure is shown above.

Figure 3.3: **Marine Extracts PNG11-190, PNG11-192, PNG11-215, and PNG11-221 Disrupt PP-1c$\alpha \bullet$iASPP$_{608\text{-}828}$ Binding.** MC-S (20 μL) was first washed with 25 column volumes of ddH$_2$O and centrifuged at 3,500 rpm for 1.5 mins at room temperature. The beads were then washed twice with 25 column volumes of Buffer J + 150 mM NaCl. PP-1cα (2 μg) was incubated with the MC-S for 1 hr at 4 °C, end over end and the beads were washed twice with 25 column volumes of Buffer J + 150 mM NaCl. iASPP$_{608\text{-}828}$ (1 μg) and marine extracts (100 μg) were incubated with the PP-1cα-bound MC-S for 1 hr at 4 °C, end over end. The beads were washed four times with 25 column volumes of Buffer J + 300 mM NaCl. 1X SDS-PAGE Buffer was added to each sample and boiled for 5 mins at 100 °C. Samples were separated by a 12 % SDS-PAGE and stained with Coomassie Blue. Each assay was carried out in duplicate with a representative figure is shown above. Arrows are pointing to the marine extracts that disrupted iASPP$_{608\text{-}828}$ from binding PP-1cα.
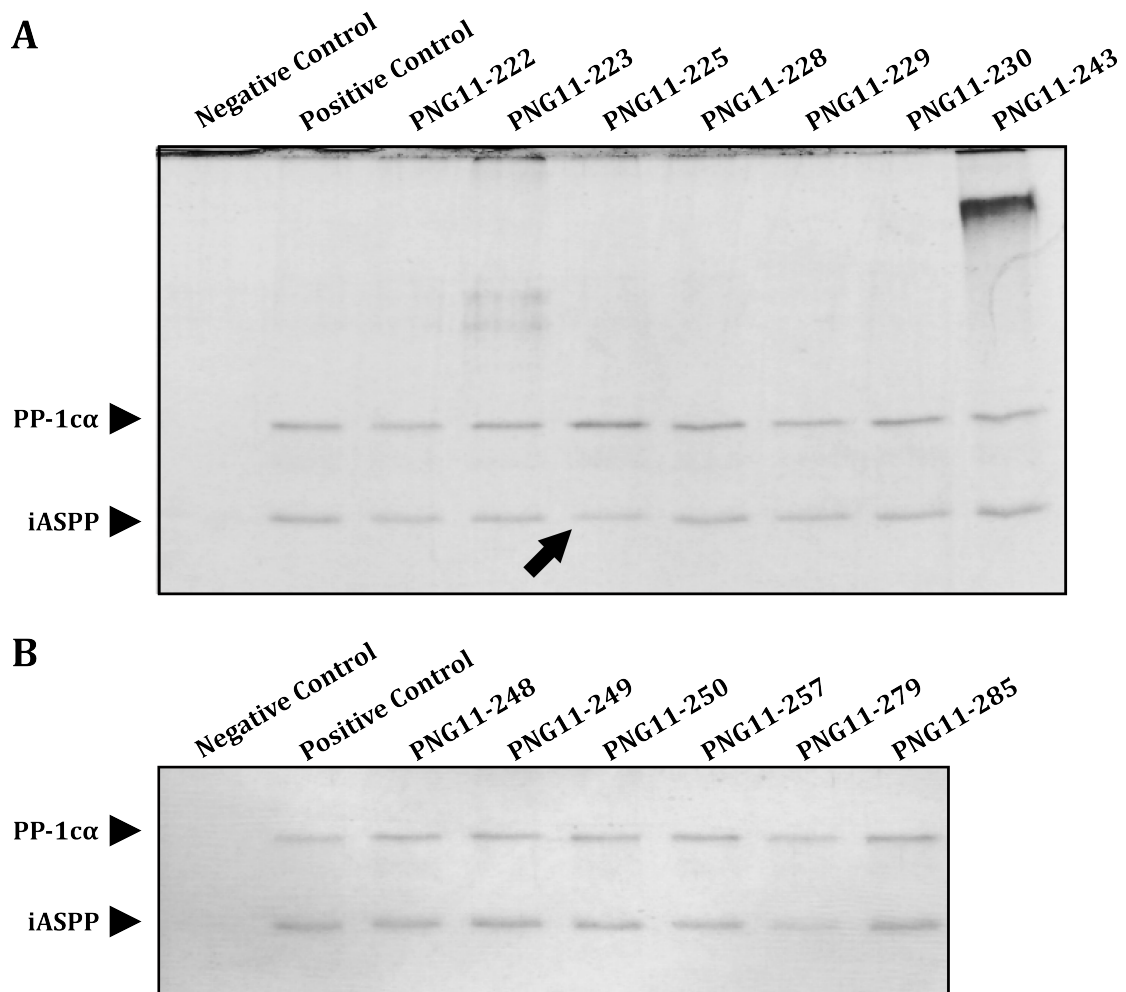
Figure 3.4: **Marine Extract PNG11-225 Disrupts PP-1c$\alpha\bullet$iASPP$_{608-828}$ Binding.** MC-S (20 μL) was first washed with 25 column volumes of ddH$_2$O and centrifuged at 3,500 rpm for 1.5 mins at room temperature. The beads were then washed twice with 25 column volumes of Buffer J + 150 mM NaCl. PP-1cα (2 μg) was incubated with the MC-S for 1 hr at 4 °C, end over end and the beads were washed twice with 25 column volumes of Buffer J + 150 mM NaCl. iASPP$_{608-828}$ (1 μg) and marine extracts (100 μg) were incubated with the PP-1cα-bound MC-S for 1 hr at 4 °C, end over end. The beads were washed four times with 25 column volumes of Buffer J + 300 mM NaCl. 1X SDS-PAGE Buffer was added to each sample and boiled for 5 mins at 100 °C. Samples were lseparated by a 12 % SDS-PAGE and stained with Coomassie Blue. Each assay was carried out in duplicate with a representative figure is shown above. The arrow is pointing to the marine extract that disrupted iASPP$_{608-828}$ from binding PP-1cα.

A

B

Figure 3.5: **Marine Extract PNG11-314 Disrupts PP-1cα•iASPP$_{608-828}$ Binding.** MC-S (20 μL) was first washed with 25 column volumes of ddH$_2$O and centrifuged at 3,500 rpm for 1.5 mins at room temperature. The beads were then washed twice with 25 column volumes of Buffer J + 150 mM NaCl. PP-1cα (2 μg) was incubated with the MC-S for 1 hr at 4 °C, end over end and the beads were washed twice with 25 column volumes of Buffer J + 150 mM NaCl. iASPP$_{608-828}$ (1 μg) and marine extracts (100 μg) were incubated with the PP-1cα-bound MC-S for 1 hr at 4 °C, end over end. The beads were washed four times with 25 column volumes of Buffer J + 300 mM NaCl. 1X SDS-PAGE Buffer was added to each sample and boiled for 5 mins at 100 °C. Samples were separated by a 12 % SDS-PAGE and stained with Coomassie Blue. Each assay was carried out in duplicate wit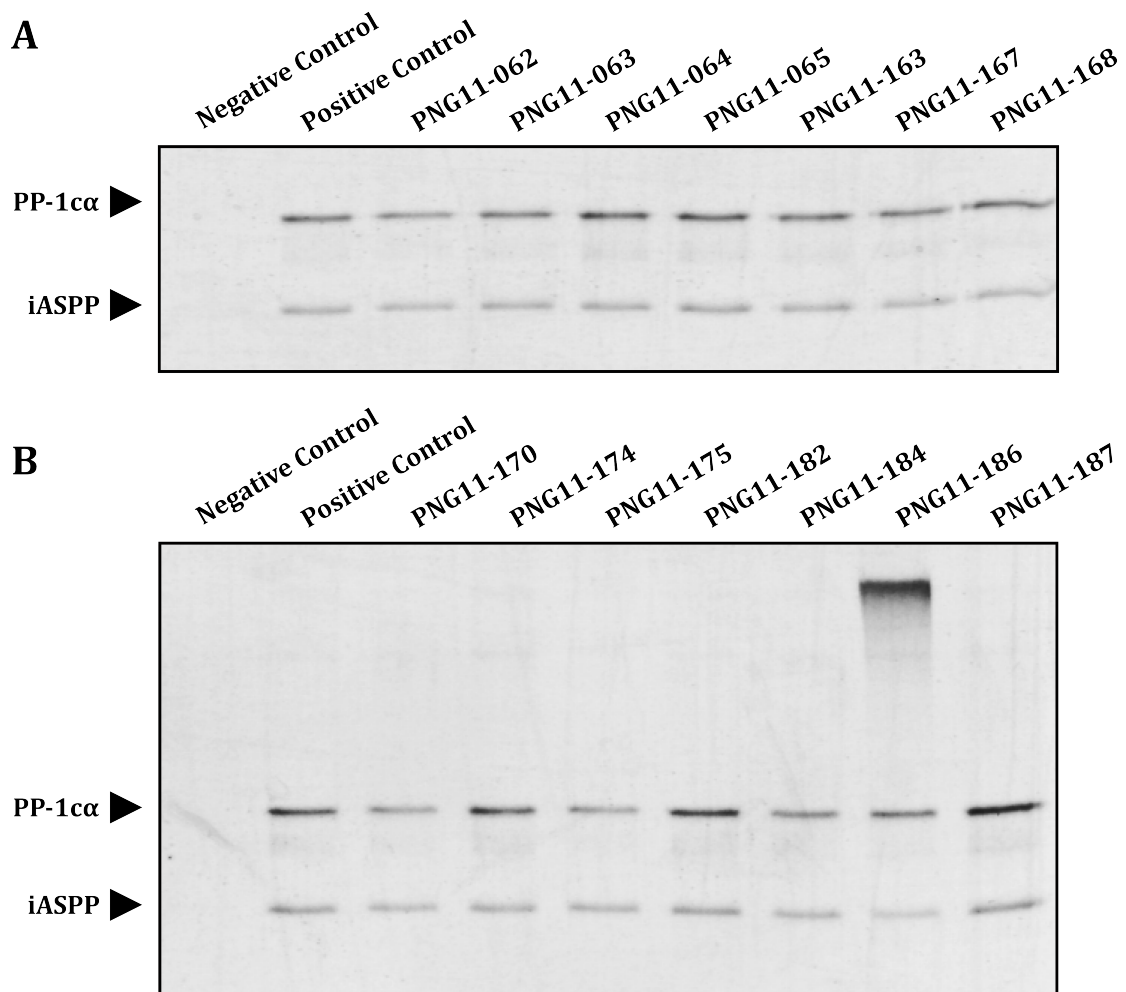h a representative figure is shown above. The arrow is pointing to the marine extract that disrupted iASPP$_{608-828}$ from binding PP-1cα.

58

Figure 3.6: **TMarine Extract RJA4150 Disrupts PP-1cα•iASPP$_{608\text{-}828}$ Binding.** MC-S (20 μL) was first washed with 25 column volumes of ddH$_2$O and centrifuged at 3,500 rpm for 1.5 mins at room temperature. The beads were then washed twice with 25 column volumes of Buffer J + 150 mM NaCl. PP-1cα (2 μg) was incubated with the MC-S for 1 hr at 4 °C, end over end and the beads were washed twice with 25 column volumes of Buffer J + 150 mM NaCl. iASPP$_{608\text{-}828}$ (1 μg) and marine extracts (100 μg) were incubated with the PP-1cα-bound MC-S for 1 hr at 4 °C, end over end. The beads were washed four times with 25 column volumes of Buffer J + 300 mM NaCl. 1X SDS-PAGE Buffer was added to each sample and boiled for 5 mins at 100 °C. Samples were separated by a 12 % SDS-PAGE and stained with Coomassie Blue. The assay was carried o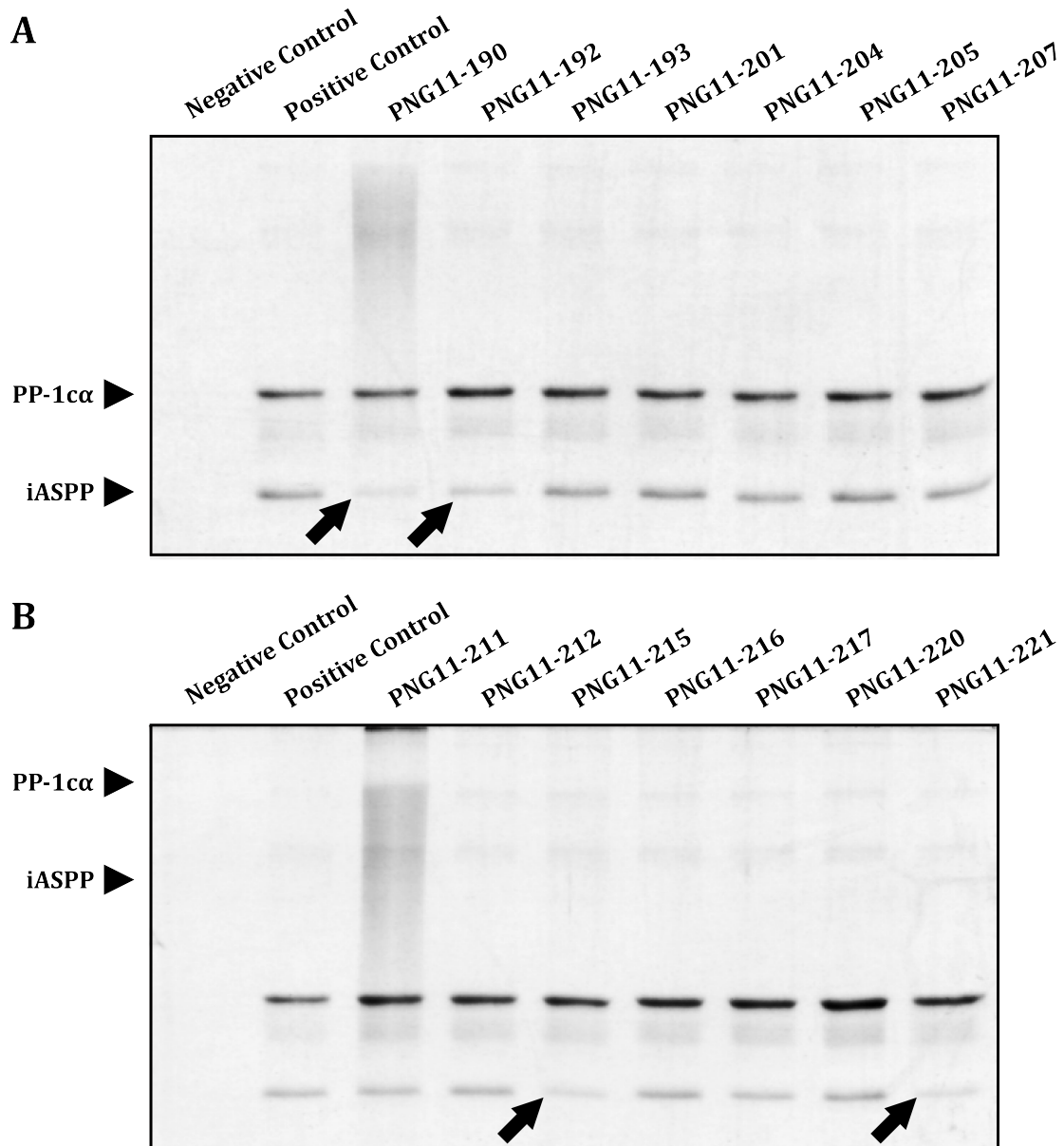ut in duplicate with a representative figure is shown above. The arrow is pointing to the marine extract that disrupted iASPP$_{608\text{-}828}$ from binding PP-1cα.

Figure 3.7: **Quantification of the Disruption of iASPP$_{608-828}$ from Binding PP-1cα in the Presence of Marine Extracts PNG11-190, PNG11-192, PNG11-215, PNG11-221, PNG11-225, PNG11-314, and RJA4150.** The amount of iASPP$_{608-828}$ present was quantified by measuring the density of the iASPP$_{608-828}$ band on the SDS-PAGE using the ImageJ program. They were then standardized against the iASPP$_{608-828}$ density in the positive control and the percentage of the control iASPP$_{608-828}$ were calculated.

Table 3.1: **The Marine Extracts Identified as Containing iASPP•PP-1cα Disruptors.**

Marine Extract Number
PNG11-190
PNG11-192
PNG11-215
PNG11-221
PNG11-225
PNG11-314
RJA4150

3.1.2 Identification of Marine Extracts that Inhibit PP-1cα Activity via pNPP Assay

Over 300 marine extracts obtained from the Dr. Ray Andersen Lab at the University of British Columbia (UBC) that were collected off the coast of Papua New Guinea were analyzed by the addition of 100 μg of crude marine extract to the pNPP phosphatase activity assay (as described in Section 2.4). The pNPP inhibition data for all marine extracts is shown in Figures 3.8 to 3.14. PP-1c inhibition indicates that a compound is bound at or near the PP-1c active site and establishing that the compound can bind PP-1cα. Most marine extracts had little or no effect on the activity of PP-1cα. Dr. Tamara Arnold aided in the screening process by repeating a portion of the assays and her data is used, in part, below. Marine extracts that were also analyzed for iASPP•PP-1c disruption in the MC-S disruption assay are listed in Table 3.2.

Two marine extracts demonstrated very potent inhibition of PP-1cα activity; PNG11-279 and PNG11-285, which inhibit PP-1cα activity to 0.36 % and 4.71 % of their original activity, respectively. These two marine extracts contain compounds that are extremely potent PP-1cα inhibitors. Finding PP-1cα inhibitors was not the main objective of the project; however, these samples are still interesting because a potent, cell permeable PP-1cα inhibitor could be a remarkably useful research tool. Therefore, the choice was made to attempt to identify the compounds in PNG11-279 and PNG11-285 responsible for this inhibition, in addition to these marine extracts being screened for iASPP•PP-1cα disruption and is described in detail in Section 4.3.
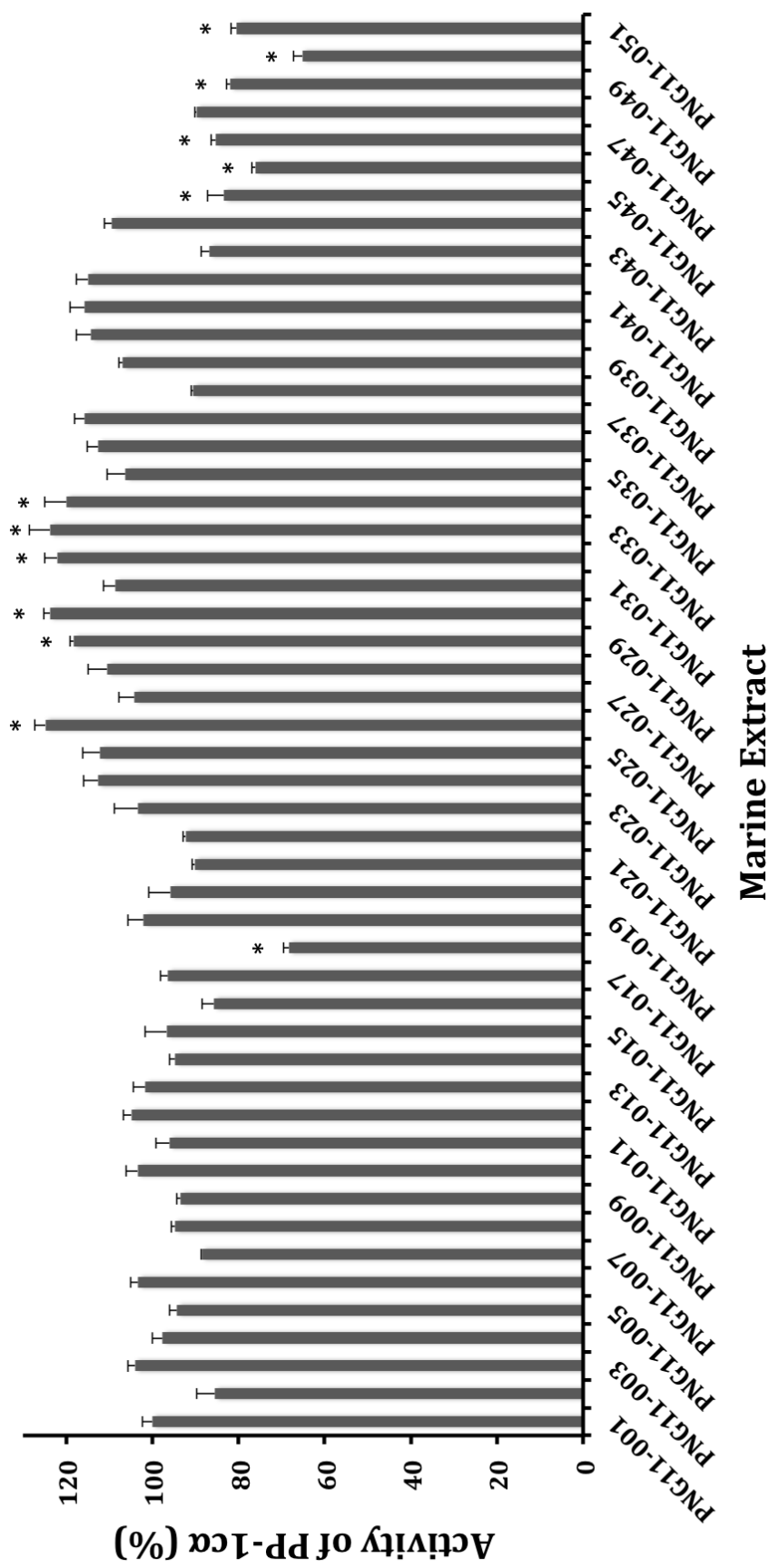
Figure 3.8: **The Effect of Marine Extracts PNG11-001 to PNG11-051 on PP-1cα Activity.** Marine extracts PNG11-001 to PNG11-051 (100 μg) along with PP-1cα (27.5 ng) were added to each well of a 96 well plate and incubated for 10 mins at 37 °C. pNPP (5 μM) was added to every well and the initial absorbance was read at 405 nm. The plate was incubated at 37 °C until the absorbance reached between 0.400 - 0.500 at 405 nm. The Abs_{final} was corrected against the $Abs_{initial}$. The $Abs_{corrected}$ was standardized against the $Abs_{control}$ value and the percent of control PP-1cα activity was calculated. The * symbol indicates marine extracts tested in the iASPP$_{608-828}$•PP-1cα disruption assay.
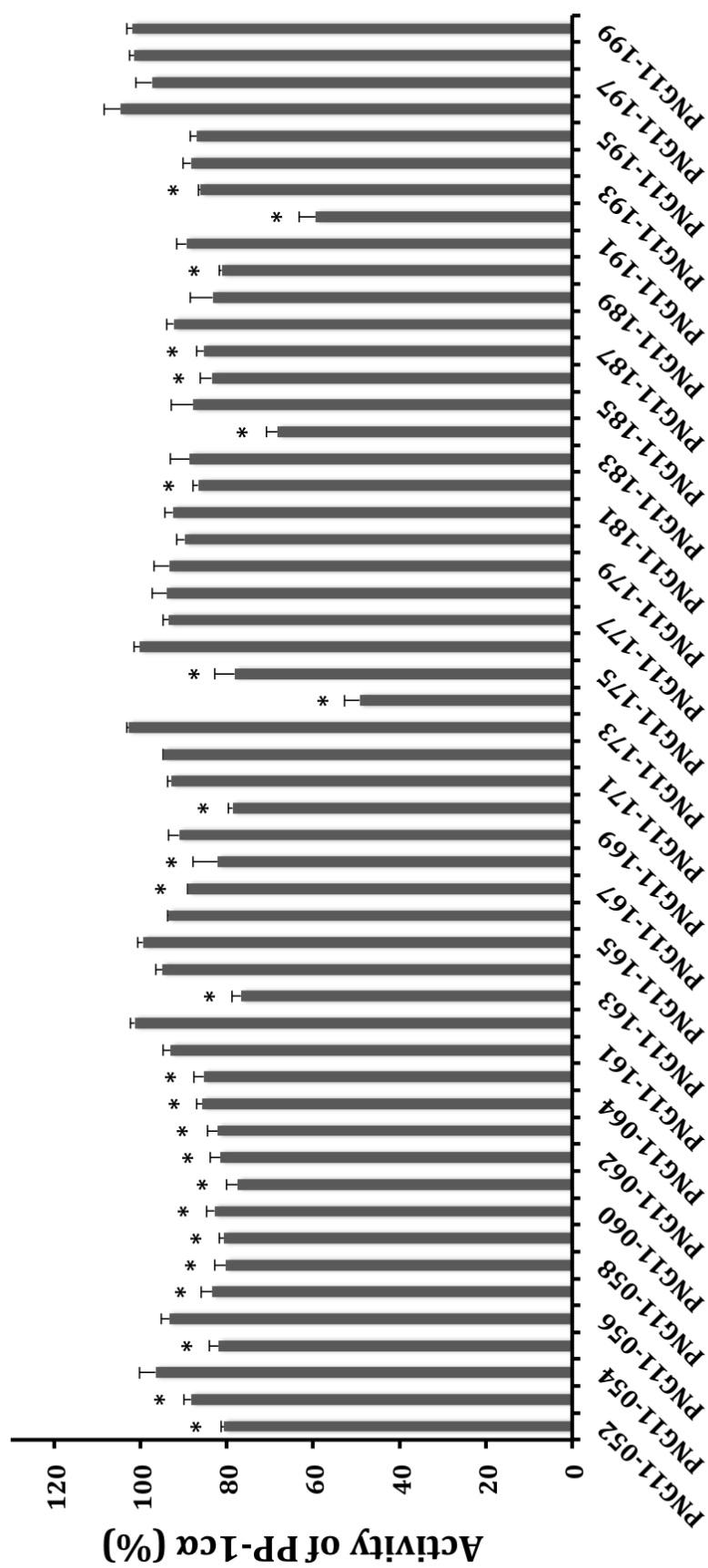
Figure 3.9: The Effect of Marine Extracts PNG11-052 to PNG11-199 on PP-1cα Activity. Marine extracts PNG11-052 to PNG11-199 (100 μg) along with PP-1cα (27.5 ng) were added to each well of a 96 well plate and incubated for 10 mins at 37 °C. pNPP (5 μM) was added to every well and the initial absorbance was read at 405 nm. The plate was incubated at 37 °C until the absorbance reached between 0.400 - 0.500 at 405 nm. The Abs$_{final}$ was corrected against the Abs$_{initial}$. The Abs$_{corrected}$ was standardized against the Abs$_{control}$ value and the percent of control PP-1cα activity was calculated. The * symbol indicates marine extracts tested in the iASPP$_{608-828}$•PP-1cα disruption assay. Each assay was carried out in duplicate.
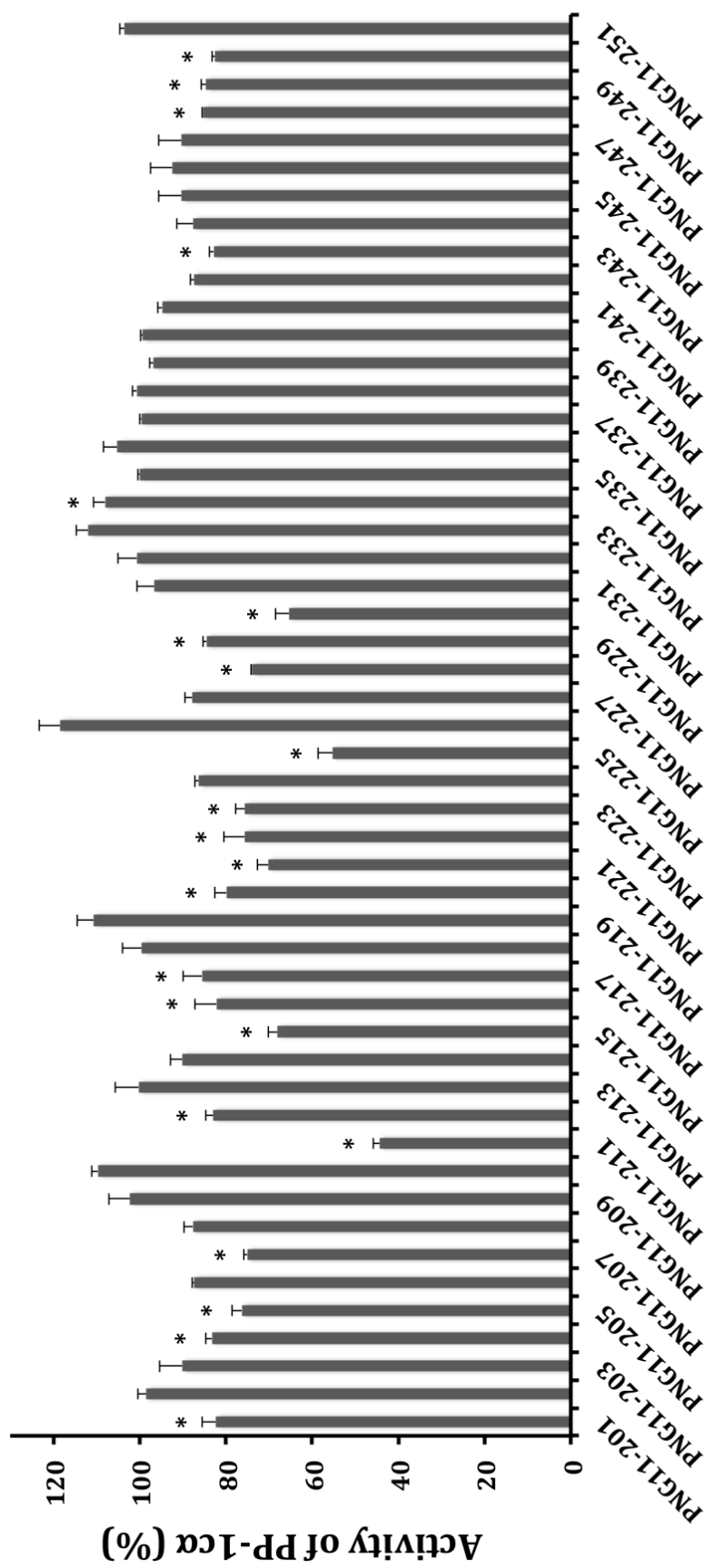
Figure 3.10: **The Effect of Marine Extracts PNG11-201 to PNG11-251 on PP-1cα Activity.** Marine extracts PNG11-201 to PNG11-251 (100 μg) along with PP-1cα (27.5 ng) were added to each well of a 96 well plate and incubated for 10 mins at 37 °C. pNPP (5 μM) was added to every well and the initial absorbance was read at 405 nm. The plate was incubated at 37 °C until the absorbance reached between 0.400 - 0.500 at 405 nm. The Abs$_{final}$ was corrected against the Abs$_{initial}$. The Abs$_{corrected}$ was standardized against the Abs$_{control}$ value and the percent of control PP-1cα activity was calculated. The * symbol indicates marine extracts tested in the iASPP$_{608-828}$•PP-1cα disruption assay. Each assay was carried out in duplicate.

64
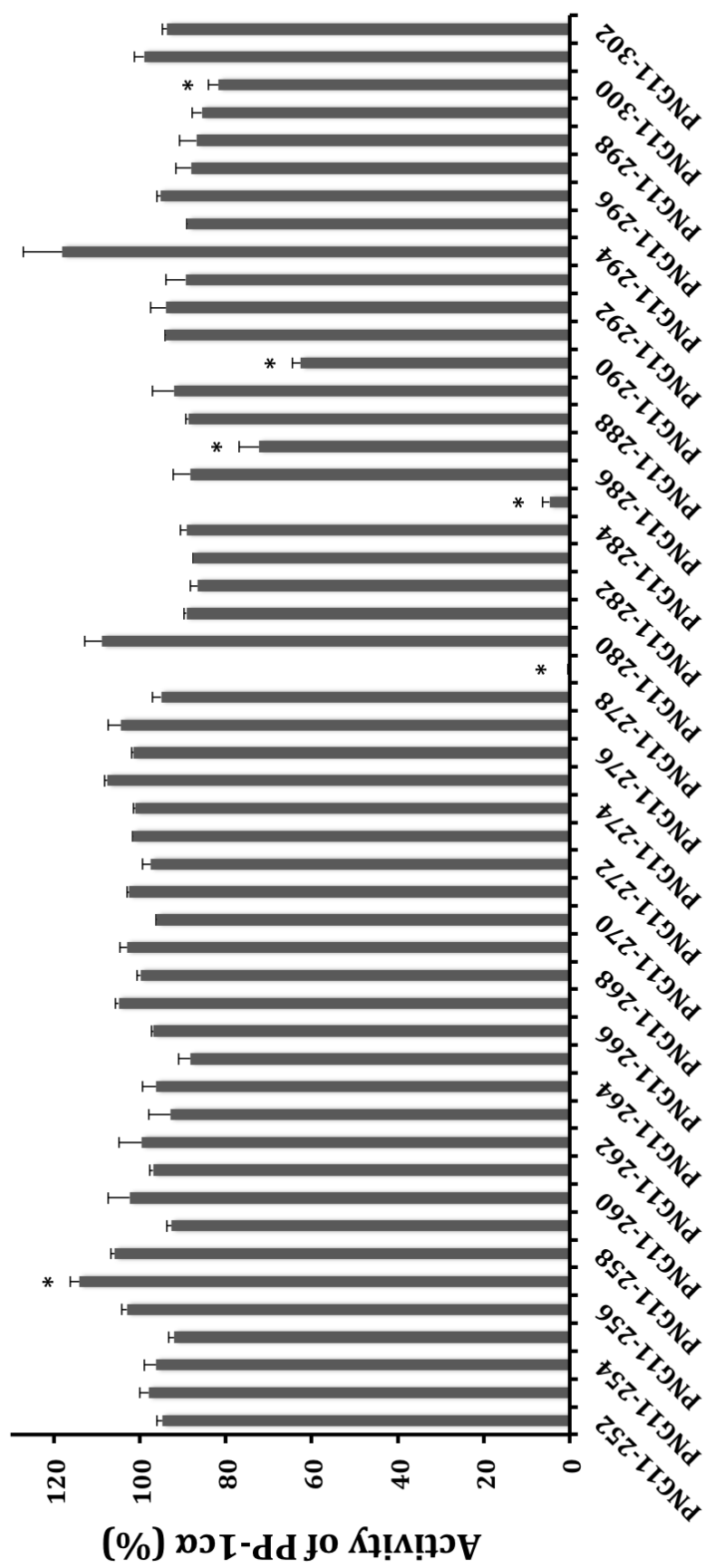
Figure 3.11: **The Effect of Marine Extracts PNG11-252 to PNG11-302 on PP-1cα Activity.** Marine extracts PNG11-252 to PNG11-302 (100 μg) along with PP-1cα (27.5 ng) were added to each well of a 96 well plate and incubated for 10 mins at 37 °C. pNPP (5 μM) was added to every well and the initial absorbance was read at 405 nm. The plate was incubated at 37 °C until the absorbance reached between 0.400 - 0.500 at 405 nm. The Abs_{final} was corrected against the $Abs_{initial}$. The $Abs_{corrected}$ was standardized against the $Abs_{control}$ value and the percent of control PP-1cα activity was calculated. The * symbol indicates marine extracts tested in the iASPP$_{608-828}$•PP-1cα disruption assay. Each assay was carried out in duplicate.
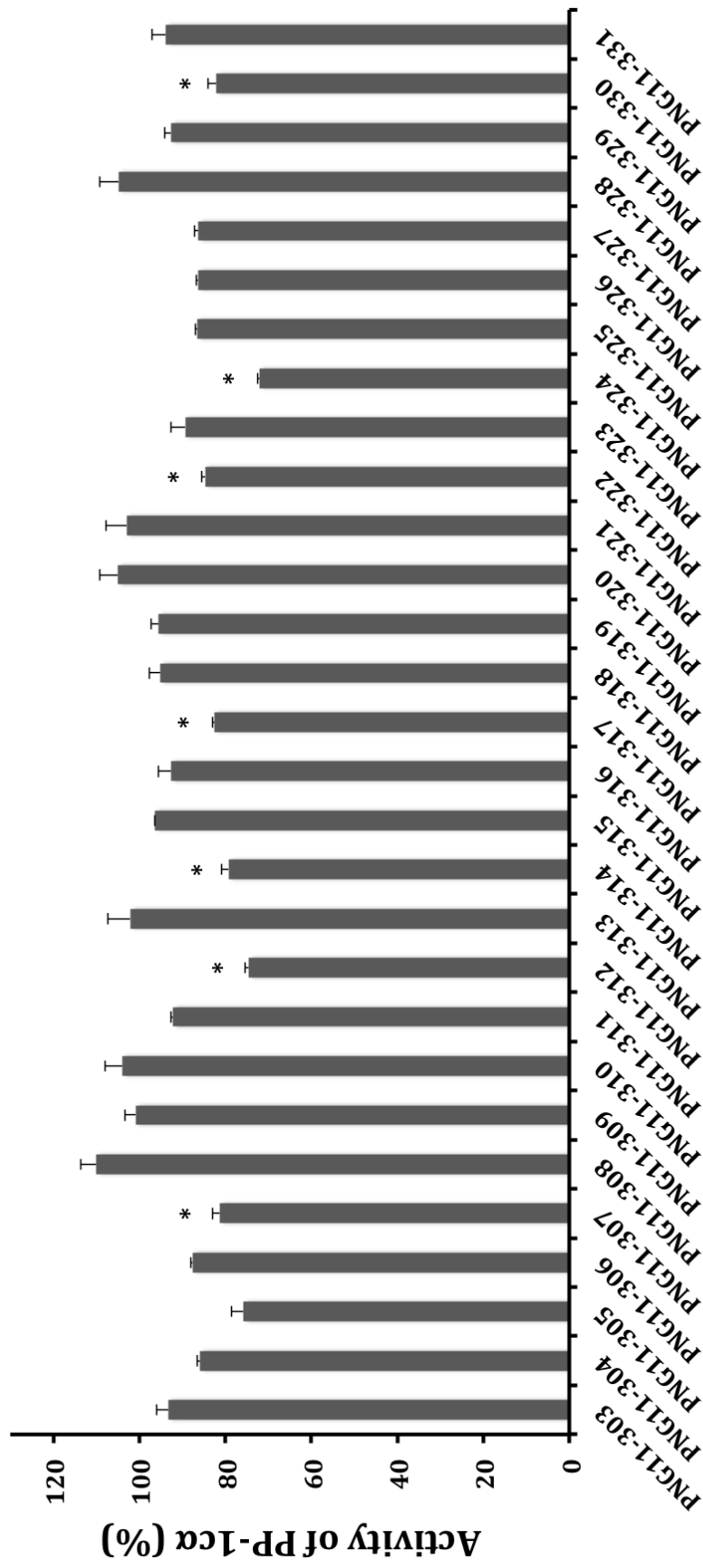
Figure 3.12: **The Effect of Marine Extracts PNG11-303 to PNG11-331 on PP-1cα Activity.** Marine extracts PNG11-303 to PNG11-331 (100 μg) along with PP-1cα (27.5 ng) were added to each well of a 96 well plate and incubated for 10 mins at 37 °C. pNPP (5 μM) was added to every well and the initial absorbance was read at 405 nm. The plate was incubated at 37 °C until the absorbance reached between 0.400 - 0.500 at 405 nm. The Abs_{final} was corrected against the $Abs_{initial}$. The $Abs_{corrected}$ was standardized against the $Abs_{control}$ value and the percent of control PP-1cα activity was calculated. The * symbol indicates marine extracts tested in the iASPP$_{608-828}$•PP-1cα disruption assay. Each assay was carried out in duplicate.
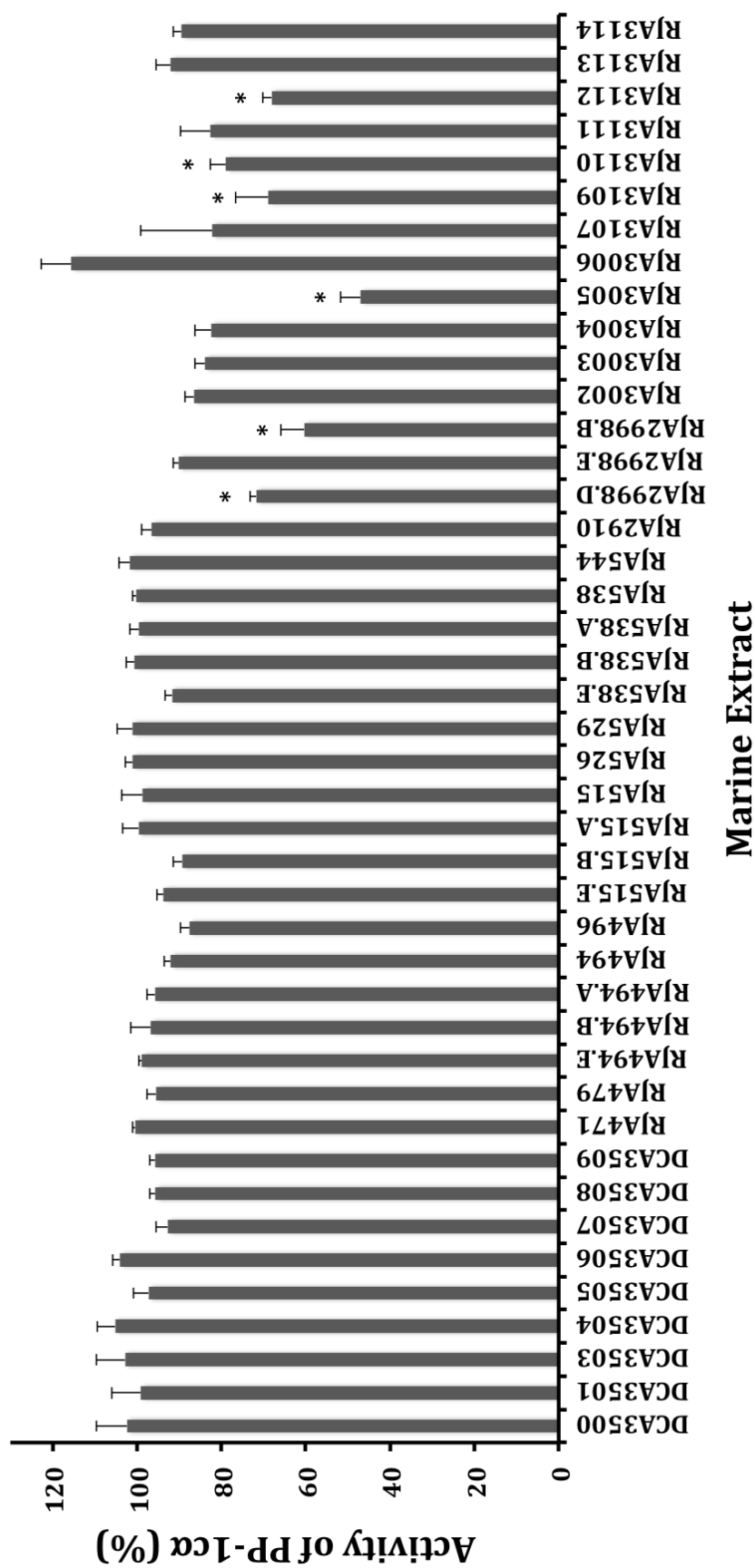
Figure 3.13: **The Effect of Marine Extracts DCA3500 to RJA3114 on PP-1cα Activity.** Marine extracts DCA3500 - RJA3114 (100 μg) along with PP-1cα (27.5 ng) were added to each well of a 96 well plate and incubated for 10 mins at 37 °C. pNPP (5 μM) was added to every well and the initial absorbance was read at 405 nm. The plate was incubated at 37 °C until the absorbance reached between 0.400 - 0.500 at 405 nm. The Abs$_{final}$ was corrected against the Abs$_{initial}$. The Abs$_{corrected}$ was standardized against the Abs$_{control}$ value and the percent of control PP-1cα activity was calculated. The * symbol indicates marine extracts tested in the iASPP$_{608-828}$•PP-1cα disruption assay. Each assay was carried out in duplicate.
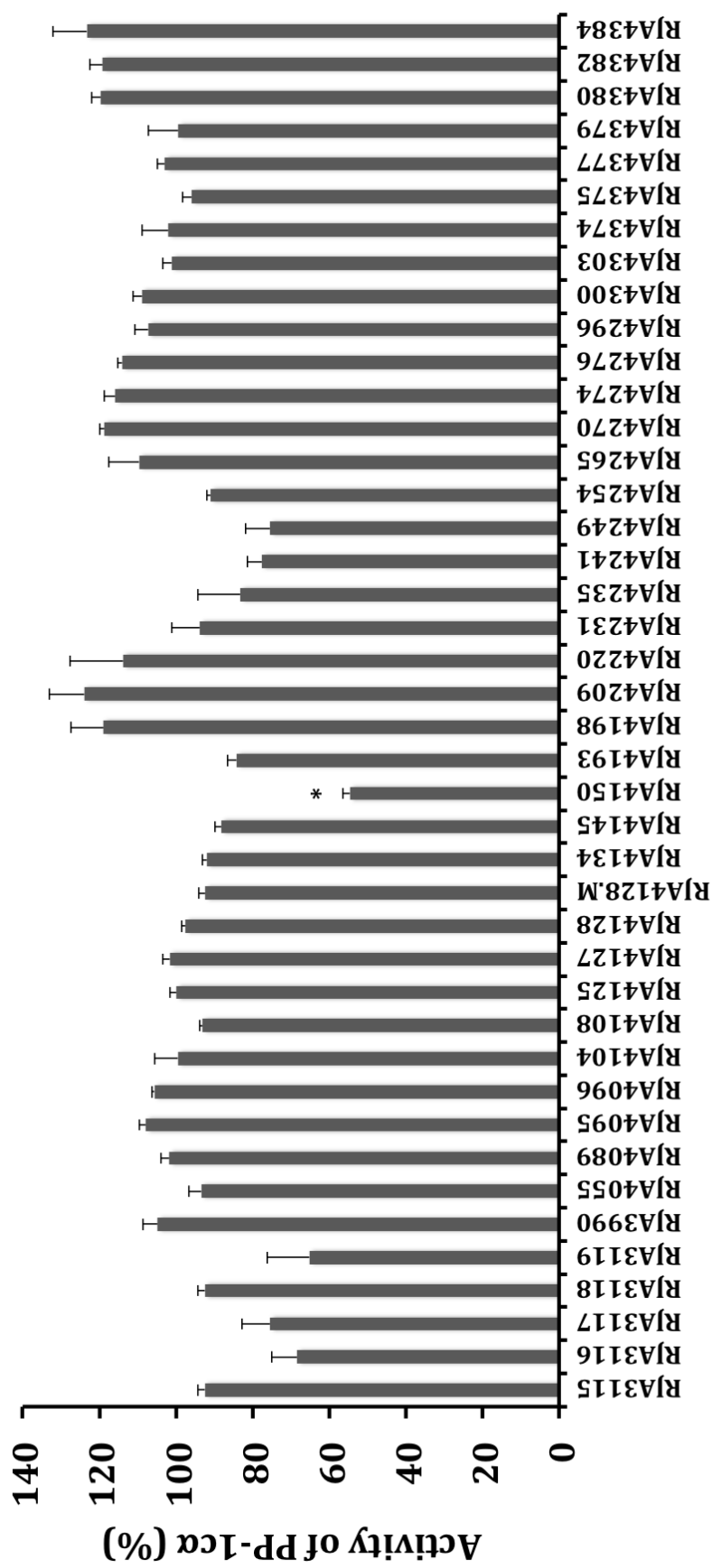
Figure 3.14: **The Effect of Marine extracts RJA3115 to RJA4384 on PP-1cα Activity.** Marine extracts RJA3115 to RJA4384 (100 μg) along with PP-1cα (27.5 ng) were added to each well of a 96 well plate and incubated for 10 mins at 37 °C. pNPP (5 μM) was added to every well and the initial absorbance was read at 405 nm. The plate was incubated at 37 °C until the absorbance reached between 0.400 - 0.500 at 405 nm. The Abs$_{final}$ was corrected against the Abs$_{initial}$. The Abs$_{corrected}$ was standardized against the Abs$_{control}$ value and the percent of control PP-1cα activity was calculated. The * symbol indicates marine extracts tested in the iASPP$_{608-828}$•PP-1cα disruption assay. Each assay was carried out in duplicate.

68

Table 3.2: **The PP-1cα Activity in the Presence of the Marine Extracts also Analyzed for iASPP•PP-1cα Disruption.**

Marine Extract	PP-1cα Activity (%)	Marine Extract	PP-1cα Activity (%)
PNG11-018	67	PNG11-230	65
PNG11-026	1245	PNG11-234	108
PNG11-029	118	PNG11-243	85
PNG11-030	124	PNG11-248	85
PNG11-032	122	PNG11-249	85
PNG11-033	124	PNG11-250	83
PNG11-034	120	PNG11-257	114
PNG11-045	83	PNG11-279	0
PNG11-046	76	PNG11-285	5
PNG11-047	82	PNG11-287	72
PNG11-049	82	PNG11-290	62
PNG11-050	65.	PNG11-300	82
PNG11-051	80	PNG11-307	75
PNG11-052	81	PNG11-312	75
PNG11-053	88	PNG11-314	79
PNG11-055	82	PNG11-317	82
PNG11-057	83	PNG11-322	85
PNG11-058	80	PNG11-324	72
PNG11-059	81	PNG11-330	82
PNG11-060	77	RJA2998 (DCM)	72
PNG11-061	77	RJA2998 (BuOH)	60
PNG11-062	81	RJA3005	47
PNG11-063	82	RJA3109	69
PNG11-064	86	RJA3110	79
PNG11-065	85	RJA3112	68
PNG11-163	79	RJA4150	55
PNG11-167	89		
PNG11-168	79		
PNG11-170	79		
PNG11-174	49		
PNG11-175	78		
PNG11-182	87		
PNG11-184	68		
PNG11-186	83		
PNG11-187	85		
PNG11-190	81		
PNG11-192	59		
PNG11-193	86		
PNG11-201	82		
PNG11-204	83		
PNG11-205	76		
PNG11-207	75		
PNG11-211	44		
PNG11-212	83		
PNG11-215	68		
PNG11-216	82		
PNG11-217	86		
PNG11-220	80		
PNG11-221	70		
PNG11-222	76		
PNG11-223	76		
PNG11-225	55		
PNG11-228	74		
PNG11-229	84		

Chapter 4

The Characterization and Functional Assay of Compounds that Disrupt Binding of iASPP from PP-1cα

4.1 The Identification of Novel Disruptors of iASPP•PP-1cα Binding

Once the marine extracts were analyzed for iASPP•PP-1c disrupt, each marine extract that contained an iASPP disruptor was further partitioned to attempt to identify the compound causing the disruption. Of the list, two novel iASPP disruptors were identified and are discussed in this Section.

4.1.1 Identification of Marine Extract PNG11-192 as Halistanol Sulfate

In collaboration with the Dr. David Williams at UBC, the crude marine extract, selected for iASPP disruption labelled as PNG11-192, underwent extensive fractionation. The extract was seperated based on polarity and size while continually being monitored for desired iASPP•PP-1cα disruption activity. The crude extract was first processed by solvent partitioning into three fractions: Aq-Aq, BuOH, and EtOAc (Figure 4.2). Fraction BuOH disrupted iASPP$_{608-828}$ from PP-1cα with the MC-S disruption assay (Figure 4.3); therefore, it was further partitioned via Sephadex LH20 chromatography. Again, follow analysis of the fractions within MC-S disruption assay, the compound of interest was identified in the BuOH-C fraction (see Figure 4.3 and 4.4).

The PNG11-192 BuOH-C fraction was pure enough for Dr. David Williams to identify the compound of interest as Halistanol Sulfate via NMR. The structure of Halistanol Sulfate, shown in Figure 4.1, was determined to possess a sulfate group at C-3 where most sterols typically have an alcohol. In addition, Halistanol Sulfate also contains two additional sulfate groups at the C-2 and C-6 positions and a long canonical aliphatic side chain C-17, in the form of a 2,2-dimethylheptane group. Halistanol Sulfate is structurally very similar to the iASPP disruptor, Sokotrasterol Sulfate, discovered by Dr. Tamara Arnold (shown in Section 1.10) with the only differences being that Halistanol Sulfate contains extra methyl groups in the long aliphatic chain.

4.1.2 Identification of Marine Extract PNG11-221 as Coscinamide B

Coscinamide B was the second compound I identified as an iASPP disruptor via the iASPP•PP-1cα disruption screening and was present in marine extract PNG11-221 (as shown in Figure 3.3). With the help of the Dr. David Williams, PNG11-221 was fractionationed first via solvent partitioning to obtain Aq-Aq, BuOH, and EtOAc fractions (Figure 4.6). The disruption activity was identified in the EtOAc fraction, see Figure 4.7, which was subsequently partitioned again, with the use of Sephadex LH20
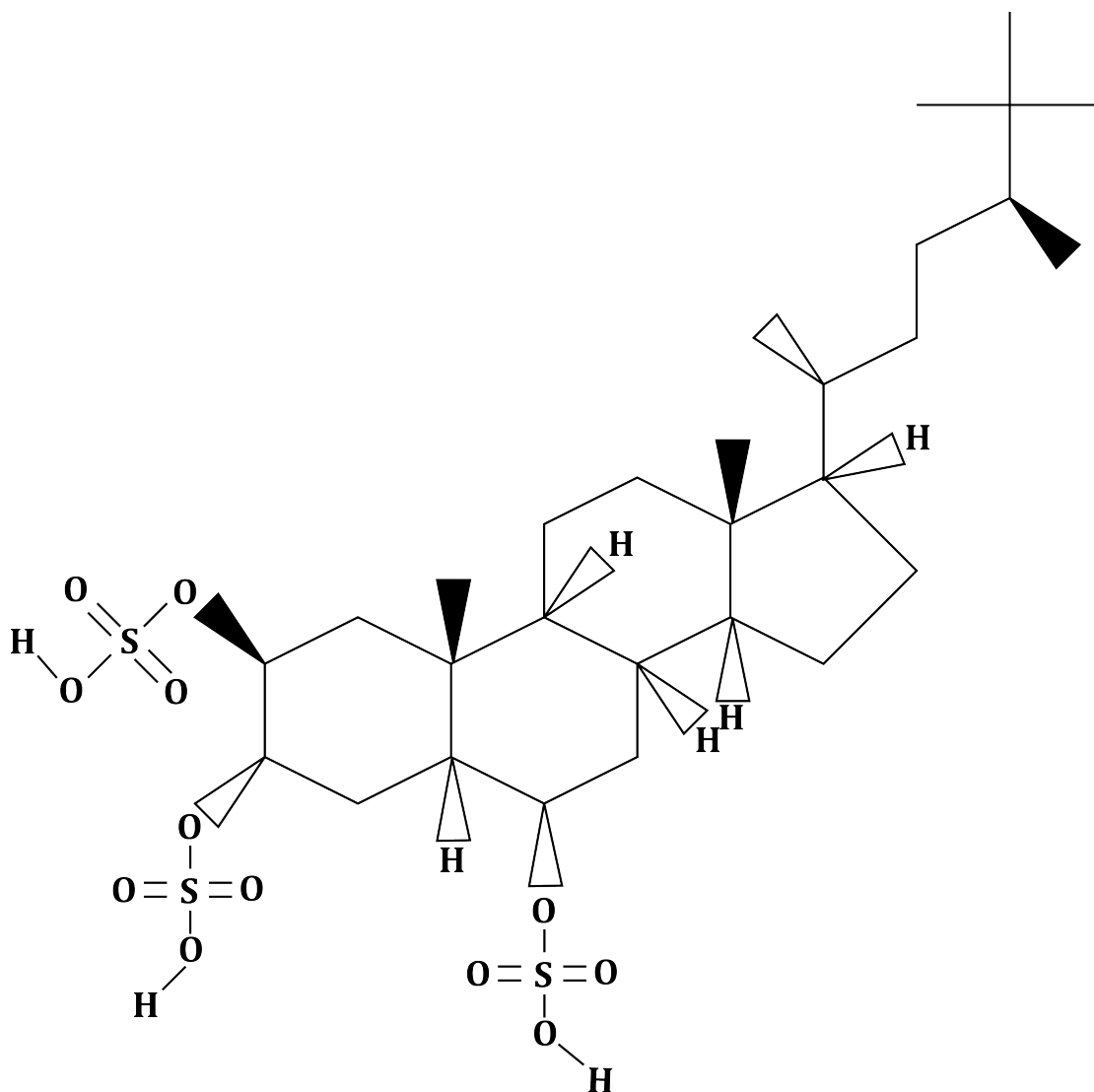
Figure 4.1: **The Chemical Structure of Halistanol Sulfate (Marine Extract PNG11-192).** Halistanol Sulfate is sterol with 3 sulfate groups attached to C-2, C-3, and C-6. As well, has a long, saturated alkyl chain attached to position 17 [124].

chromatography based on molecular size, to obtain the fractions EtOAc-A to EtOAc-J. The disruption assay results showed that Coscinamide B was located within the last four fractions; EtOAc-G, EtOAc-H, EtOAc-I, and EtOAc-J based on disruption activity seen (Figure 4.8). Unfortunately, there was less than 30 μg of this compound remaining and I could not analyze it further.

Figure 4.5 shows that Coscinamide B is a bisindolic endamide, largely composed of
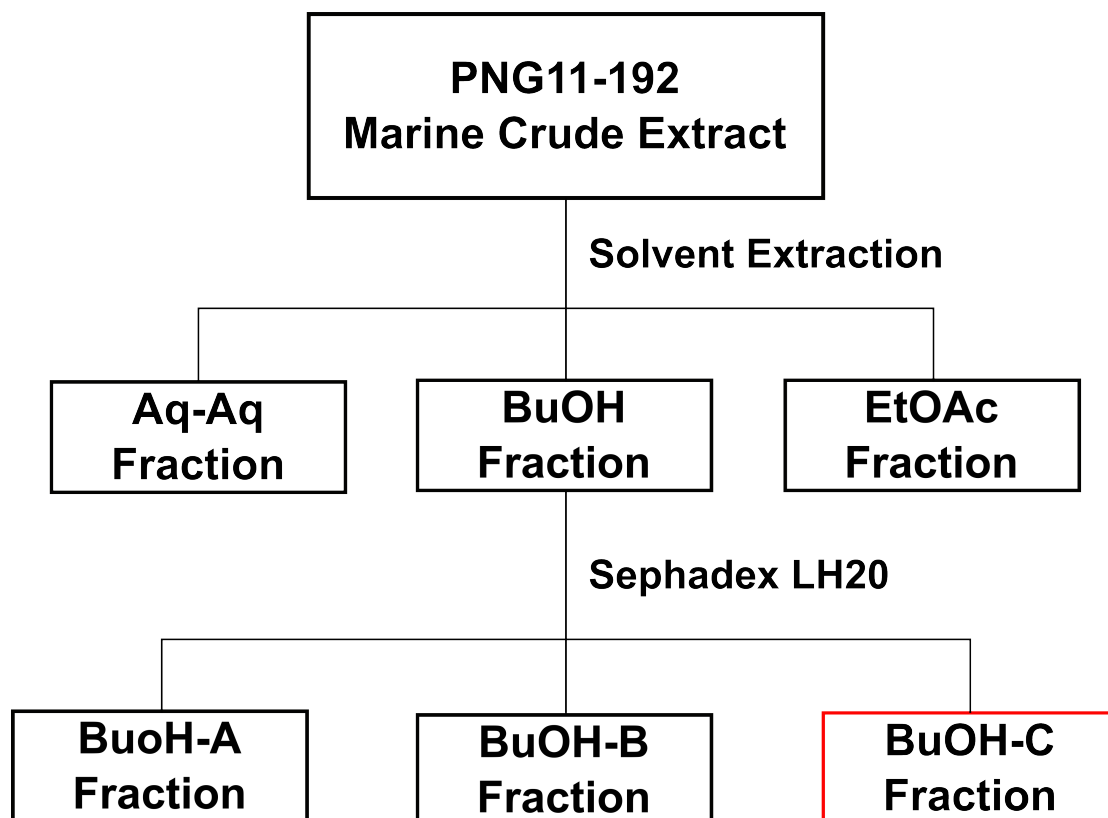
Figure 4.2: **Fractionation of Marine Extract PNG11-192.** The solvent and size fraction of marine extract PNG11-192 that lead to the identification of the compound, Halistanol Sulfate. The red box indicates the fraction that Halistanol Sulfate was identified within, namely BuOH-C.

two indole groups at either end which connect to one another by their C-3 positions. The connector group is a long alkyl chain that is formed by a 2,3-butanedione followed by a nitrogen and a propylene group. But, unlike typical amines, Coscinamide B is not basic. As well, unlike the Halistanol Sulfate, Sokotrasterol Sulfate, and Suvanine, Coscinamide B contains no sulfate groups. The indole rings make Coscinamide B structurally similar to the amino acid, tryptophan. Tryptophan has a single indole ring with a D-2-aminobutyric acid at the C3 position.
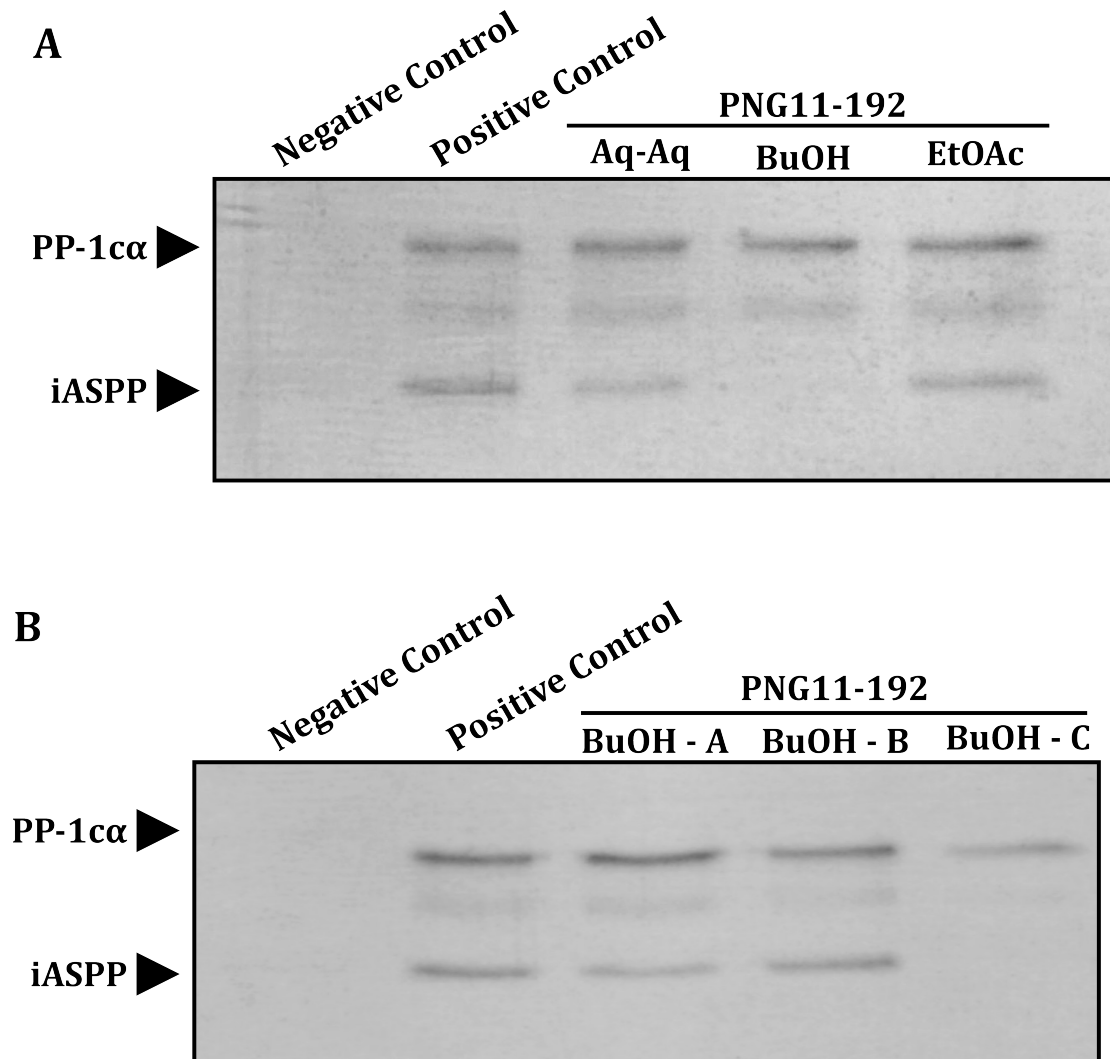
Figure 4.3: **Disruption of the PP-1cα•iASPP$_{608\text{-}828}$ by PNG11-192 Fractions.**
MC-S (20 μL) was first washed with 25 column volumes of ddH$_2$O and centrifuged at
3,500 rpm for 1.5 mins at room temperature. The beads were then washed twice with
25 column volumes of Buffer J + 150 mM NaCl. PP-1cα (2 μg) was incubated with
the MC-S for 1 hr at 4 °C, end over end and the beads were washed twice with 25
column volumes of Buffer J + 150 mM NaCl. iASPP$_{608\text{-}828}$ (1 μg) and PNG11-192
Fractions (A) Aq-Aq, BuOH, and EtOAc (B) BuOH-A, BuOH-B, and BuOH-C (100
μg) were incubated with the PP-1cα-bound MC-S for 1 hr at 4 °C, end over end. The
beads were washed four times with 25 column volumes of Buffer J + 300 mM NaCl. 1X
SDS-PAGE Buffer was added to each sample and boiled for 5 mins at 100 °C. Samples
were separated by a 12 % SDS-PAGE and stained with Coomassie Blue. The assay was
carried out in duplicate with a representative figure shown above.
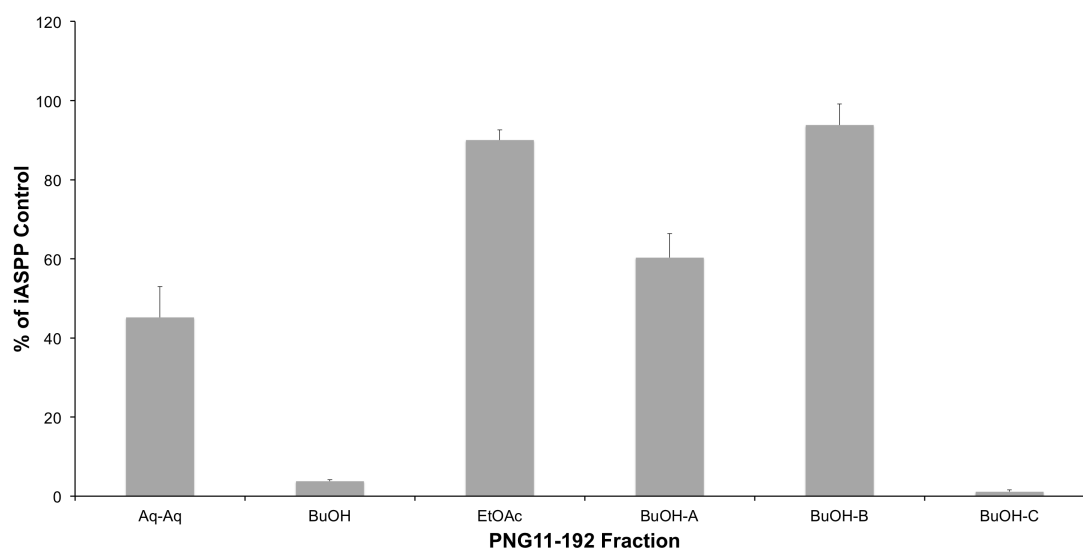
Figure 4.4: **Quantification of the Disruption of iASPP$_{608\text{-}828}$ from Binding PP-1cα in the Presence of PNG11-192 Fractions.** The amount of iASPP$_{608\text{-}828}$ present was quantified by measuring the density of the iASPP$_{608\text{-}828}$ band on the SDS-PAGE using the ImageJ program. They were then standardized against the iASPP$_{608\text{-}828}$ density in the positive control lane. These values were averaged with the duplicate experiment and plotted.
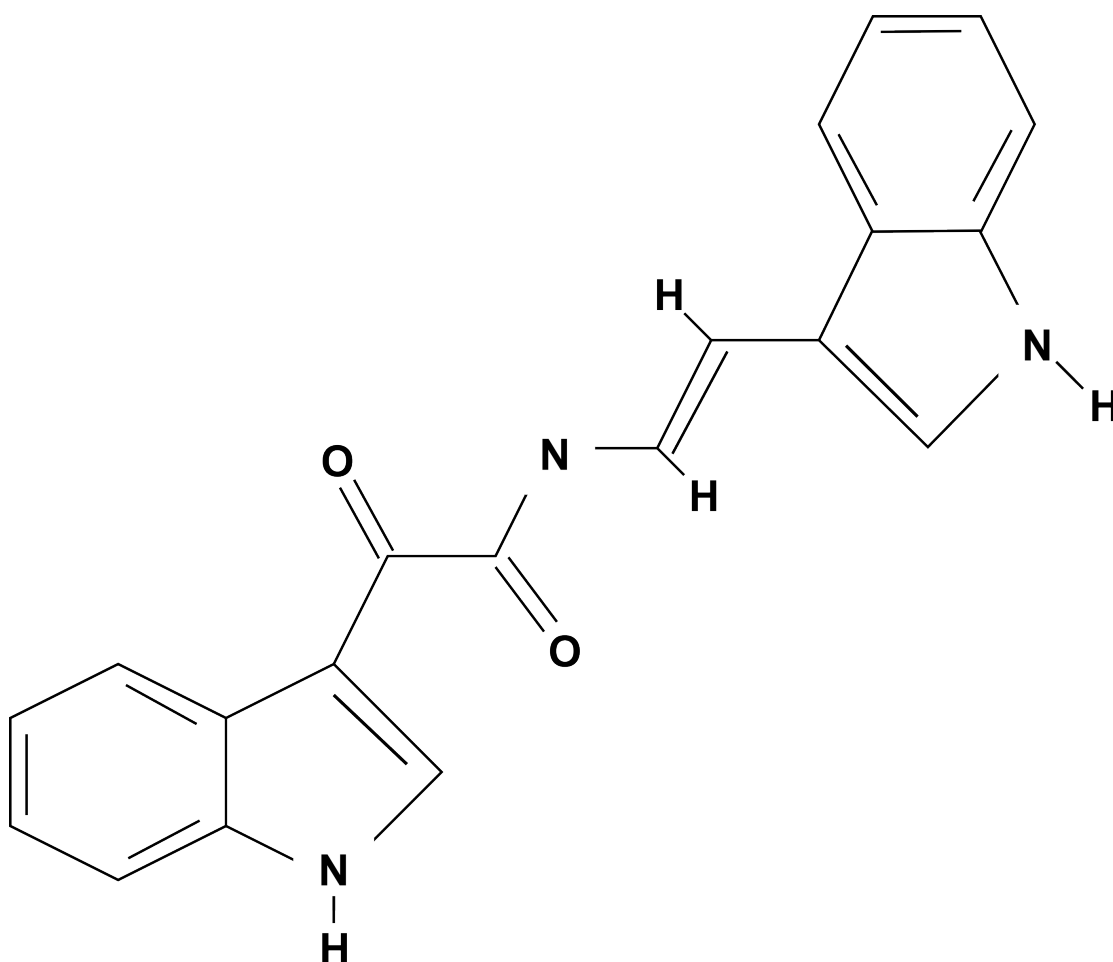
Figure 4.5: **The Chemical Structure of Coscinamide B (Marine Extract PNG11-221).** Coscinamide B is largely composed of two indole groups that are attached to one another via a long alkyl chain. This chain is formed by a 2,3-butanedione groove, followed by a nitrogen, and a propylene group [124].
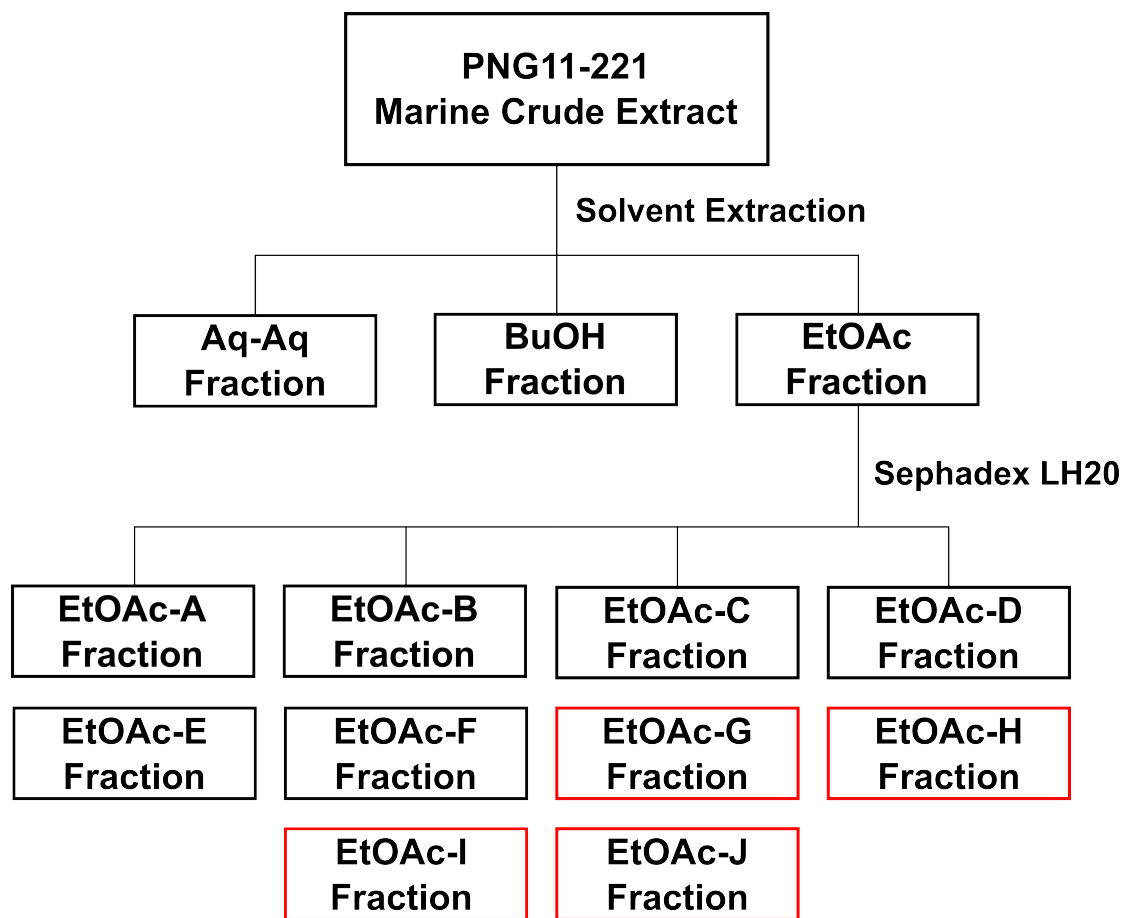
Figure 4.6: **Fractionation of Marine Extract PNG11-221.** The solvent and size fraction of marine extract PNG11-221 that lead to the identification of the compound of interest, Coscinamide B. The red boxes indicate the fractions that Coscinamide B was identified namely within; EtOAc-G, EtOAc-H, EtOAc-I and EtOAc-J.
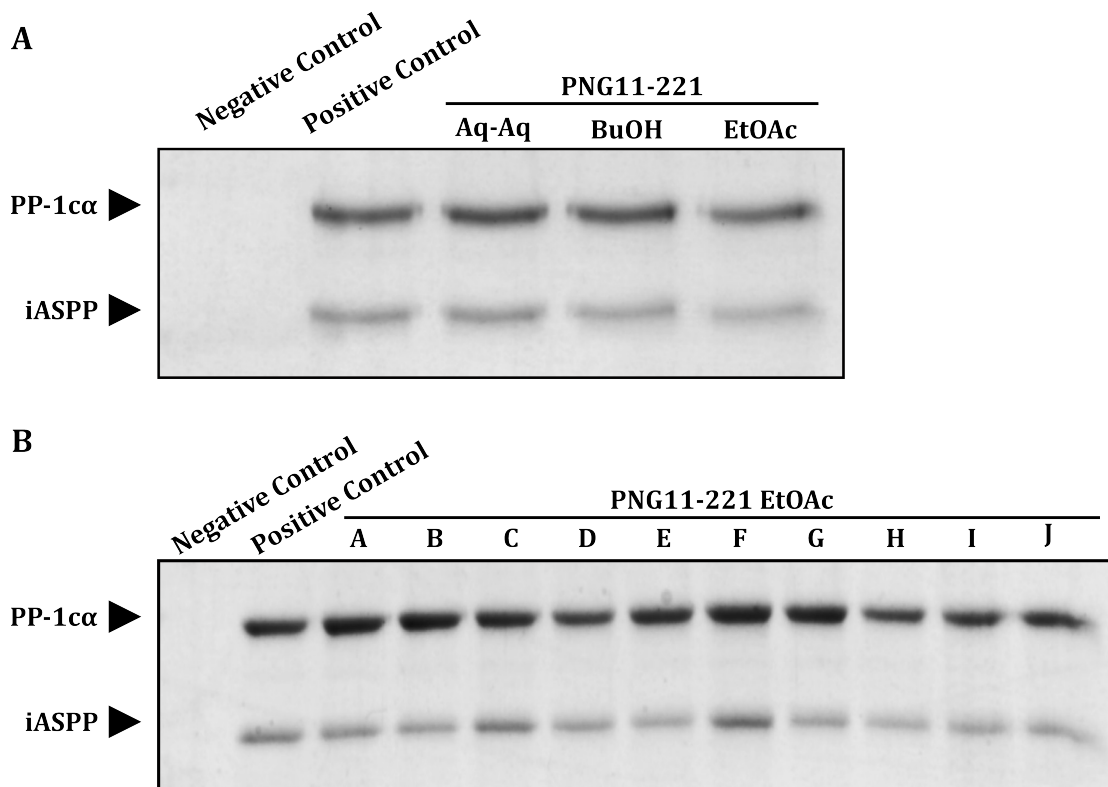
Figure 4.7: **Disruption of iASPP$_{608\text{-}828}$ from PP-1cα by PNG11-221 Fractions.** MC-S (20 μL) was washed first with 25 column volumes of ddH$_2$O and centrifuged at 3,500 rpm for 90 seconds at room temperature. The beads were then washed twice with 25 column volumes of Buffer J + 150 mM NaCl. PP-1cα (2 μg) was incubated with the MC-S for 1 hr at 4 °C, end over end and the beads were washed twice with 25 column volumes of Buffer J + 150 mM NaCl. iASPP$_{608\text{-}828}$ (1 μg) and PNG11-221 Fractions (A) Aq-Aq, BuOH, and EtOAc (B) EtOAc-A to EtOAc-J (100 μg) were incubated with the PP-1cα-bound MC-S for 1 hr at 4 °C, end over end. The beads were washed four times with 25 column volumes of Buffer J + 300 mM NaCl. 1X SDS-PAGE Buffer was added to each sample and boiled for 5 mins at 100 °C. Samples were separated by a 12 % SDS-PAGE and stained with Coomassie Blue. The assay was carried out in duplicate with a representative figure shown above.

Figure 4.8: **Quantification of the Disruption of iASPP$_{608-828}$ from binding PP-1cα in the Presence of PNG11-221 Fractions.** The amount of iASPP$_{608-828}$ present was quantified by measuring the density of the iASPP$_{608-828}$ band on the SDS-PAGE using the ImageJ program. They were then standardized against the iASPP$_{608-828}$ density in the positive control lane. These values were averaged with the duplicate experiment and plotted.

4.2 Determination of the Potency and Specificity of Halistanol Sulfate, Sokotrasterol Sulfate, and Suvanine on the Binding of PP-1c to iASPP, TIMAP and ASPP2 Regulatory Subunits

Once the iASPP disruptors, Halistanol Sulfate, Sokotrasterol Sulfate, and Suvanine, were identified and purified, the potency of each of the compounds was then established. Specifically, what was the minimum concentration required to disrupt the binding of iASPP to PP-1α. To substantiate this, I ascertained the concentration at which 50 % of the iASPP$_{608\text{-}828}$ was prevented from binding PP-1cα; this was termed the half maximal disruption concentration or DC$_{50}$. Due to limited amounts of each compound, I approximated how much of each compound was required based on the fractions in Section 3.1.1 and selected concentrations around that value to test further with the MC-S disruption assay.

4.2.1 Halistanol Sulfate, Sokotrasterol Sulfate, and Suvanine Disrupt the Binding of iASPP$_{608\text{-}828}$ to PP-1cα

Figure 4.9 shows the effect of Halistanol Sulfate on the iASPP$_{608\text{-}828}$•PP-1cα complex at 50 μM, 75 μM, and 100 μM concentrations. As the concentration of Halistanol Sulfate increased, so did the disruption of iASPP binding, demonstrating that the effect of Halistanol Sulfate is dose-dependent. The MC-S disruption assay results also showed that the presence of 100 μM Halistanol Sulfate disrupted the binding of PP-1cα to MC-S beads. Panel A of Figure 4.10 shows the relative percent of iASPP bound, quantifying that iASPP is being disrupted in a dose-dependent manner. Panel B of Figure 4.10 represents the slope of percent iASPP bound. The slope equation was used to extrapolate the DC$_{50}$ value, which was calculated as approximately equal 102 μM.

Next, the potency of Sokotrasterol Sulfate as an iASPP disruptor was determined. Figure 4.11 shows significant iASPP$_{608\text{-}828}$ disruption within the range of 10 μM to

50 μM concentrations. As well, a small amount of PP-1cα was disrupted from the MC-S beads, as seen with Halistanol Sulfate above. Panel A of Figure 4.12 shows the quantification the percent iASPP bound in Figure 4.11, confirming that iASPP is being disrupted by Sokotrasterol Sulfate in a dose-dependent manner. Panel B of Figure 4.12 determines the slope equation which was used to establish the DC$_{50}$ to equal 40 μM.

Lastly, I analyzed the potency of the compound Suvanine using MC-S disruption assay between iASPP and PP-1cα at 25 μM, 50 μM, and 75 μM concentrations (Figure 4.13). Figure 4.14 Panel A shows the quantification the iASPP bound to PP-1cα after the addition of Suvanine and shows that Suvanine disrupts in a dose-dependent manner. The slope equation was calculated (Figure 4.14 Panel B) and it was determined that the DC$_{50}$ was 60 μM.
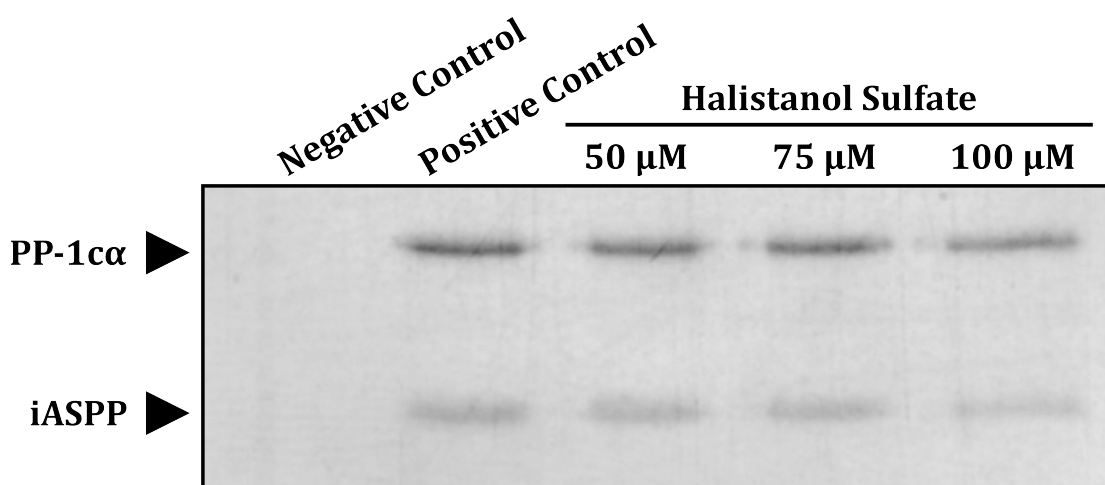
Figure 4.9: **The Disruption of PP-1c$\alpha\bullet$iASPP$_{608\text{-}828}$ Binding by 50 μM, 75 μM, and 100 μM of Halistanol Sulfate.** MC-S (20 μL) was washed first with 25 column volumes of ddH$_2$O and centrifuged at 3,500 rpm for 1.5 mins at room temperature. The beads were then washed twice with 25 column volumes of Buffer J + 150 mM NaCl. PP-1cα (2 μg) was incubated with the MC-S for 1 hr at 4 $^\circ$C, end over end and the beads were washed twice with 25 column volumes of Buffer J + 150 mM NaCl. iASPP$_{608\text{-}828}$ (1 μg) along with 50 μM, 75 μM, or 100 μM of Halistanol Sulfate was incubated with the PP-1cα-bound MC-S for 1 hr at 4 $^\circ$C, end over end. The beads were washed four times with 25 column volumes of Buffer J + 300 mM NaCl. 1X SDS-PAGE Buffer was added to each sample and boiled for 5 mins at 100 $^\circ$C. Samples were separated by a 12 % SDS-PAGE and stained with Coomassie Blue. The assay was carried out in duplicate with a representative figure shown above.

Figure 4.10: **Quantification of the Disruption of iASPP$_{608\text{-}828}$ from Binding PP-1cα in the Presence of 50 μM, 75 μM, and 100 μM of Halistanol Sulfate.** The amount of iASPP$_{608\text{-}828}$ density in a positive control lane. These values were averaged with the duplicate experiment and plotted.
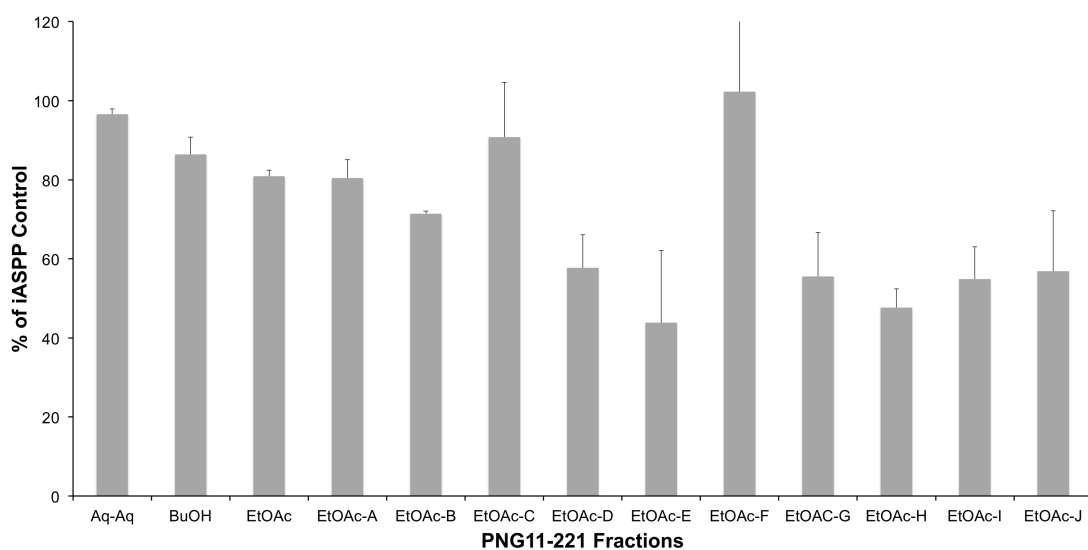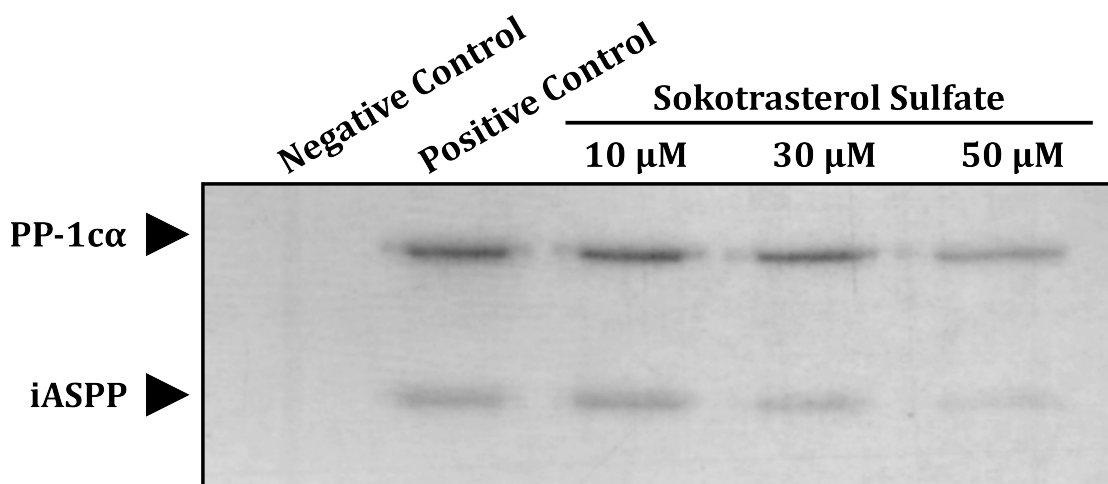
Figure 4.11: **The Disruption of PP-1cα•iASPP$_{608\text{-}828}$ Binding by 10 μM, 30 μM, and 50 μM of Sokotrasterol Sulfate.** MC-S (20 μL) was washed first with 25 column volumes of ddH$_2$O and centrifuged at 3,500 rpm for 1.5 mins at room temperature. The beads were then washed twice with 25 column volumes of Buffer J + 150 mM NaCl. PP-1cα (2 μg) was incubated with the MC-S for 1 hr at 4 °C, end over end and the beads were washed twice with 25 column volumes of Buffer J + 150 mM NaCl. iASPP$_{608\text{-}828}$ (1 μg) along with 10 μM, 30 μM, or 50 μM of Sokotrasterol Sulfate was incubated with the PP-1cα-bound MC-S for 1 hr at 4 °C, end over end. The beads were washed four times with 25 column volumes of Buffer J + 300 mM NaCl. 1X SDS-PAGE Buffer was added to each sample and boiled for 5 mins at 100 °C. Samples were separated by a 12 % SDS-PAGE and stained with Coomassie Blue. The assay was carried out in duplicate with representative figure shown above.

Figure 4.12: **Quantification of the Disruption of iASPP$_{608-828}$ from Binding PP-1cα in the Presence of 10 μM, 30 μM, and 50 μM of Sokotrasterol Sulfate.** The amount of iASPP$_{608-828}$ density in a positive control lane. These values were averaged with the duplicate experiment and plotted.

Figure 4.13: **The Disruption of PP-1cα•iASPP$_{608\text{-}828}$ Binding by 25 μM, 50 μM, and 75 μM of Suvanine.** MC-S (20 μL) was washed first with 25 column volumes of ddH$_2$O and centrifuged at 3,500 rpm for 1.5 mins at room temperature. The beads were then washed twice with 25 column volumes of Buffer J + 150 mM NaCl. PP-1cα (2 μg) was incubated with the MC-S for 1 hr at 4 °C, end over end and the beads were washed twice with 25 column volumes of Buffer J + 150 mM NaCl. iASPP$_{608\text{-}828}$ (1 μg) along with 25 μM, 50 μM, or 75 μM of Suvanine was incubated with the PP-1cα-bound MC-S for 1 hr at 4 °C, end over end. The beads were washed four times with 25 column volumes of Buffer J + 300 mM NaCl. 1X SDS-PAGE Buffer was added to each sample and boiled for 5 mins at 100 °C. Samples were separated by a 12 % SDS-PAGE and stained with Coomassie Blue. The assay was carried out in duplicate with a representative figure shown above.

Figure 4.14: **Quantification of the Disruption of iASPP$_{608\text{-}828}$ from Binding PP-1cα in the Presence of 25 μM, 50 μM, and 75 μM of Suvanine.** The amount of iASPP$_{608\text{-}828}$ density in a positive control lane. These values were averaged with the duplicate experiment and plotted.

4.2.2 Halistanol Sulfate, Sokotrasterol Sulfate, and Suvanine do not Disrupt the Binding of GST-TIMAP Binding to PP-1cγ

Once the potency of Halistanol Sulfate, Sokotrasterol Sulfate, and Suvanine was established, the next important step was to test the specificity of the compounds. The ef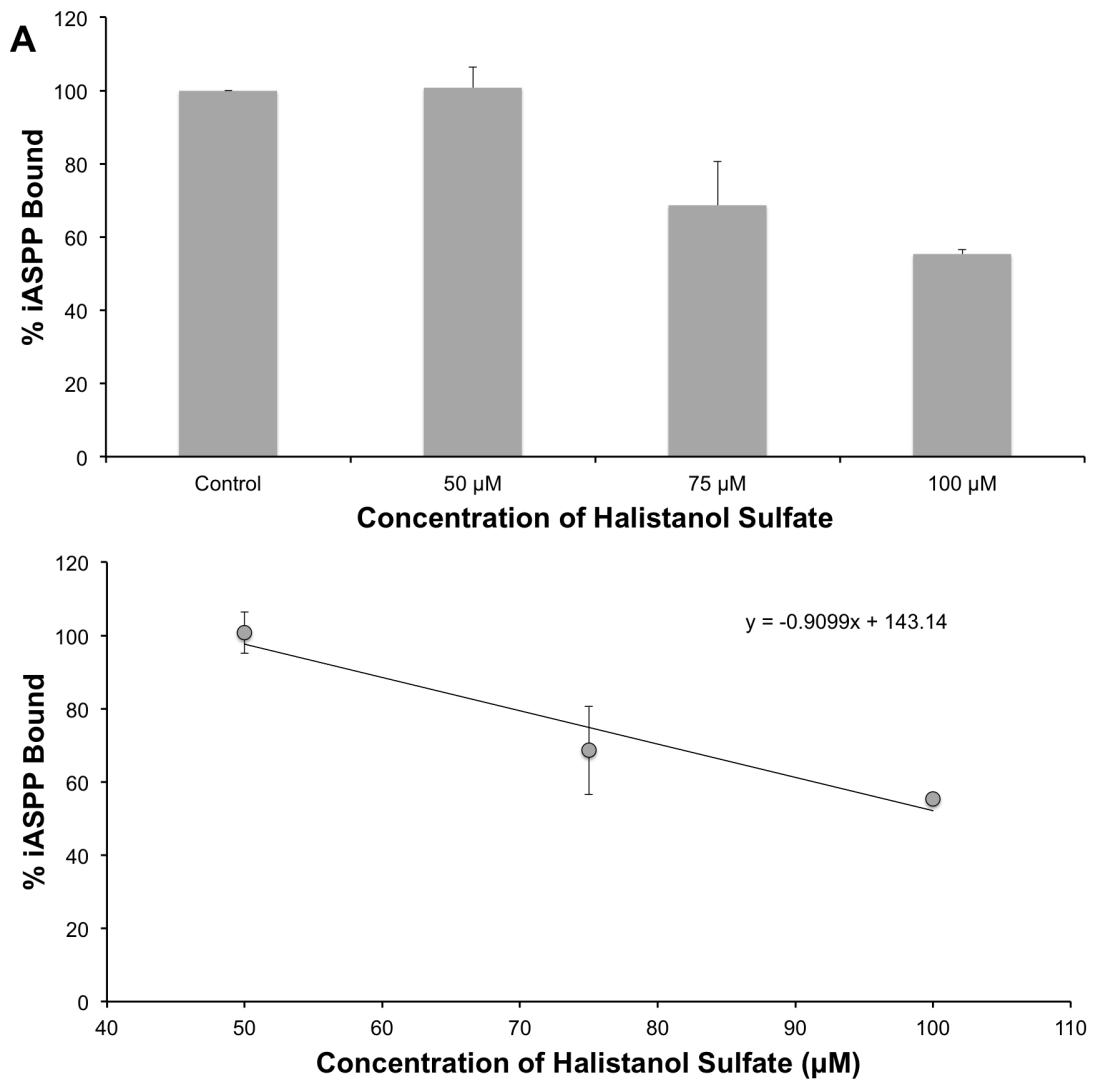fects of each compound against the binding of TGF-β-inhibited membrane-associated protein (TIMAP) to PP-1c were investigated. As mentioned in Section 1.5, TIMAP is a member of the myosin phosphatase targeting protein (MYPT) family of PP-1 regulatory subunits. Testing Halistanol Sulfate, Sokotrasterol Sulfate, and Suvanine against binding of TIMAP•PP-1cγ serves as a control to determine if there is specificity for the disruption of the ASPP family. As well, MYPT1 is one of the few crystal structures of PP-1c bound to a regulatory subunit [145]. This gives huge insight into how PP-1c is interacting with TIMAP and how the compounds might be affecting the protein complex.

The compounds were tested at the same concentrations as were used in the iASPP•PP-1cα disruption assay, to obtain the most accurate comparison as possible (as described in Section 2.8). When compared to the MC-S disruption assay used in Section 4.2.1, there are two major differences in this assay. Firstly, Glutathione-4B Sepharose (GS) beads were used, which bound full-length TIMAP (1.5 μg) first followed by PP-1c (1 μg). Secondly, the gamma (γ) isoform of PP-1c was used instead of PP-1cα because PP-1cγ has been shown to bind to TIMAP more efficiently.

The specificity of 50 μM, 75 μM, and 100 μM of Halistanol Sulfate towards TIMAP•PP-1cγ binding was tested and results are shown in Figure 4.15. The results indicate that there is no significant disruption of PP-1cγ from TIMAP. This was quantified in Figure 4.16, which depicts the values of PP-1cγ relative to the control and also shows that as the concentration of Halistanol Sulfate increased, the amount of PP-1cγ present remained unchanged.

Secondly, Sokotrasterol Sulfate was tested against TIMAP•PP-1cγ binding to measure the effect affect against other PP-1c regulatory proteins at 10 μM, 30 μM, and 50 μM

concentrations (Figure 4.17). Sokotrasterol Sulfate also did not demonstrate disruption of TIMAP•PP-1cγ binding at the concentrations capable of disrupting iASPP$_{608\text{-}828}$. As depicted in Figure 4.18, the quantities of PP-1cγ remained the same relative to the control when 10 μM, 30 μM, and, 50 μM of Sokotrasterol Sulfate was present.

Finally, the compound Suvanine was analyzed at 25 μM, 50 μM, and 75 μM concentrations in the presence of TIMAP and PP-1cγ. Similar to Halistanol Sulfate and Sokotrasterol Sulfate, Suvanine does not impact the binding of PP-1cγ at these concentrations (Figure 4.19). The levels of PP-1cγ stayed equal across all lanes in this assay (Figure 4.20).
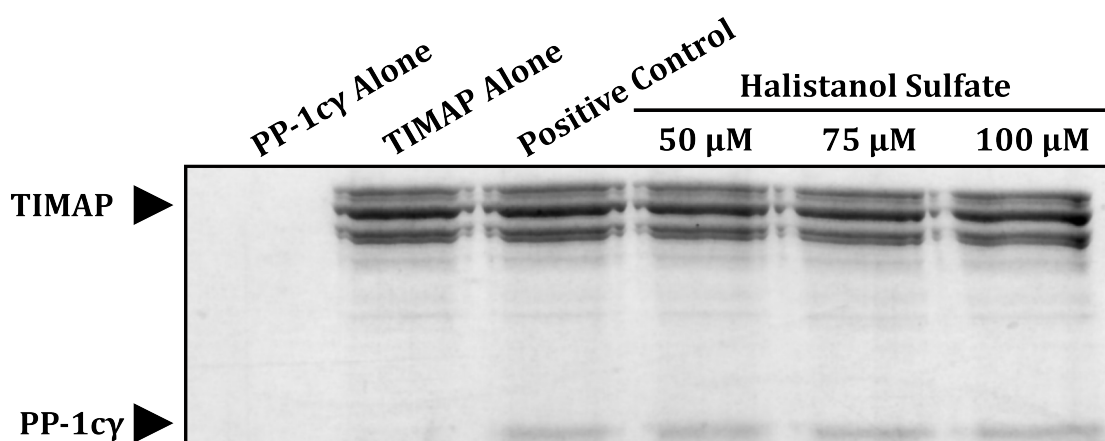
Figure 4.15: **Halistanol Sulfate Does Not Disrupt Binding of PP-1cγ to TIMAP.** GS (20 μL) was washed first with 25 column volumes of ddH$_2$O and centrifuged at 3,500 rpm for 1.5 mins at room temperature. The beads were then washed twice with 25 column volumes of Buffer K + 150 mM NaCl. TIMAP (1.5 μg) was incubated with the GS for 1 hr at 4 °C, end over end and the beads were washed twice with 25 column volumes of Buffer K + 150 mM NaCl. PP-1cγ (1 μg) along with 50 μM, 75 μM, or 100 μM of Halistanol Sulfate was incubated with the TIMAP-bound GS for 1 hr at 4 °C, end over end. The beads were washed four times with 25 column volumes of Buffer K + 300 mM NaCl. 1X SDS-PAGE Buffer was added to each sample and boiled for 5 mins at 100 °C. Samples were separated by a 10 % SDS-PAGE and stained with Coomassie Blue. The assay was carried out in duplicate with a representative figure shown above.
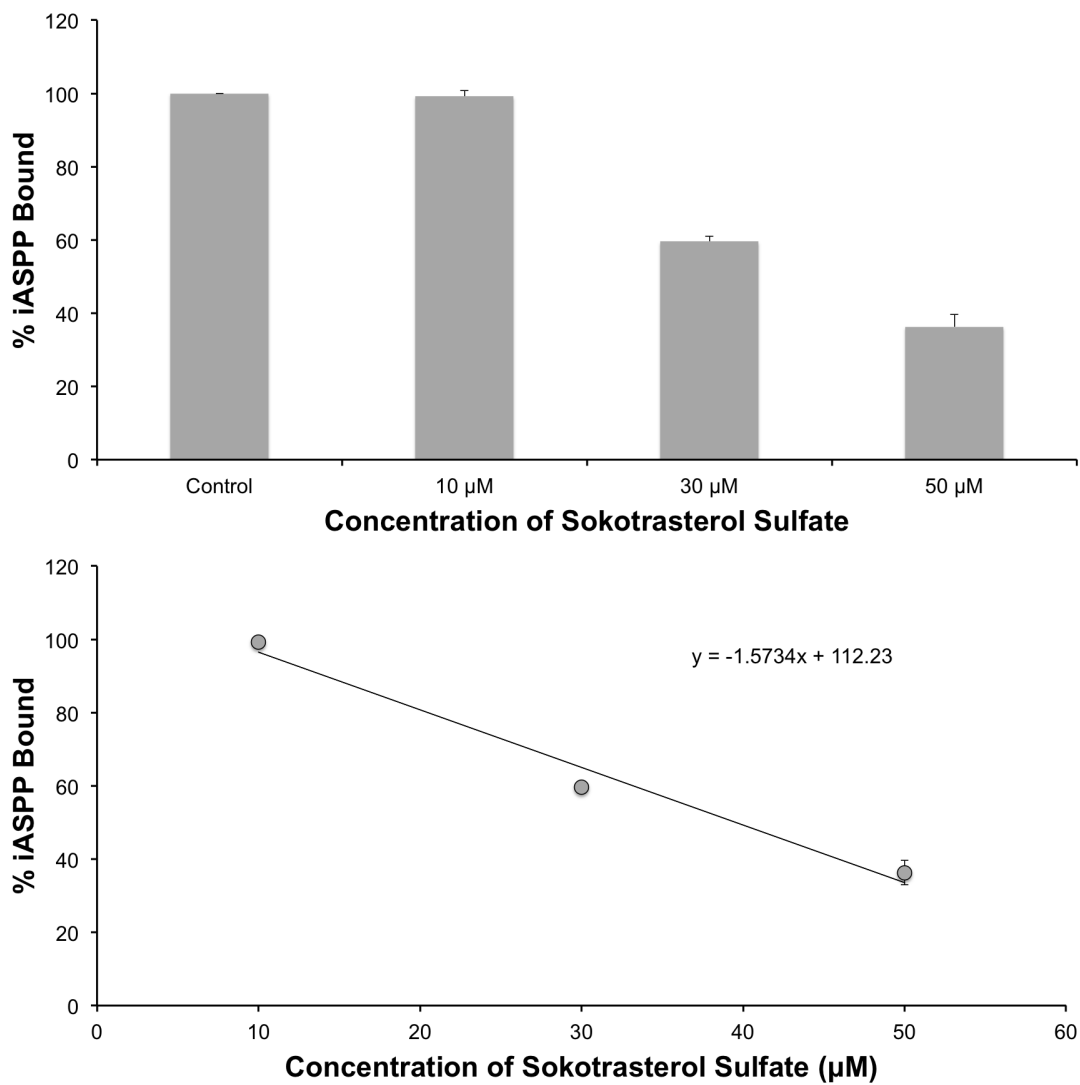
Figure 4.16: **Quantitative of the Disruption of PP-1cγ from Binding TIMAP in the Presence of 50 μM, 75 μM, and 100 μM of Halistanol Sulfate.** The amount of PP-1γ density in a positive control lane. These values were averaged with the duplicate experiment and plotted.
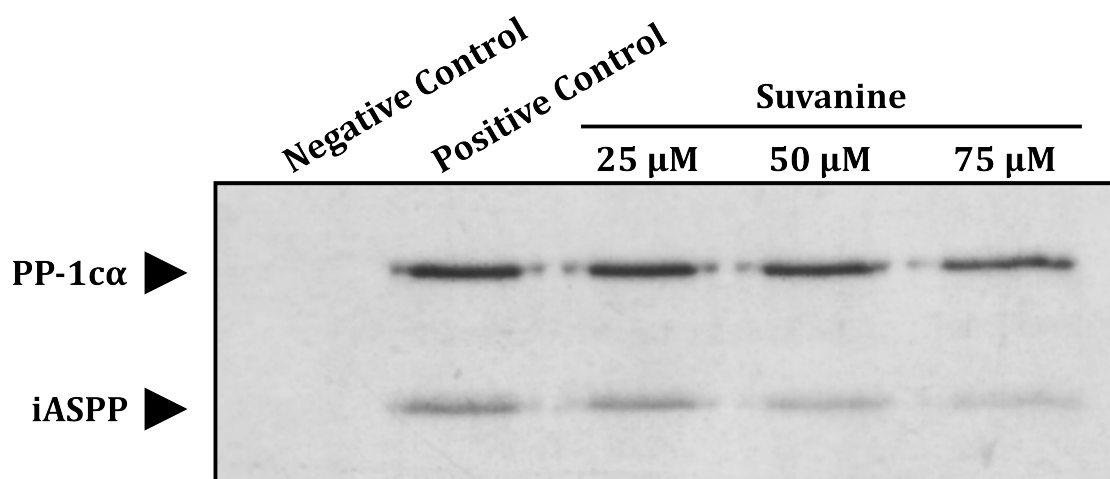
Figure 4.17: **Sokotrasterol Sulfate Does Not Disrupt Binding of PP-1cγ to TIMAP.** GS (20 μL) was washed first with 25 column volumes of ddH$_2$O and centrifuged at 3,500 rpm for 1.5 mins at room temperature. The beads were then washed twice with 25 column volumes of Buffer K + 150 mM NaCl. TIMAP (1.5 μg) was incubated with the GS for 1 hr at 4 °C, end over end and the beads were washed twice with 25 column volumes of Buffer K+ 150 mM NaCl. PP-1cγ (1 μg) along with 10 μM, 30 μM, or 50 μM of Sokotrasterol Sulfate was incubated with the TIMAP-bound GS for 1 hr at 4 °C, end over end. The beads were washed four times with 25 column volumes of Buffer K + 300 mM NaCl. 1X SDS-PAGE Buffer was added to each sample and boiled for 5 mins at 100 °C. Samples were separated by a 10 % SDS-PAGE and stained with Coomassie Blue. The assay was carried in duplicate with a representative figure shown above.
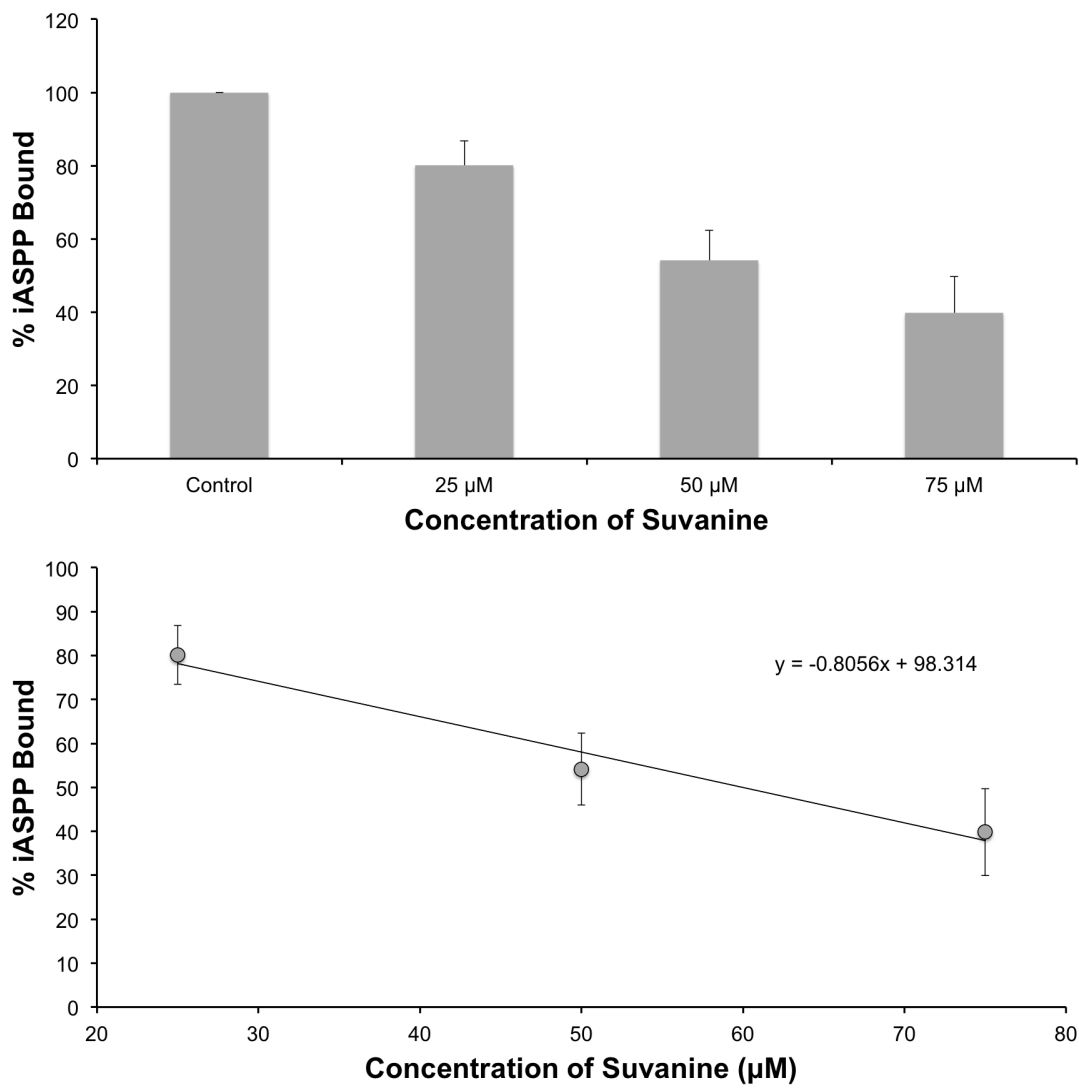
Figure 4.18: **Quantification of the Disruption of PP-1cγ from Binding TIMAP in the Presence of 10 μM, 30 μM, or 50 μM of Sokotrasterol Sulfate.** The amount of PP-1γ density in a positive control lane. These values were averaged with the duplicate experiment and plotted.
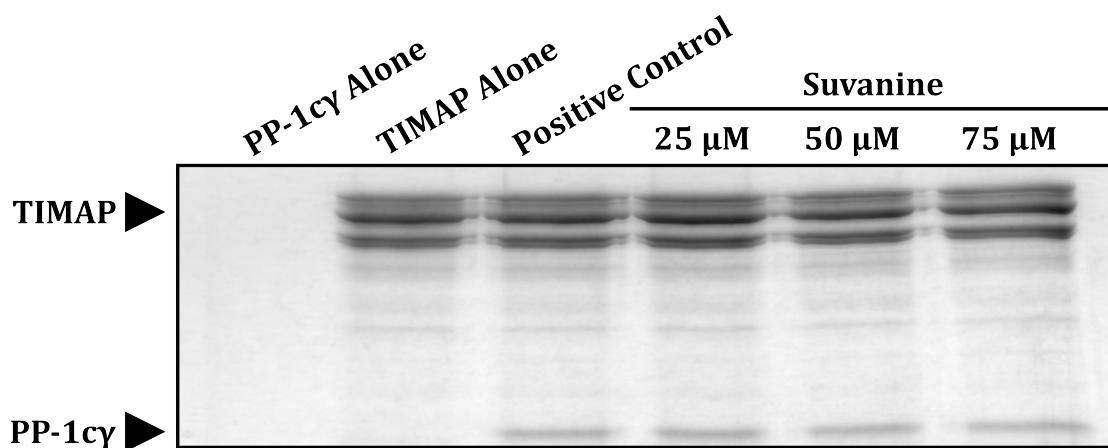
Figure 4.19: **Suvanine Does Not Disrupt Binding of PP-1cγ to TIMAP.** GS (20 μL) was washed first with 25 column volumes of ddH$_2$O and centrifuged at 3,500 rpm for 1.5 mins at room temperature. The beads were then washed twice with 25 column volumes of Buffer K + 150 mM NaCl. TIMAP (1.5 μg) was incubated with the GS for 1 hr at 4 °C, end over end and the beads were washed twice with 25 column volumes of Buffer K + 150 mM NaCl. PP-1cγ (1 μg) along with 25 μM, 50 μM, or 75 μM of Suvanine was incubated with the TIMAP-bound GS for 1 hr at 4 °C, end over end. The beads were washed four times with 25 column volumes of Buffer K + 300 mM NaCl. 1X SDS-PAGE Buffer was added to each sample and boiled for 5 mins at 100 °C. Samples were separated by a 10 % SDS-PAGE and stained with Coomassie Blue. The assay was carried out in duplicate with a representative sample shown above.

Figure 4.20: **Quantification of the Disruption of PP-1cγ from Binding TIMAP in the Presence of 25 μM, 50 μM, or 75 μM of Suvanine.** The amount of PP-1γ density in a positive control lane. These values were averaged with the duplicate experiment and plotted.

4.2.3 Halistanol Sulfate and Sokotrasterol Sulfate, but not Suvanine were able to Disrupt the ASPP2•PP-1cα Binding Complex

Once it was established that Halistanol Sulfate, Sokotrasterol Sulfate displayed specificity for disruption of the ASPP family by not disrupting the MYPT family at the similar concentrations, it was important to determine their specificity for the different members within the ASPP family. Specifically, I analyzed the effects of each compound on the binding of ASPP2$_{905\text{-}1128}$ to PP-1cα were tested. As mentioned previously, ASPP2 is an ASPP family member that is responsible for the activation p53 pro-apoptotic activity. The effects of the three compounds were analyzed using the same MC-S disruption assay that was used for testing iASPP•PP-1c disruption (Section 4.2.1).

Figure 4.21 shows the results from the ASPP2$_{608\text{-}828}$•PP-1cα disruption assay in the presence of 50 μM, 75 μM, and 100 μM of Hali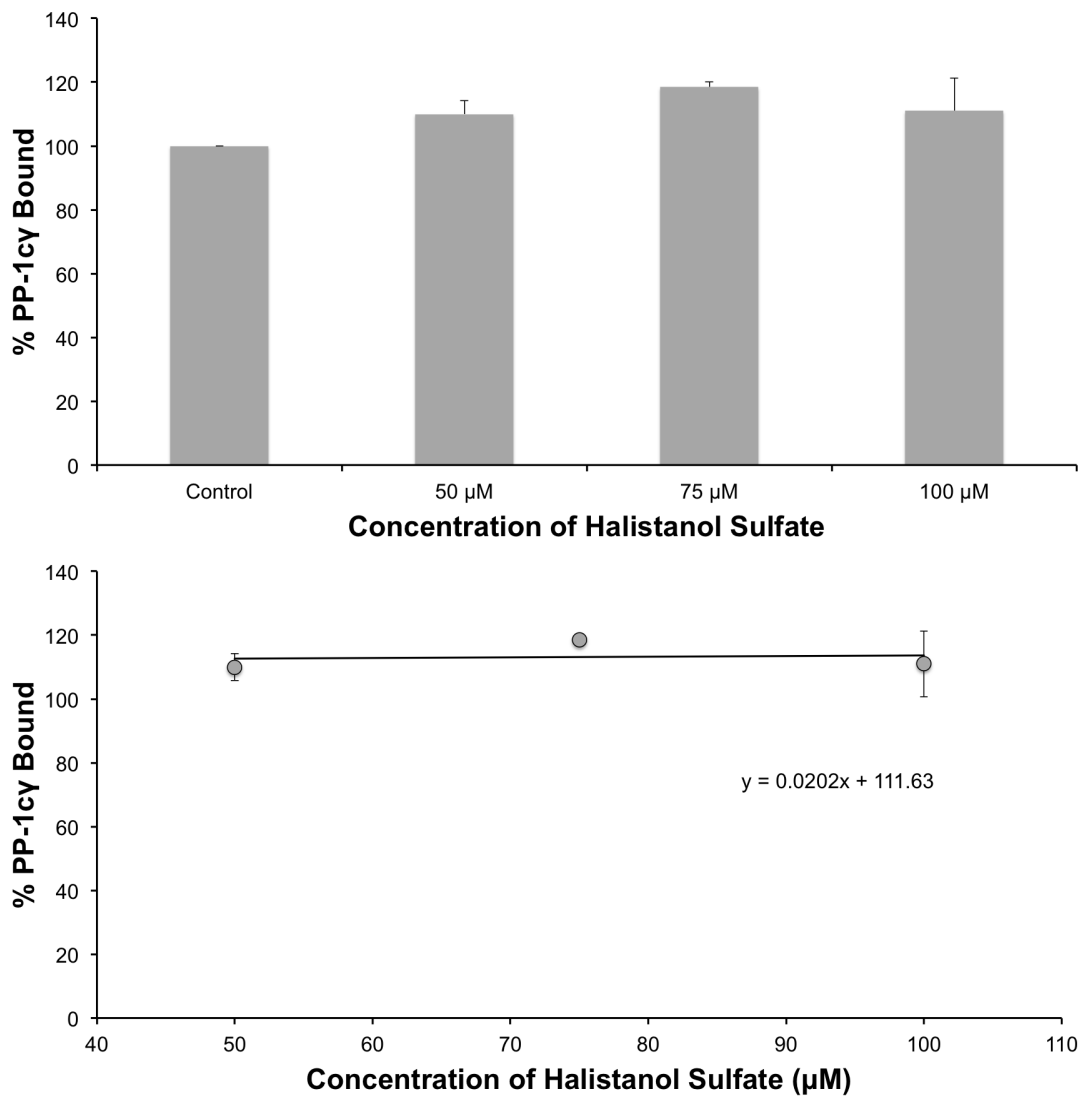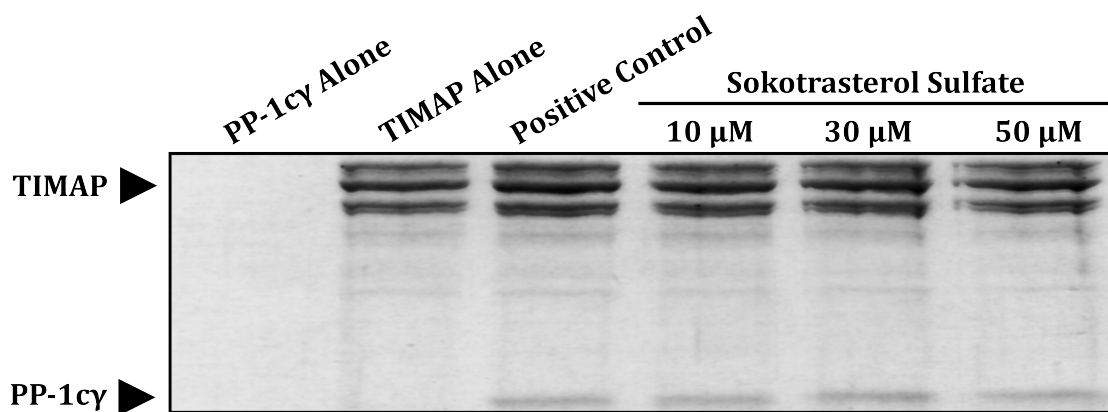stanol Sulfate. There was significant disruption of ASPP2 from PP-1c (Figure 4.22) and Halistanol Sulfate disrupted ASPP2 to a greater extent than it disrupted iASPP. Therefore, it appears there is a greater potency against ASPP2•PP-1cα disruption than iASPP•PP-1cα disruption. Based on the data in Figure 4.22, it can be said that the DC$_{50}$ of Halistanol Sulfate against ASPP2 is less than 50 μM in this assay. This is significantly lower that the DC$_{50}$ for iASPP disruption. As well, there was significant disruption of PP-1cα from the MC-S beads which again suggests that Halistanol Sulfate might bind near the active site of PP-1cα.

Secondly, 10 μM, 30 μM, and 50 μM of Sokotrasterol Sulfate was tested in the ASPP2$_{905\text{-}1128}$•PP-1cα disruption assay (shown in Figure 4.23). Sokotrasterol Sulfate disrupted ASPP2 at approximately the same potency to its disruption of iASPP to PP-1c (as seen previously in Figure 4.24). Therefore, Sokotrasterol Sulfate did not demonstrate significant specificity for iASPP over ASPP2. The DC$_{50}$ is 32 μM, which is similar the DC$_{50}$ value in the iASPP binding assay (40 μM).

Lastly, Suvanine was tested within the PP-1cα•ASPP2$_{905\text{-}1128}$ disruption assay at concentrations of 25 μM, 50 μM, and 75 μM. Unlike Sokotrasterol Sulfate and Halistanol Sulfate, Suvanine did not disrupt the binding of ASPP2$_{905\text{-}1128}$ to PP-1cα (Figure 4.26).

Suvanine demonstrated increased iASPP disruption from PP-1cα than ASPP2. Again, the DC$_{50}$ for each compound within the slope equation was not established due to very limited amounts of each compound. This assay was performed for comparison with iASPP disruption .
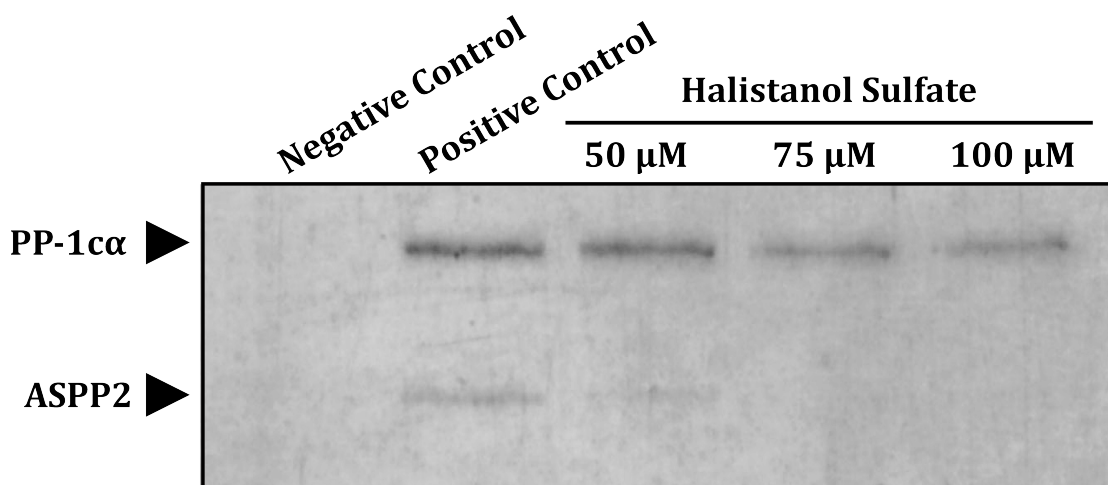
Figure 4.21: **The Disruption of PP-1c$\alpha \bullet$ASPP2$_{905\text{-}1128}$ Binding by 50 μM, 75 μM, and 100 μM of Halistanol Sulfate.** MC-S (20 μL) was washed first with 25 column volumes of ddH$_2$O and centrifuged at 3,500 rpm for 1.5 mins at room temperature. The beads were then washed twice with 25 column volumes of Buffer J + 150 mM NaCl. PP-1cα (2 μg) was incubated with the MC-S for 1 hr at 4 °C, end over end and the beads were washed twice with 25 column volumes of Buffer J + 150 mM NaCl. ASPP2$_{905\text{-}1128}$ (2 μg) along with 50 μM, 75 μM, or 100 μM of Halistanol Sulfate was incubated with the PP-1cα-bound MC-S for 1 hr at 4 °C, end over end. The beads were washed four times with 25 column volumes of Buffer J + 300 mM NaCl. 1X SDS-PAGE Buffer was added to each sample and boiled for 5 mins at 100 °C. Samples were separated by a 12 % SDS-PAGE and stained with Coomassie Blue. The assay was carried out in duplicate with a representative figure shown above.
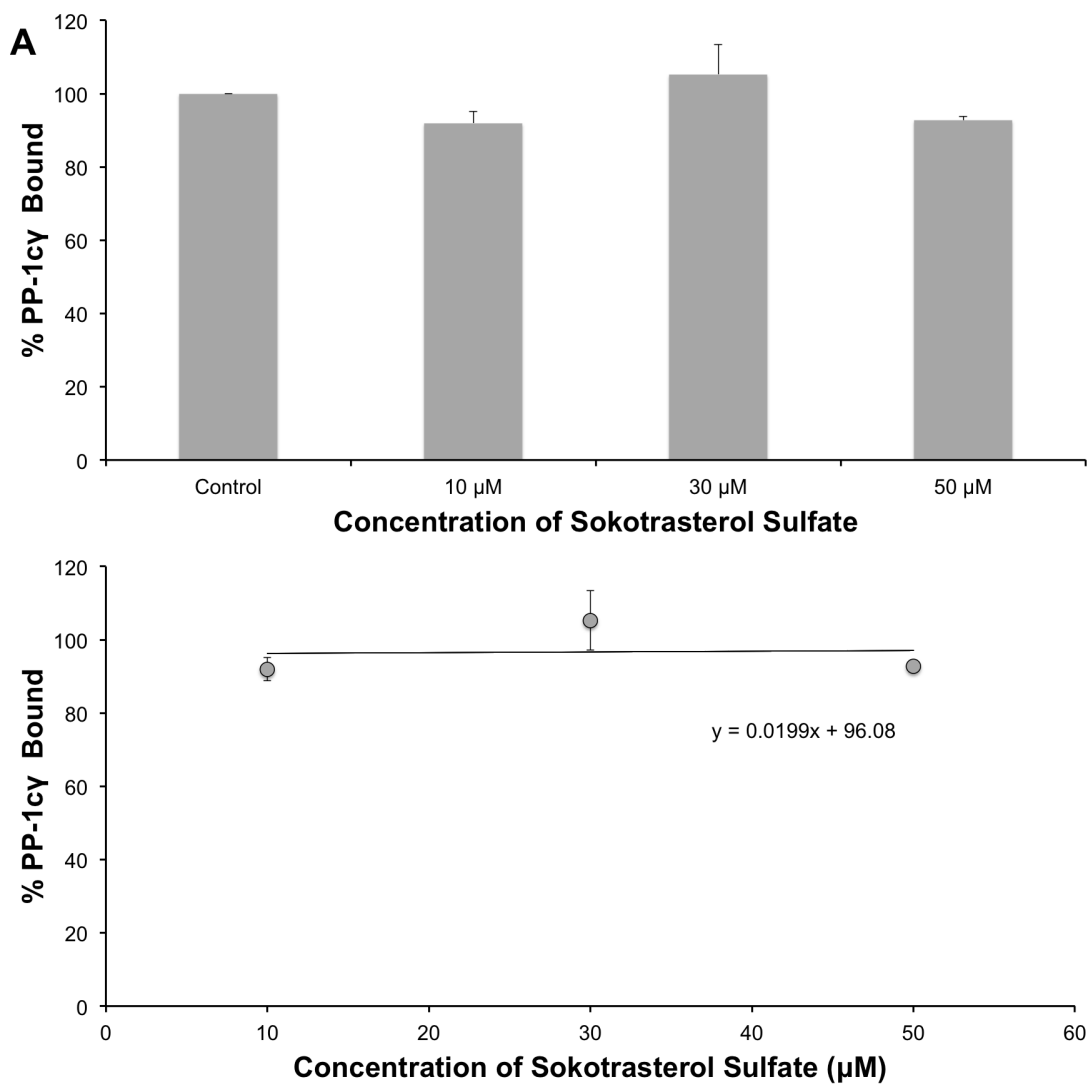
Figure 4.22: **Quantification of the Disruption of ASPP2$_{905\text{-}1128}$ from Binding PP-1cα in the Presence of 50 μM, 75 μM, and 100 μM of Halistanol Sulfate.** The amount of ASPP2$_{905\text{-}1128}$ density in a positive control lane. These values were averaged with the duplicate experiment and plotted.
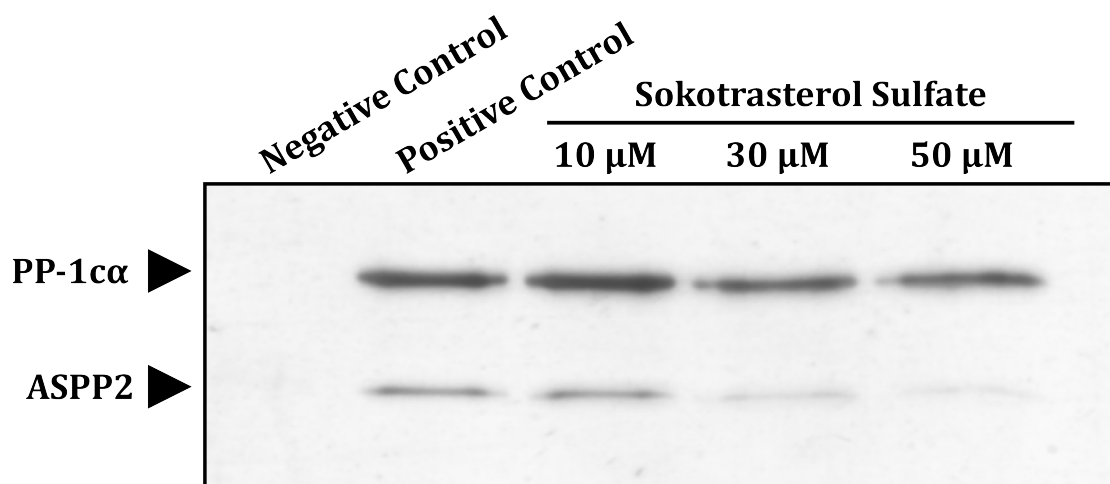
Figure 4.23: **The Disruption of PP-1c$\alpha\bullet$ASPP2$_{905\text{-}1128}$ Binding by 10 μM, 30 μM, and 50 μM Sokotrasterol Sulfate.** MC-S (20 μL) was washed first with 25 column volumes of ddH$_2$O and centrifuged at 3,500 rpm for 1.5 mins at room temperature. The beads were then washed twice with 25 column volumes of Buffer J + 150 mM NaCl. PP-1cα (2 μg) was incubated with the MC-S for 1 hr at 4 $^\circ$C, end over end and the beads were washed twice with 25 column volumes of Buffer J + 150 mM NaCl. ASPP2$_{905\text{-}1128}$ (2 μg) along with 10 μM, 30 μM, or 50 μM of Sokotrasterol Sulfate was incubated with the PP-1cα-bound MC-S for 1 hr at 4 $^\circ$C, end over end. The beads were washed four times with 25 column volumes of Buffer J + 300 mM NaCl. 1X SDS-PAGE Buffer was added to each sample and boiled for 5 mins at 100 $^\circ$C. Samples were separated by a 12 % SDS-PAGE and stained with Silver Stain. The assay was carried out in duplicate with a representative figure shown above.
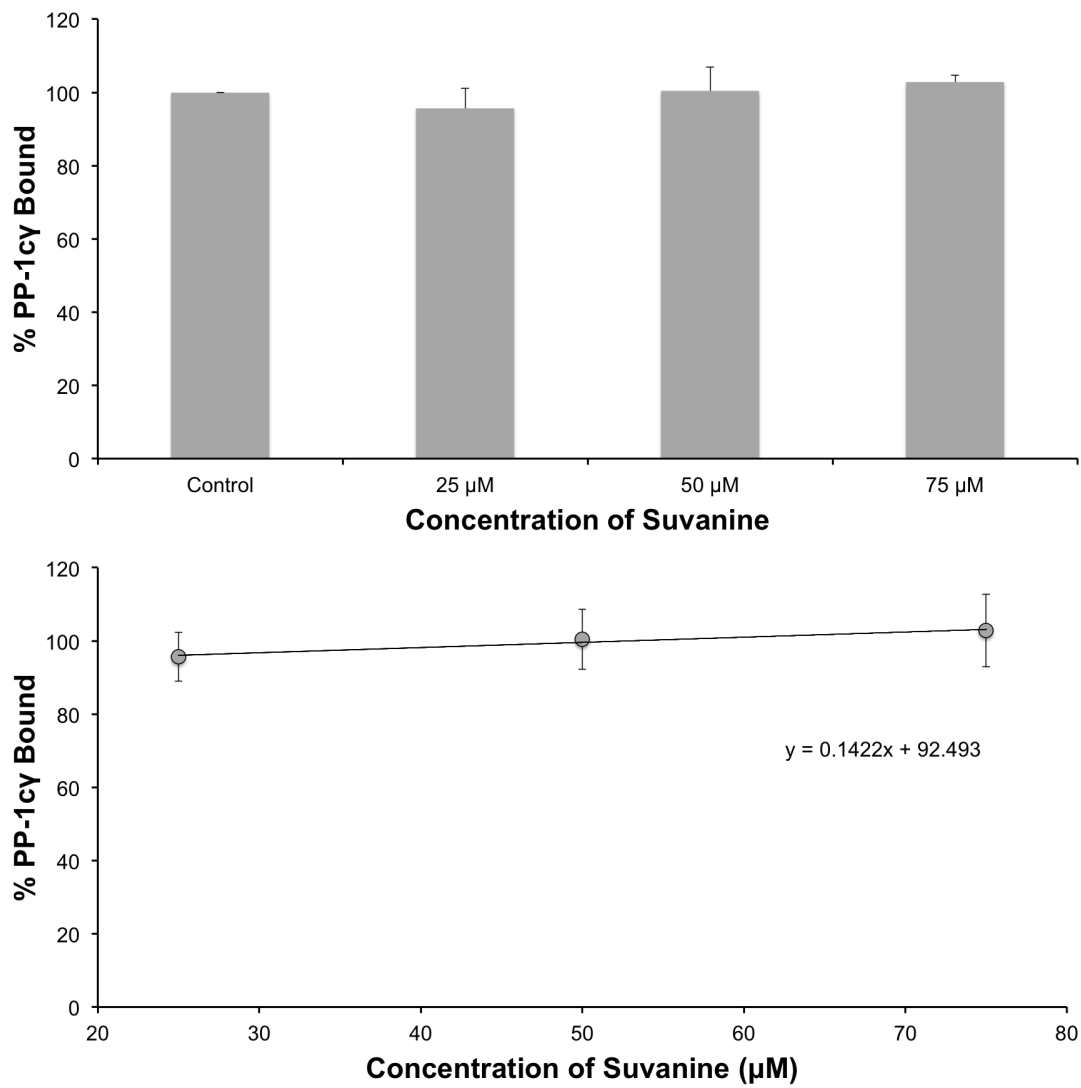
Figure 4.24: **Quantification of the Disruption of ASPP2$_{905\text{-}1128}$ from Binding PP-1cα in the Presence of 10 μM, 30 μM, or 50 μM of Sokotrasterol Sulfate.** The amount of ASPP2$_{905\text{-}1128}$ density in a positive control lane. These values were averaged with the duplicate experiment and plotted.
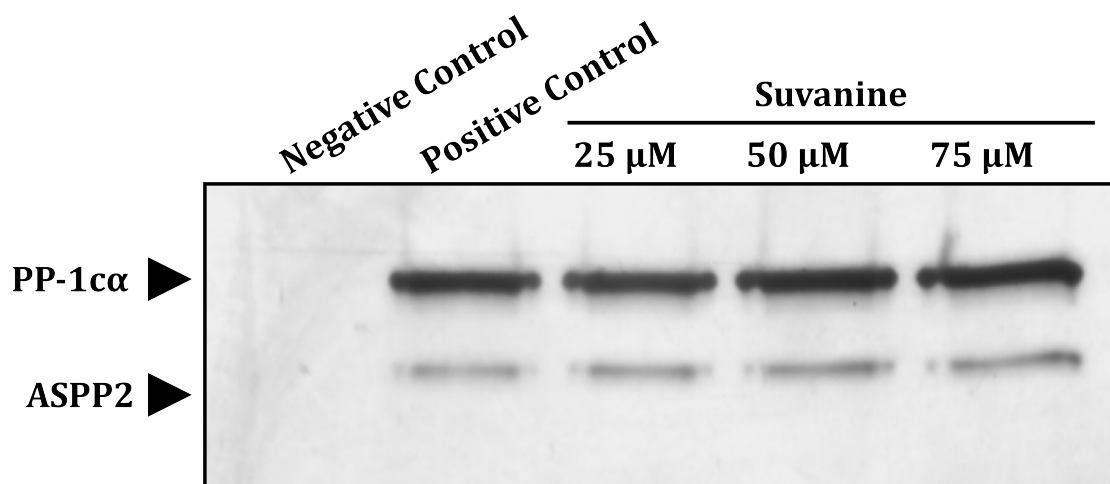
Figure 4.25: **The Disruption of PP-1cα•ASPP2$_{905-1128}$ Binding by 25 μM, 50 μM, and 75 μM of Suvanine.** MC-S (20 μL) was washed first with 25 column volumes of ddH$_2$O and centrifuged at 3,500 rpm for 1.5 mins at room temperature. The beads were then washed twice with 25 column volumes of Buffer J + 150 mM NaCl. PP-1cα (2 μg) was incubated with the MC-S for 1 hr at 4 °C, end over end and the beads were washed twice with 25 column volumes of Buffer J + 150 mM NaCl. ASPP2$_{905-1128}$ (2 μg) along with 125 μM, 50 μM, or 75 μM of Suvanine was incubated with the PP-1cα-bound MC-S for 1 hr at 4 °C, end over end. The beads were washed four times with 25 column volumes of Buffer J + 300 mM NaCl. 1X SDS-PAGE Buffer was added to each sample and boiled for 5 mins at 100 °C. Samples were separated by a 12 % SDS-PAGE and stained with Silver Stain. The assay was carried out in duplicate with a representative figure shown above.

Figure 4.26: **Quantification of the Disruption of ASPP2$_{905\text{-}1128}$ from Binding PP-1cα in the Presence of 25 μM, 50 μM, or 75 μM of Suvanine.** The amount of ASPP2$_{905\text{-}1128}$ density in a positive control lane. These values were averaged with the duplicate experiment and plotted.

4.3   Identification of Potent Protein Phosphatase-1c Inhibitors

During the initial screening with the pNPP phosphatase activity assay in Section 3.1.2, two marine extracts exhibited potent PP-1cα inhibition. Marine extract PNG11-279 resulted in 99 % PP-1cα inhibition while PNG11-285 resulted in 95 % inhibition. Although, the main goal of the thesis was to identify iASPP•PP-1cα disruptors, we wanted to identity the compounds responsible for this inhibition. Small molecules that are potent and specific inhibitors of PP-1c are extremely useful research tools. As well, if found to be cell permeable, these compounds could also be used in biological studies.

4.3.1   Identification of Marine Extract PNG11-279 as Motuporin

Marine extract PNG11-279 was previously identified as a potent inhibitor of PP-1cα by me prior to the start of my Masters project (inhibition data seen in Table 3.2). Using the assay-guided purification process described 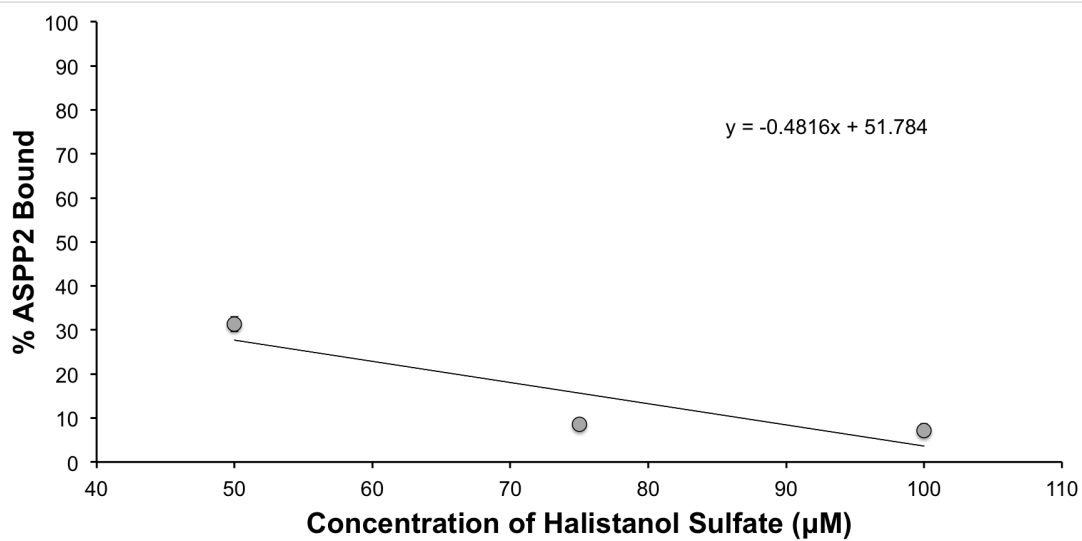in Section 2.9, the compound responsible for the inhibition was identified via NMR as a small molecule known as Motuporin (shown in Figure 4.27). This conclusion was confirmed when the crude PNG11-279 extract (750 μg) in 1 mL of Solvent A was analyzed via high performance liquid chromatography (HPLC) at $\text{Abs}_{214 \text{ nM}}$ (chromatograph shown in Figure 4.28). The crude extract was injected onto a C18 reverse phase column and eluted using a linear solvent gradient of 0-100 % Solvent B over 80 mins at a flowrate of 1 mL/min. This was followed by 100 % Solvent B for 10 mins and 0 % Solvent A for 5 mins. Fractions (1 mL) were collected and analyzed by addition (10 μL) to a pNPP assay. Fraction 54, in Figure 4.29, produced significant PP-1cα inhibition ($\sim$ 100 %) suggesting it contains the inhibitory compound. There is a large peak at the corresponding chromatograph fraction (53.31 mins). Based on standards carried out by Ply Pasarj, a fellow lab-member, under the same conditions, Motuporin had the same retention time. This strongly suggested that PNG11-279 contained the compound Motuporin, which was responsible for the PP-1cα activity inhibition.

Motuporin is a cyclic pentapeptide from the Nodularin class of toxins that are structurally related to Microcystins. Most notably, they contain an ADDA amino acid at position 5 like Microcystin, but Nodularins only have one variable position at position 4, rather than two. At said variable position, Motuporin contains a valine residue, hence its second name, Nodularin-V.
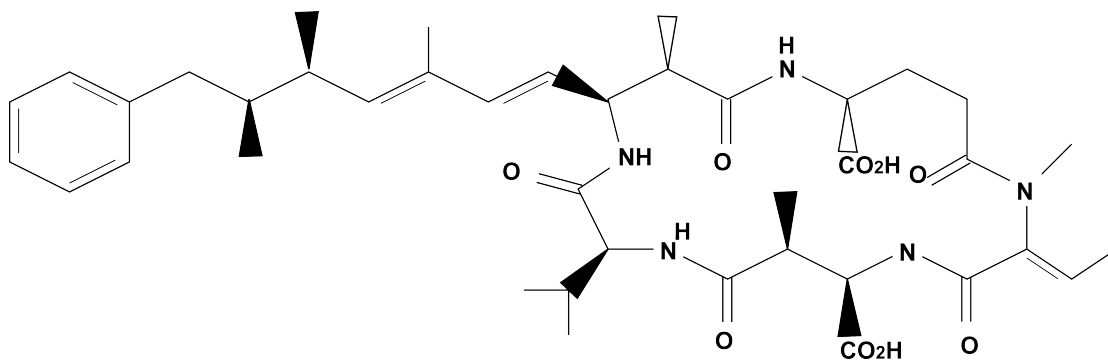
Figure 4.27: **The Chemical Structure of Motuporin (Marine Extract PNG11-279).** Motuporin, also known as Nodularin-V, is cyclic pentapeptide from the Nodularin class of PP-1c toxins. Motuporin contains the β-amino acid ADDA and a valine in the Nodularin variable residue position [124].

4.3.2 Identification of Marine Extract PNG11-285 as a Novel PP-1c Inhibitor

Marine extract PNG11-285 was the second marine extract identified as a potent PP-1cα inhibitor. Figure 4.31 depicts the assay-guided partitioning as described previously in Section 2.9 resulting in fractions Aq-Aq, BuOH, EtOAc, BuOH-A to BuOH-D and BuOH-A-1 to BuOH-A-3. All fractions were analyzed for PP-1cα inhibition via the pNPP activity assay (Figure 4.32). Fraction BuOH-A contained the majority of the inhibition activity and the compound responsible was identified via NMR. It was identified as a novel 4-trimethyl(prop-1-enzyl)azanium, 2-bromophenol compound and the structure is depicted in Figure 4.30. The structure of the compound contains a phenol group with a bromide group attached. As well, there is a two-carbon alkyl chain consisting of an ethene group bound to a trimethylamine, resulting in a positively charged nitrogen.
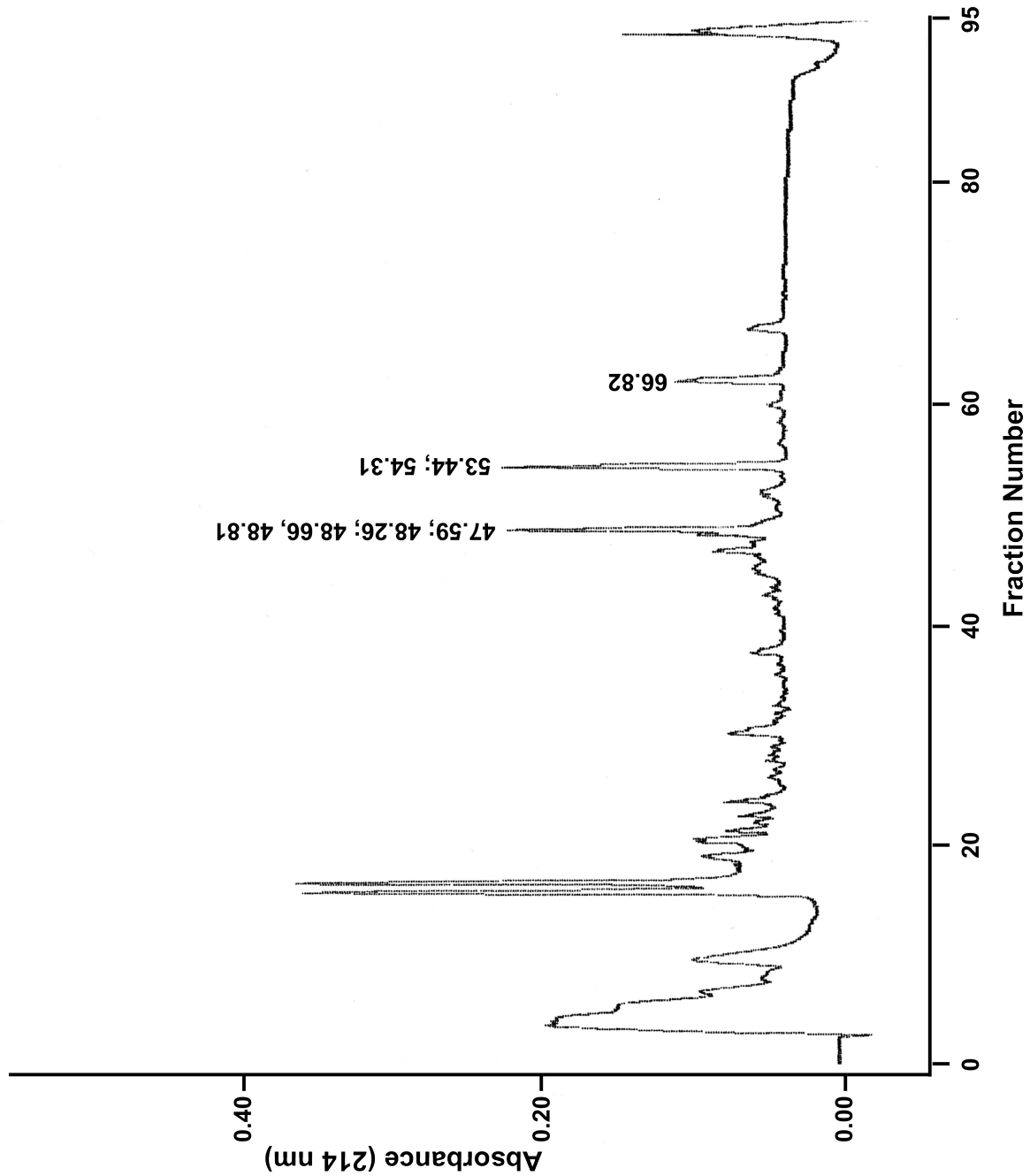
Figure 4.28: **The HPLC Chromatograph of Marine Extract PNG11-279.** Marine extract PNG11-279 (750 μg) was resuspended into 1 mL of Solvent A. The sample was injected onto a HPLC C-18 reverse phase column at a flowrate of 1 mL/min from 100 % Solvent F to 100 % Solvent B over 80 mins. This was followed by 10 mins at 100 % Solvent B and 100 % Solvent A for 5 mins. The absorbance was measured at 214 nm while 1 mL fractions were collected. The largest peaks were present at ∼ 48 mins, ∼ 54 mins, and ∼ 66 mins.

Figure 4.29: **The Inhibition of PP-1cα Activity by HPLC Fractions of Marine Extract PNG11-279.** Fractions (1 mL) were eluted from C18 HPLC column in a solvent gradient of 100 % Solvent A to 100 % Solvent B over 80 mins at a flow rate of 1 mL/min. These fractions along with PP-1cα (27.5 ng) were added to each well of a 96 well plate and incubated for 10 mins at 37 °C. pNPP (5 μM) was added to every well and the initial absorbance was read at 405 nm. The plate was incubated at 37 °C until the absorbance reached between 0.400-0.500 at 405 nm. The Abs$_{final}$ was correct against the Abs$_{initial}$. The Abs$_{corrected}$ was standardized against the Abs$_{control}$ value and the percent of PP-1cα inhibition was calculated and plotted above. The most inhibition was seen in Fraction 54.

104

This small molecule has never before been isolated for having bioactivity. Unfortunately, once this sample was fractionated further into fractions BuOH-A-1 to BuOH-A-3, the activity of the compound was lost and could no longer be used (Figure 4.32).

Additionally, the PNG11-279 and PNG11-285 marine extracts were screened in MC-S disruption assay. Figure 3.4 shows that PNG11-279 decreases PP-1cα binding to the MC-S beads, while PNG11-285 decreased PP-1cα binding less significantly. Disrupting PP-1cα off the MC-S beads indicate that the marine extracts are binding at the PP-1cα active site. Both marine extracts appear to have minimal effect on the binding of iASPP; therefore, are likely binding far from iASPP interactions sites. Again, this confirms that both of these compounds are binding near the PP-1cα active site.
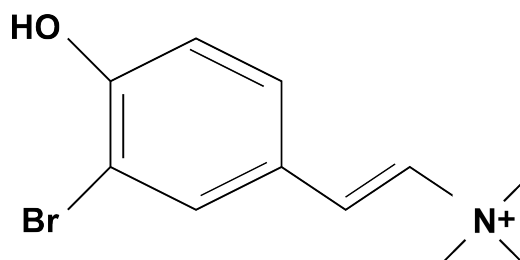
Figure 4.30: **The Chemical Structure of a Novel Bromophenol PP-1cα Inhibitor (Marine Extract PNG11-285).** Above is the chemical structure of the novel compound identified in marine extract PNG11-285. The structure is a bromophenol with alkyl group at position 4. The alkyl chains is a two-carbon chain that has trimethyl amide group holding a positive charge [124].

105
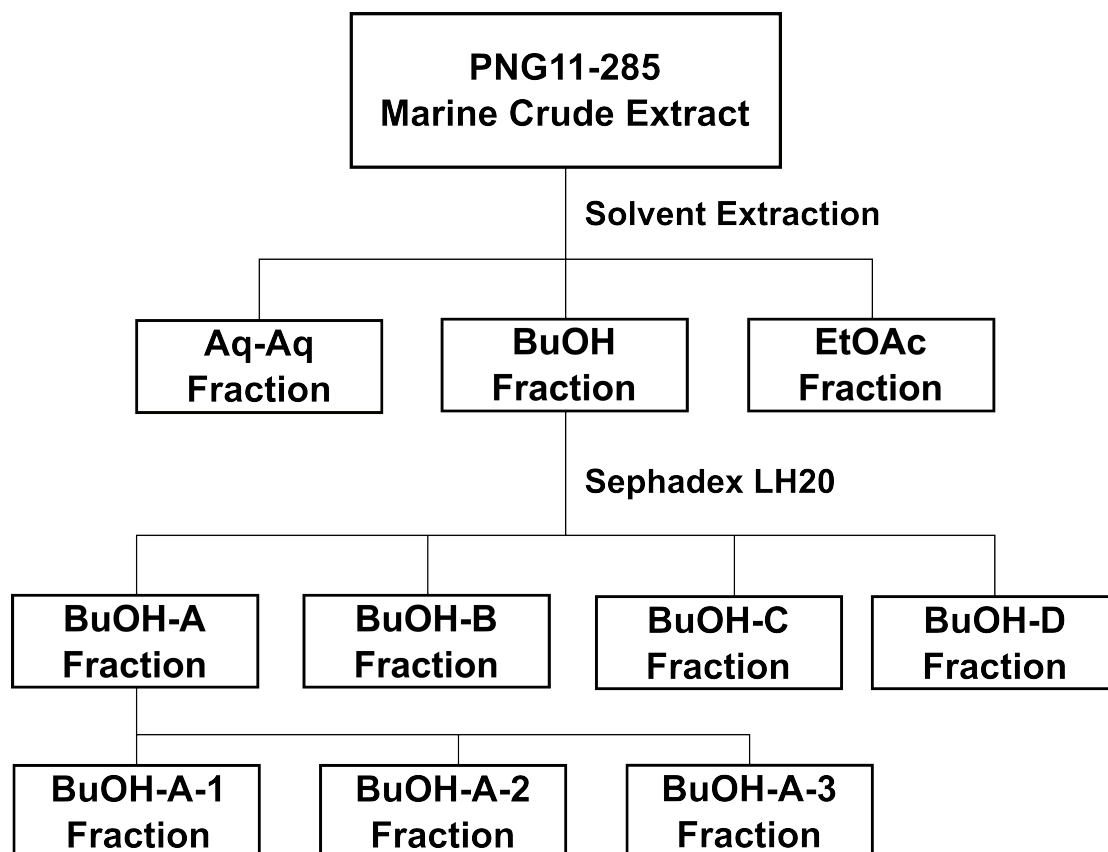
Figure 4.31: **The Fractionation of Marine Extract PNG11-285.** The solvent partitioning lead to Aq-Aq, BuOH, and EtOAc fractions and fraction BuOH was identified to contain the PP-1cα inhibition activity. The BuOH fraction was further purified by Sephadex LH20 fractionation resulting in three additional BuOH fraction (A-C). The activity was identified in the BuOH-A fraction and Coscinamide was identified in this fraction by NMR. The BuOH-A was underwent a second round of Sephadex LH20 partitioning (BuOH-A-1 to BuOH-A-3), but the Coscinamide B activity could no longer be found.
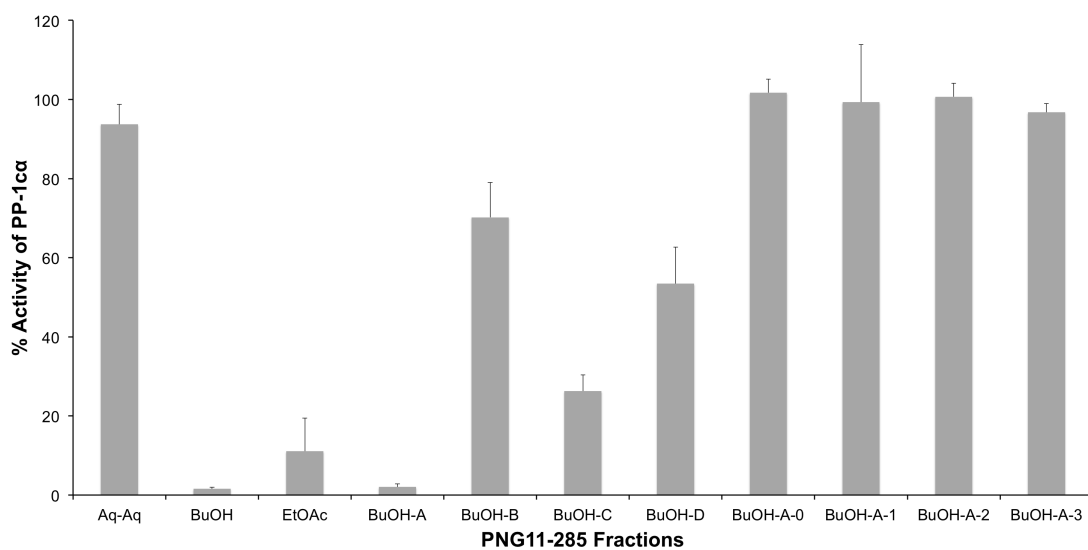
Figure 4.32: **Inhibition of PP-1cα pNPP Activity by PNG11-285 Fractions.**
PNG11-285 fractions (100 μg) along with PP-1cα (27.5 ng) were added to a 96 well
plate and incubated for 10 mins at 37 °C. pNPP (5 μM) was added to every well and
the initial absorbance was read at 405 nm. The plate was incubated at 37 °C until the
absorbance reached between 0.400 - 0.500 at 405 nm. The Abs_{final} was corrected against
the $Abs_{initial}$. The $Abs_{corrected}$ was standardized against the $Abs_{control}$ value and the
percent of control PP-1cα activity was calculated. The assay was complete in triplicate.

Chapter 5

Discussion

5.1 Identification of Marine Extracts that Disrupt the iASPP•PP-1cα Binding Complex

A subset of the marine extracts were tested within the iASPP•PP-1cα disruption assay, as described in Section 2.7. iASPP interacts with PP-1cα in part via its SH3 domain and its RVxF motif, RARL. The SH3 domain interacts with a PxxP motif present on the C-terminus of PP-1c, while the RVxF motif interacts with the RVxF-hydrophobic binding pocket of PP-1c located ~ 20 $\mathring{A}$ away from the PP-1c active site. The disruption of iASPP•PP-1cα by a marine extract indicates that the compounds present in these marine extracts are likely binding at one or both of these interaction points.

In future experiments, it could be useful to test the effect of the marine extracts in a reversed binding assay. This assay can be performed by binding iASPP to Ni-NTA beads via its His tag, followed by the hydrophobic binding pocket and PxxP ligand binding motif of PP-1c then binding iASPP. In comparison, the MC-S beads occupy some of the surface area around the PP-1c active site, whereas, the reverse binding order would leave the active site and the area around it available. Any compounds that require this area for PP-1c binding are free to access the active site rather than being in competition with

the potent toxin, Microcystin. The screening could then be preformed on the remaining marine extracts to determine any other iASPP disruptors that were previously missed. As well, already selected marine extracts that contain iASPP disruptors could also be reconfirmed using this method and further the understanding on how the compounds interact with the binding complex.

5.2 Newly Discovered iASPP Disruption Activity by Halistanol Sulfate and Coscinamide B

Marine extract PNG11-192 was identified as Halistanol Sulfate. Halistanol Sulfate (also known as Halistanol Trisulfate) was originally found in the sponge *Halichondra* cf. *moorei* in 1981 for its antimicrobial activity [39, 110]. Halistanol Sulfate has been show to demelanize human melanoma cells at non-toxic levels [148] and has also demonstrated anti-viral activity against HSV-1 and HIV-1 [26, 62]. Halistanol Sulfate promotes cell-death in the cancerous cell line L929 by disrupting the cell membrane [102], evidence that Halistanol Sulfate is behaving like a detergent [62, 148]. Due to the fact that Halistanol Sulfate is known to disrupt cell membranes, in the future it might be worth trying to alter the chemical structure in such a way that it could fully enter cell and preform its iASPP disruption activity.

The structure of Halistanol Sulfate is very similar to the iASPP disruptor discovered by Dr. Tamara Arnold, Sokotrasterol Sulfate (see Figure 5.1), and discussed previously in Section 1.10. The only differences are in the aliphatic side chain. First, the aliphatic side-chain attached to C-17 is slightly longer on Sokotrasterol Sulfate, containing two extra methyl groups to extend the tail, and secondly, it is unsaturated.

Typically, when looking for novel bioactive compounds, it is more beneficial to obtain a diverse group of compounds to increase the likelihood of specific function. But, these structural similarity of these two compound provides an unique opportunity. Throughout the assays, it now is possible to compare and contrast the differences in their activ-

ities, knowing the resulting differences would be caused by these nuances in structure. This information would give large insight into how these compounds maybe interacting with proteins and perhaps how modifications in structures would impact the desired activity.

Both Halistanol Sulfate and Sokotrasterol Sulfate are steroids and one of the most well-known steroids is cholesterol. This raises the obvious question; is cholesterol able to disrupt the iASPP$_{608\text{-}828}$•PP-1cα binding complex? In data not shown, this very idea was tested by Dr. Tamara Arnold and she was able to demonstrated that cholesterol alone was not able to prevent iASPP from binding PP-1cα [3]. This evidence suggests that either one or more the sulfate groups or the long aliphatic side-chain present on Halistanol Sulfate and Sokotrasterol Sulfate may be responsible for the disruption of the iASPP•PP-1cα protein complex. Figure 5.1 highlights the subtle, but significant differences between Halistanol Sulfate, Sokotrasterol Sulfate, and cholesterol. In future experiments, it would be worth selecting a variety of sulfated cholesterol-like compounds and testing them in the MC-S disruption assay. The results would demonstrate what specific chemical groups are responsible for iASPP•PP-1cα disruption and add to the knowledge of the binding interactions in this protein complex.

Coscinamide B was the second novel iASPP disruptor identified and discovered in marine extract PNG11-221. Coscinamide B, along with Coscinamide A and C, was first discovered in 2000 in the sponge *Coscicoderma* collected off the coast of Papua, New Guinea [12]. Indole alkaloids like the Coscinamides have been extensively shown to be a promising source of compounds with bioactivity including anti-cancer drugs [47]. Coscinamide B exhibited partial cytoprotection against human host cells infected with HIV and some anti-tumour activity against a human prostate cancer cell line [12, 93]. Coscinamide B is the most unique iASPP antagonist identified to date. Coscinamide B is an indole alkaloid, as well as, is the first iASPP disruptor that does not contain a sulfate group.

Due to the limited availability of Coscinamide B, I believe it worth while to synthetically produce more of this compound in order to test for its potency and specificity in

110

the same manner as Halistanol Sulfate, Sokotrasterol Sulfate, and Suvanine (Sections 4.2.1 to 4.2.3). Due to the unique structure of Coscinamide B, these results would give further insight into the iASPP•PP-1cα binding interactions, and therefore, how to antagonize it. Other labs have already been able to produce Coscinamide B, therefore, it should not be difficult to obtain [20, 93].
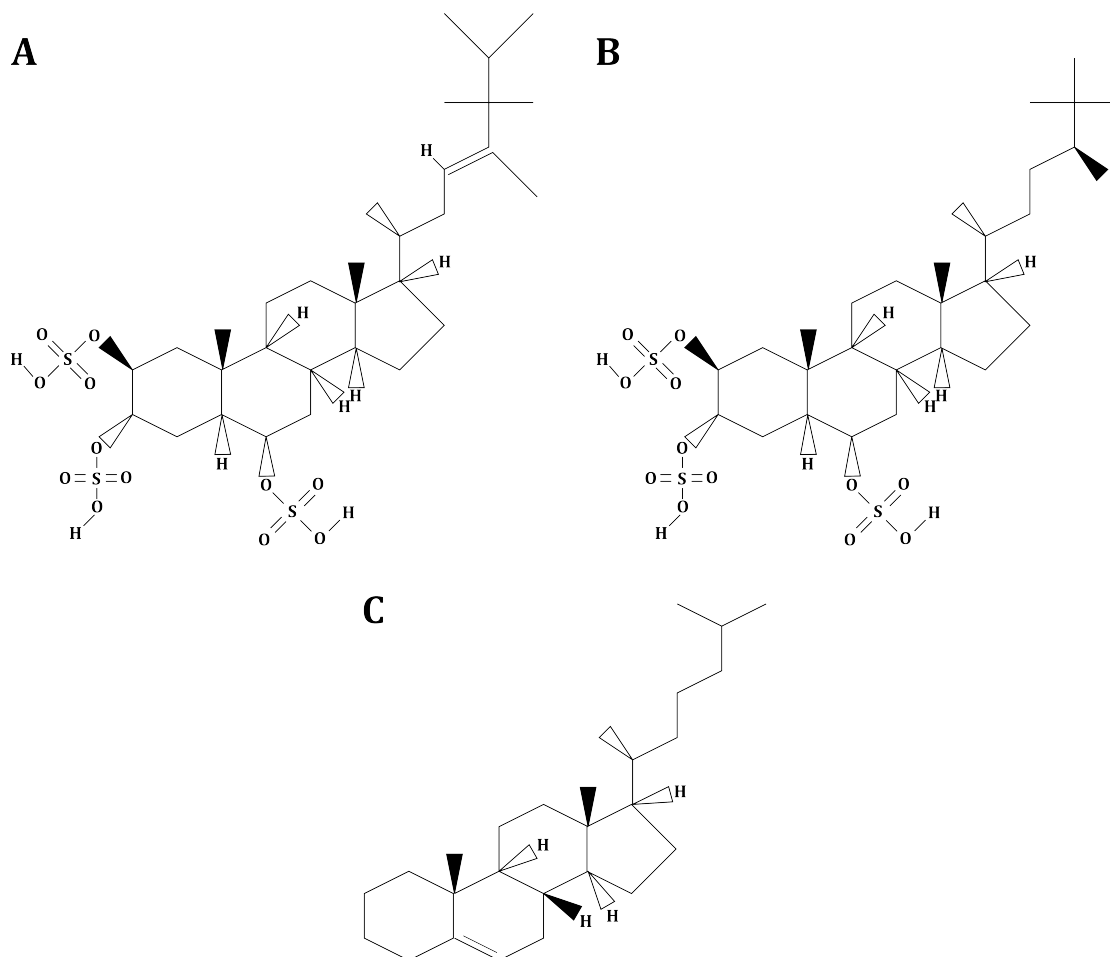
Figure 5.1: **The Chemical Structures of the Three Sterols Sokotrasterol Sulfate, Halistanol Sulfate, and Cholesterol.** The two iASPP disruptors, Sokotrasterol Sulfate (A) and Halistanol Sulfate (B), are structural similar to the cholesterol (C). The major difference is that the two antagonists contain three sulfate groups attached to positions C2, C3, and C6 of their steroid group, whereas cholesterol contains none. As well, there is a slight difference between the three alkyl chains they each have, differing in the total number of carbons in each.

5.3 The Potency and Specificity of Halistanol Sulfate, Sokotrasterol Sulfate, and Suvanine

The effects of Halistanol Sulfate, Sokotrasterol Sulfate, and Suvanine were tested towards iASPP, TIMAP, and ASPP2 binding of PP-1c to determine their potency and specificity as disruptors. The DC_{50} values can be found in Table 5.1. Halistanol Sulfate and Sokotrasterol were the two most structurally similar compounds identified as iASPP disruptors. Despite this, Sokotrasterol Sulfate was about twice a potent than Halistanol Sulfate against iASPP disruption. Secondly, Sokotrasterol maintained approximately equal potency when tested against ASPP2, while Halistanol Sulfate demonstrated higher potency against ASPP2 disruption. As well, both Halistanol Sulfate and Sokotrasterol Sulfate demonstrated disruption of PP-1cα off the MC-S beads, again suggesting that it is interacting at or near the active site of PP-1c. As a result of these compounds likely binding PP-1cα, we are planning to collaborate with another lab to produce crystal structures of the compounds bound to PP-1cα to determine exactly where they are binding.

Suvanine demonstrated a moderate potency against iASPP disruption, only slightly higher than that of Sokotrasterol Sulfate. But, unlike the other Halistanol Sulfate and Sokotrasterol Sulfate, Suvanine demonstrates no disruption of ASPP2 binding to PP-1c. None of the three compounds demonstrated disruption of the PP-1cγ•TIMAP protein complex, suggesting they have specificity towards the disruption of the ASPP family over TIMAP.

Table 5.1: **The DC_{50} of Halistanol Sulfate, Sokotrasterol Sulfate, and Suvanine Against the Regulatory Subunits iASPP, TIMAP, and ASPP2 Binding to PP-1c.**

iASPP Disruptor Name	iASPP DC_{50}	TIMAP DC_{50}	ASPP2 DC_{50}
Halistanol Sulfate	102 μM	>100 μM	<50 μM
Sokotrasterol Sulfate	40 μM	>50 μM	32 μM
Suvanine	60 μM	>75 μM	>75 μM

The TIMAP disruption assay does have some limitations when in comes to interpreting the results. As a result of the regulatory subunit TIMAP binding the beads, first followed by PP-1cγ binding to TIMAP, different surfaces of PP-1c were exposed for compound interaction. The active site of PP-1c remains available, while the RVxF hydrophobic binding pocket is largely hidden. If the compounds require interaction with any of these hidden surfaces, the compound may not demonstrate any disruption. If the TIMAP and PP-1cγ were bound in the reverse order, the results may change. But overall, the purpose of the assay was to be a control for the iASPP•PP-1c binding assay. As a control assay, the TIMAP•PP-1c binding assay serves its purpose.

Current protein-protein disruptor drugs, such as the Nutlins discussed in Section 1.8, have nanomolelor potencies. Halistanol Sulfate, Sokotrasterol Sulfate, and Suvanine do not have nanomolelar potencies in the iASPP•PP-1c disruption assays; therefore, they likely require modifications to their structure to increase their potencies. It is reasonable to suggest that these small molecules with potencies in the micromolelar range can still be promising small molecules leads, because as our knowledge of how Halistanol Sulfate, Sokotrasterol Sulfate, and Suvanine interact with iASPP•PP-1c binding complex increases, informed decisions about chemical modifications can be made and their structures changes to increase their potency.

5.4 Identification of Potent Protein Phosphatase-1 Inhibitors

Some marine extracts tested had a drastic affects on PP-1cα activity, resulting in almost complete inhibition of PP-1cα activity towards pNPP. Specifically, marine extracts PNG11-279 and PNG11-284 inhibit PP-1cα at 99 % and 95 %, respectively.

The identification of a potent PP-1c inhibitor in marine extract PNG11-279 lead to the rediscovery of the small molecule, Motuporin. This is the first time Motuporin has been seen since its initial discovery in 1992 [27] in the sponge *Theonella swinhoei* Gray. It is one of the most potent PP-1c inhibitors known [27]. Motuporin is a cyclic pentapeptide inhibitor, classified as a nodularin, and contains the β-amino acid, ADDA, that is also

seen on microcystin [27] (structure shown in Figure 4.27). Nodularins contain only one variable residue position. Motutporin has a valine residue at this position leading to its second name, Nodularin-V [27].

The crystal structure of Motuporin bound to PP-1cγ was solved in 2006 (see Figure 5.2). Similarly to Microcystin and other known toxins, the large ring of the toxin interacts with the active site of PP-1c, while the hydrophobic ADDA amino acid occupies the hydrophobic groove. The negatively charged residues bind indirectly to the Mn^{2+} metal ions via hydrogen-bonding to water molecules [105].

Now that we are again in possession of the this cytotoxin, in the future it would be useful to test the cell permeability of Motuporin in order to determine if it could be potentially used as a research tool. Motuporin is already known to enter the liver, but could be useful in biological studies if Motuporin was cell permeable similar to Okadaic Acid.

Secondly, a novel compound was discovered in marine extract PNG11-285 due to its PP-1c inhibition activity. The compound is unique in that it contains a bromine group, an element found naturally in only marine compounds. This compound could not be isolated by our traditional fractionation methods, but perhaps it could be synthetically produced. If able to obtain more of this compound, it would be beneficial to test for an IC_{50} and for cell permeability. The compound could then be used to further our understanding of PP-1c activity and potentially used as a PP-1c inhibitor for research.
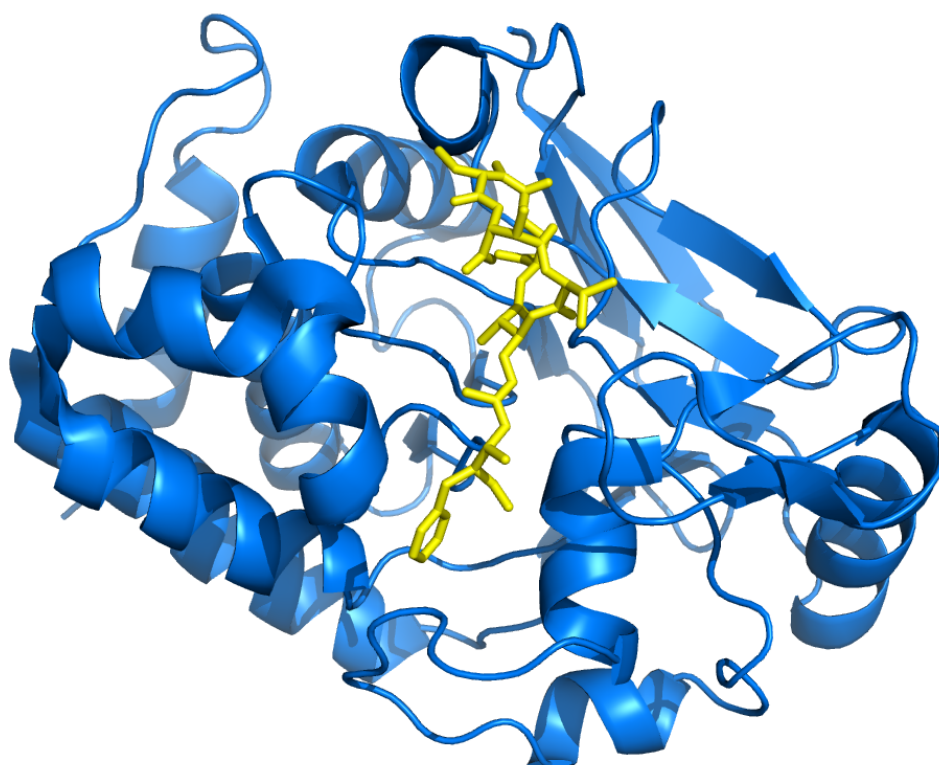
Figure 5.2: **The Three-Dimensional Crystal Structure of Motuporin Bound to PP-1cγ.** The structure of PP-1cγ is represented in marine blue. Motuporin is shown in yellow lying across the active site of PP-1c. The ADDA amino acid binds in the hydrophobic groove of the catalytic cleft. Motuporin also interacts with the metal ions within the active site. This figure was produced with *PyMOL*. [PDB 2BCD] [27].

5.5 The Recently Elucidation Three-Dimensional Crystal Structure of iASPP Bound to PP-1cα

Recently, Dr. Mark Glover *et. al.* have elucidated the crystal structure of the regulatory subunit, iASPP, bound to PP-1cα (unpublished data). Figure 5.3 shows that the non-canonical RVxF motif, RARL, of iASPP binds the RVxF-hydrophobic binding pocket of PP-1cα. As well, the SH3 domain of iASPP interacts with the PxxP motif present in PP-1cα, confirming data seen in previous studies [138]. Lastly, the two Ank repeats present in iASPP bind PP-1c at the C-terminal of PP-1cα. The Ank repeats bind PP-1c in similar manner to the Ank repeats of MYPT1 (see Figure 1.9), as predicted. The crystal structure provides confirmation of the key binding interactions between iASPP•PP-1c as predicted before I began my thesis project. Now that the binding interactions of the iASPP•PP-1cα are established, the targeting of bioactive compounds for disruption can be even more specific. In the future, Halistanol Sulfate, Sokotrasterol Sulfate, and Suvanine can be chemically modified to target these interactions to increase their potency for iASPP disruption. Furthermore, if the crystal structure of Halistanol Sulfate, Sokotrasterol Sulfate, and Suvanine bound to PP-1cα can be elucidated, it would provide evidence of which of these iASPP binding interactions the compounds are disrupting. This information would further the understanding of the importance of each iASPP•PP-1cα binding interactions.
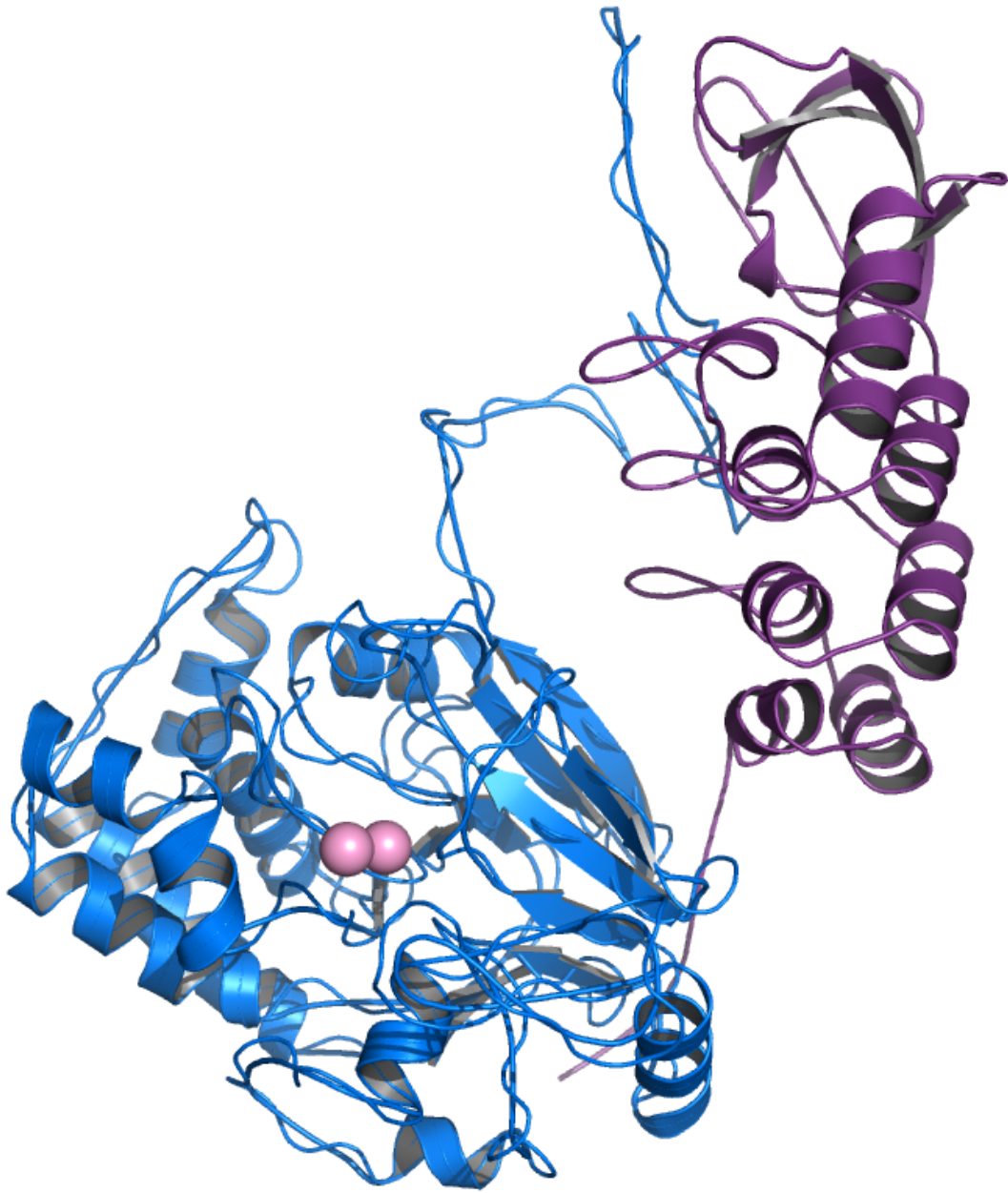
Figure 5.3: **The Three-Dimensional Crystal Structure of iASPP bound to PP-1cα.** The non-canonical RVxF motif of iASPP binds the RVxF-hydrophobic binding pocket of PP-1cα. The SH3 domains and the two Ank repeats of iASPP bind the C-terminal tail of PP-1cα. The SH3 domain bind the PxxP motif of PP-1cα (unpublished data).

Chapter 6

Conclusion

In conclusion, one of the major goals of this research project was to attempt to identify if small molecules from marine organisms can disrupt the iASPP•PP-1cα complex. I have identified that Halistanol Sulfate, Sokotrasterol Sulfate, and Suvanine can antagonize the above protein complex. As well, I have demonstrated that these three compounds contain some specificity because they do not disrupt a second regulatory subunit, TIMAP, from PP-1c. Furthermore, the bioactive compound Suvanine demonstrated that it does not disrupt the binding of PP-1c from another member of the ASPP family, ASPP2. This new evidence has been added to the p53 scheme regulation described in Chapter 1 and depicted in Figure 6.1. These compounds possess the potential to disrupt the p53•PP-1cα•iASPP binding complex. Inhibition of the dephosphorylation of p53 would allow the negative regulator, MDM2, to again bind p53. MDM2 would then promote the cell-cycle arrest and pro-apoptotic functions of p53 by exporting p53 from the nucleus, increasing the transactivational activity of p53, and inducing p53 proteolysis. With further testing and modifications, the compounds can be tested for effects on the down-stream functions of p53. Therefore, they have the potential to be used as novel anti-cancer drugs that decrease the dephosphorylation of p53 by PP-1c.

Based on the data above, Suvanine is perhaps our best lead for a potential novel biologically active drug. In the future, it will be critical to establish whether Suvanine

can decrease dephosphorylation of p53 by PP-1cα (although preliminary studies were consistent with this possibility). As well, it would be very useful to elucidate the crystal structure of Suvanine bound to PP-1cα allowing us, to further understand how Suvanine interacts with PP-1cα, and ultimately modulates ASPP protein binding. Also, it may be useful to develop a method to synthetically produce Suvanine. Lastly, it is important to know whether or not Suvanine is cell permeable or not in order for it to be a potential drug. If not, Suvanine can undergo chemical modifications to improve its cell permeability and potency.
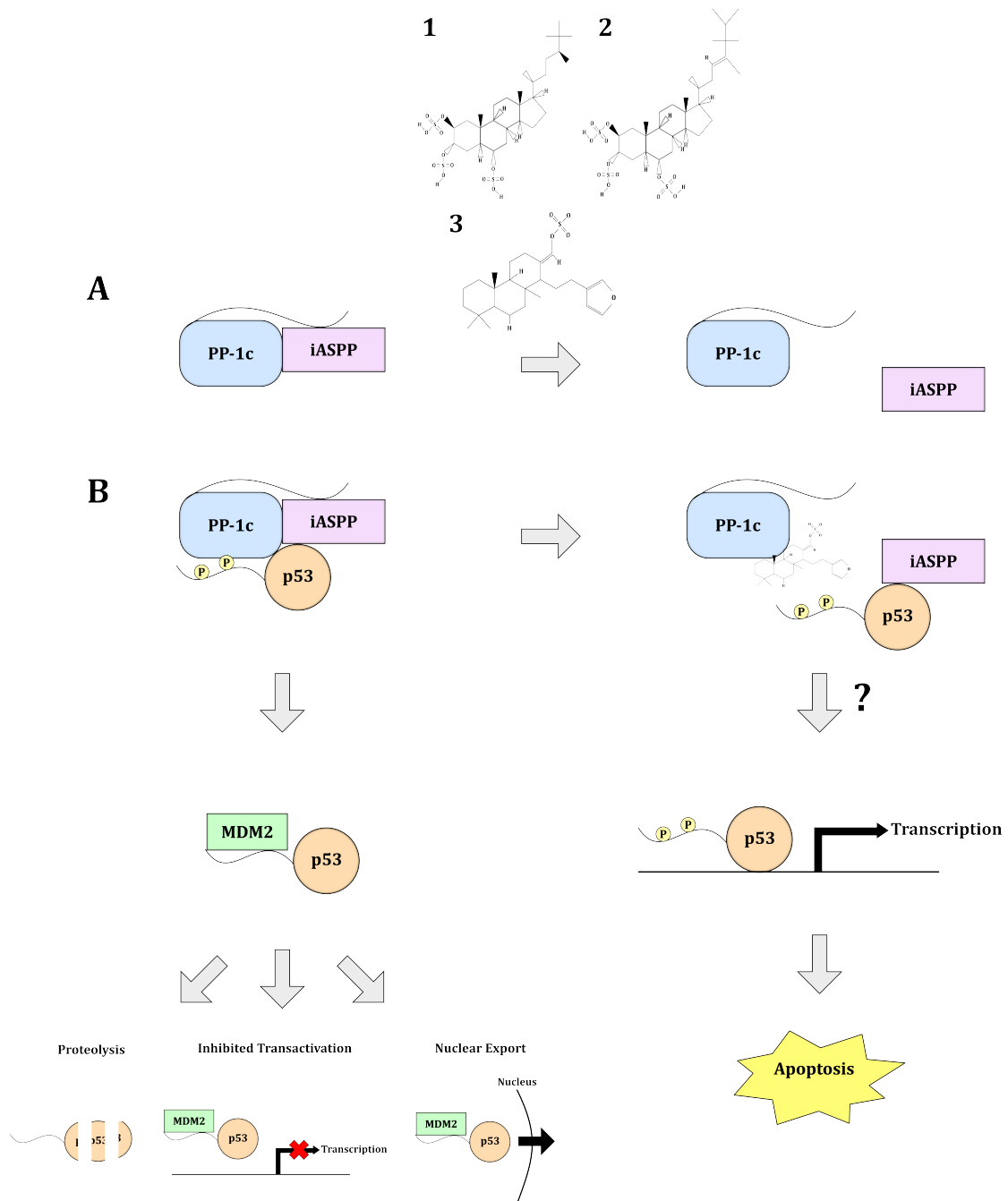
Figure 6.1: **PP-1cα and iASPP Binding can be Targeted with Small Molecules with the Potential to Affect Down-stream Regulation of p53.** (A) The binding of PP-1cα and iASPP can be targeted and disrupted with the small molecules (1) Halistanol Sulfate, (2) Sokotrasterol Sulfate, and (3) Suvanine. (B) The disruption of the iASPP●PP-1c binding complex could lead to the disruption of the iASPP●PP-1c●p53 binding complex and to the decreased dephosphorylation of p53 by PP-1c. Therefore, this would have the potential to retain the pro-apoptotic activity of p53.

Bibliography

[1] X. Agirre, J. Roman-Gomez, A. Jimenez-Velasco, L. Garate, C. Montiel-Duarte, G. Navarro, I. Vazquez, M. Zalacain, M. J. Calasanz, A. Heiniger, A. Torres, J. D. Minna, and F. Prosper. Aspp1, a common activator of tp53, is inactivated by aberrant methylation of its promoter in acute lymphoblastic leukemia. *Oncogene*, 13(25):1862–1870, 2006.

[2] P. R. Andreassen, F. B. Lacroix, E. Villa-Moruzzi, and R. L. Margolis. Differential subcellular localization of protein phosphatase-1 alpha, gamma1, and beta isoforms during both interphase and mitosis in mammalian cells. *J. Cell. Biol.*, 141(5):1207–1215, 1998.

[3] T. Arnold. Molecular mechanisms underlying the regulation of protein phosphatase-1c by the apoptotic stimulating proteins of p53. *Doctoral Thesis, University of Alberta, Canada*, 2013.

[4] J. Bae, J. Jeon, Y. Lee, H. Lee, C. J. Sim, K. Oh, and J. Shin. Sesterterpenes from the tropical sponge coscinoderma sp. *J. Nat. Prod.*, 74:1805–1811, 2011.

[5] D. Barford, A. K. Das, and M. P. Egloff. The structure and mechanism of protein phosphatases: insights into catalysis and regulation. *Annu. Rev. Biophys. Biomol. Struct.*, 27:133–164, 1998.

[6] D. Bergamaschi, Y. Samuels, B. Jin, S. Duraisingham, T. Crook, and X. Lu. Aspp1 and aspp2: common activators of p53 family members. *Mol. Cell. Biol.*, 24(3):1341–1350, 2004.

[7] D. Bergamaschi, Y. Samuels, N. J. O'Neil, G. Trigiante, T. Crook, J. Hsieh, D. J. O'Connor, S. Zhong, I. Campargue, M. L. Tomlinson, P. E. Kuwabara, and X. Lu. iaspp oncoprotein is a key inhibitor of p53 conserved from worm to human. *Nat. Genet.*, 33:162–167, 2003.

[8] D. Bergamaschi, Y. Samuels, A. Sullivan, M. Zvelebil, H. Breyssens, A. Bisso, G. Del Sal, N. Syed, P. Smith, M. Gasco, T. Crook, and X. Lu. iaspp preferentially binds p53 proline-rich region and modulates apoptotic function of codon 72-polymorphic p53. *Nat. Genet.*, 10(38):1133–1141, 2006.

[9] I. Bhatnagar and S. K. Kim. Immense essence of excellence: marine microbial bioactive compounds. *Mar. Drugs*, 10(8):2673–2701, 2010.

[10] J. W. Blunt, B. R. Copp, R. A. Keyzers, M. H. G. Murno, and M. R. Prinsep. Marine natural products. *Nat. Prod. Rep*, 3(34):235–294, 2017.

[11] A. M. Bode and Z. Dong. Post-translational modification of p53 in tumorigenesis. *Nat. Rev. Cancer*, 10(4):793–805, 2004.

[12] H. R. Bokesch, L. K. Pannell, T. C. McKee, and M. R. Boyd. Coscinamides a, b and c, three new bis indole alkaloids from the marine sponge coscinoderma sp. *Tetrahedron Lett.*, 41:6305–6308, 2000.

[13] M. Bollen. Combinatorial control of protein phosphatase-1. *Trends Biochem Sci.*, 26(7):426–431, 2001.

[14] M. Bollen, W. Peti, M. J. Ragusa, and M. Beullens. The extended pp1 toolkit: designed to create specificity. *Trends Biochem Sci.*, 35(8):450–458, 2010.

[15] M. Bollen and W. Stalmans. The structure, role and regulation of type 1 protein phosphatases. *Crit. Rev. Biochem. Mol. Biol.*, 27:227–281, 1992.

[16] W. Cao, S. N. Mattagajasingh, H. Xu, K. Kim, W. Fierlbeck, H. Deng, C. J. Lowenstein, and B. J. Ballermann. Timap, a novel caax box protein regulated by tgf-1 and expressed in endothelial cells. *Am. J. Physiol. Cell Physiol.*, 1(282):327–337, 2002.

[17] L. C. Carmody, A. J. Baucum II, M. A. Bass, and R. J. Colbran. Selective targeting of the gamma1 isoform of protein phosphatase 1 to f-actin in intact cells requires multiple domains in spinophilin and neurabin. *FASEB J.*, 22(6):1660, 2008.

[18] C. Cassiano, M. C. Monti, C. Festa, A. Zampella, R. Riccio, and A. Casapullo. Chemical proteomics reveals heat shock protein 60 to be the main cellular target of the marine bioactive sesterterpene suvanine. *Chem. Bio. Chem.*, 13:1953–1958, 2012.

[19] H. Ceulemans, W. Stalmans, and M. Bollen. Regulator-driven functional diversification of protein phosphatase-1 in eukaryotic evolution. *BioEssays*, 24:371–381, 2002.

[20] M. Chakrabarty, R. Basak, and Y. Harigaya. Concise synthesis of coscinamide b, a bisindolic enamide from marine sponge. *Synthesis*, 13:2011–2014, 2003.

[21] J. Chatterjee, M. Beullens, R. Sukachaite, J. Qian, B. Lesage, D. J. Hart, M. Bollen, and M. Kohn. Development of a peptide that selectively activates protein phosphatase-1 in living cells. *Angew. Chem. Int. Ed. Engl.*, 40:10054–10059, 2012.

[22] D. Chen, E. Padiernos, F. Ding, I. S. Lossos, and C. D. Lopez. Apoptosis-stimulating protein of p53-2 (aspp2/53bp2l) is an e2f target gene. *Cell Death Differ.*, 4:358–368, 2005.

[23] M. A. Cobleigh, B. Tabesh, P. Bitterman, J. Baker, M. Cronin, M. L. Liu, R. Borchik, J. M. Mosquera, M. G. Walker, and S. Shak. Tumor gene expression and prognosis in breast cancer patients with 10 or more positive lymph nodes. *Clin. Cancer Res.*, 24 Pt 1:8623–8631, 2005.

[24] P. Cohen, C. F. Holmes, and Y. Tsukitani. Okadaic acid: a new probe for the study of cellular regulation. *Trends Biochem. Sci.*, 15(3):98–102, 1990.

[25] C. Csortos, I. Czikora, N. V. Bogatcheva, D. M. Adyshev, C. Poireir, G. Olah, and A. D. Verin. Timap is a positive regulator of pulmonary endothelial barrier function. *Am. J. Physiol. Lung Cell. Mol. Physiol.*, 295:440–450, 2008.

[26] T. da Rosa Guimaraes, C. G. Quiroz, C. R. Borges, S. Q. de Oliveira, M. T. de ALmeida, E. M. Bianco, M. I. Moritz, J. L. Carraro, J. A. Palermo, G. Cabrera, E. P. Schenkel, F. H. Reginatto, and C. M. Simoes. Anti hsv-1 activity of halistanol sulfate and halistanol sulfate c isolated from brazilian marine sponge petromica citrina (demospongiae). *Mar. Drugs*, 11:4176–4192, 2013.

[27] E. Dilip de Silvia, D. E. Williams, R. J. Anderson, H. Klix, C. F. B. Holmes, and T. M. Allen. Motuporin, a potent protein phosphatase inhibitor isolate from the papua new guinea sponge theonella swinhoei gray. *Tetrahedron Lett.*, 33:1561–1564, 1992.

[28] K. M. Dohoney, C. Guillerm, C. Whiteford, C. Elbi, P. F. Lambert, G. L. Hager, and J. N. Brady. Phosphorylation of p53 at serine 37 is important for transcriptional activity and regulation in response to dna damage. *Oncogene*, 23(1):49–57, 2004.

[29] M. Dowhadwala, E. F. da Cruz e Silva, F. L. Hall, R. T. Williams, D. A. Carbonaro-Hall, A. C. Nairn, P. Greengard, and N. Berndt. Phosphorylation and inactivation of protein phosphatase 1 by cyclin-dependent kinases. *Proc. Natl. Acad. Sci. USA*, 14:6408–6412, 1994.

[30] M. Egloff, P. T. W. Cohen, P. Reinemer, and D. Barford. Crystal structure of the catalytic subunit of human protein phosphatase 1 and its complex with tungstate. *J. Mol. Biol.*, 254:942–959, 1995.

[31] M. P. Egloff, D. F. Johnson, G. Moorhead, P. T. Cohen, P. Cohen, and D. Barford. Structural basis for the recognition of regulatory subunits by the catalytic subunit of protein phosphatase 1. *EMBO J.*, 8(16):1876–1887, 1997.

[32] S. Endo, X. Zhou, J. Connor, B. Wang, and S. Shenolikar. Multiple structural elements define the specificity of recombinant human inhibitor-1 as a protein phosphatase-1 inhibitor. *Biochemistry*, 16:5220–5228, 1996.

[33] J. J. Fernandez, M. L. Candenas, M. L. Souto, M. M. Trujillo, and M. Norte. Okadaic acid, useful tool for studying cellular processes. *Curr. Med. Chem.*, 9(2):229–262, 2002.

[34] J. Floter, I. Kaymak, and A. Schulze. Regulation of metabolic activity by p53. *Metabolites*, 2(7):E21, 2017.

[35] V. Fogal, N. N. Kartasheva, G. Trigiante, S. Llanos, D. Yap, K. H. Vousden, and X. Lu. Aspp1 and aspp2 are new transcriptional targets of e2f. *Cell Death Differ.*, 4:369–379, 2005.

[36] J. G. Foulkes, L. S. Jefferson, and P. Cohen. The hormonal control of glycogen metabolism: dephosphorylation of protein phosphatase inhibitor-1 in vivo in response to insulin. *FEBS Lett.*, 1:21–24, 1980.

[37] M. Fujioka, N. Takahashi, H. Odai, S. Araki, K. Ichikawa, J. Feng, M. Nakamura, K. Kaibuchi, D. J. Hartshorne, T. Nakano, and M. Ito. A new isoform of human myosin phosphatase targeting/regulatory subunit (mypt2): cdna clong, tissue expression, and chromosomal mapping. *Genomics*, 49:59–68, 1998.

[38] A. Furuta, K. A. Salam, I. Hermawan, N. Akimitsu, J. Tanaka, H. Tani, A. Yamashita, K. Moriishi, M. Nakakoshi, M. Tsubuki, P. W. Peng, Y. Suzuki, N. Yamamoto, Y. Sekiguchi, S. Tsuneda, and N. Noda. Idenificiation and biochemical characterizaiton of halisulfate 3 and suvanine as novel inhibitors of hepatitis c virus ns3 helicase from a marine sponge. *Mar. Drugs*, 12:462476, 2014.

[39] N. Fusetani, S. Matsunaga, and S. Konosu. Bioactive marine metabolistes ii. halistanol sulfate, an antimicrobial novel steroid sulfate from the marin sponge halichondria cf. moorei bergquist. *Tetrahedron Lett.*, 22(21):1985–1988, 1981.

[40] V. M. Galubovskaya and W. G. Cance. Targeting the p53 pathway. *Surg. Oncol. Clin. N. Am.*, 4(22):747–764, 2013.

[41] W. H. Gerwick and A. M. Fenner. Drug discovery from marine microbes. *Microb. Ecol.*, 4(65):800–806, 2013.

[42] J. A. Gibbons, L. Kozubowski, K. Tatchell, and S. Shenolikar. Expression of human protein phosphatase-1 in saccharomyces cerevisiae highlights the role of phosphatase isoforms in regulating eukaryotic functions. *J. Biol. Chem.*, 282(30):21838–21847, 2007.

[43] J. Goldberg, H. Huang, Y. Kwon, P. Greengard, A. C. Nairn, and J. Kuriyan. Three-dimensional structure of the catalytic subunit of protein phosphatase-1 serine/threonine phosphatase-1. *Nature*, 376:745–753, 1995.

[44] I. Goldstein, V. Marcel, M. Olivier, M. Oren, V. Rotter, and P. Hainaut. Understanding wild-type and mutant p53 activities in human cancer: new landmarks on the way to targeted therapies. *Cancer Gene Ther.*, 1(8):2–11, 2011.

[45] S. Gorina and N. P. Pavletich. Structure of the p53 tumor suppressor bound to the ankyrin and sh3 domains of 53bp2. *Science*, 274:1001–1005, 1996.

[46] M. E. Grassie, L. D. Moffat, M. P. Walsh, and J. A. MacDonald. The myosin phosphatase targeting protein (mypt) family: A regulated mechanism for achieving substrate specificity of the catalytic subunit of protein phosphatase type 1b. *Arch. Biochem. Biophys.*, 510:147–159, 2011.

[47] W. Gul and M. T. Hamann. Indole alkaloid marine natural products: An established source of cancer drug leads with considerable promise for the control of parasitic, neurological and other diseases. *Life Sci.*, 78:442–453, 2005.

[48] Z. He, Y. Wang, G. Huang, Q. Wang, D. Zhao, and L. Chen. The lncrna uca1 interacts with mir-182 to modulate glimo proliferation and migration by targeting iaspp. *Arch. Biochem. Biophys.*, 623-624:1–8, 2017.

[49] A. Hendrickx, M. Beullens, H. Ceulemans, T. D. Abt, A. Van Eynde, E. Nicolaescu, B. Lesage, and M. Bollen. Docking motif-guided mapping of the interactome of protein phosphatase-1. *Chemistry and Biology*, 16:365–371, 2009.

[50] E. Heroes, B. Lesage, J. Go rnemann, M. Beullens, L. V. Meervelt, and M. Bollen. The pp1 binding code: a molecular-lego strategy that governs specificity. *FEBS J.*, 280:584–595, 2013.

[51] E. Heroes, J. Rip, M. Beullens, L. V. Meervelt, S. De Gendt, and M. Bollen. Metals in the active site of native protein phosphatase-1. *J. Inorg. Biochem.*, 149:1–5, 2015.

[52] T. Hershko, M. Chaussepied, M. Oren, and D. Ginsberg. Novel link between e2f and p53: proapoptotic cofactors of p53 are transcriptionally upregulated by e2f. *Cell Death Differ.*, 4:377–383, 2005.

[53] H. Hou, L. Sun, B. A. Siddoway, R. Petralia, H. Yang, H. Gu, A. C. Nairn, and H. Xia. Synaptic nmda receptor stimulation activates pp1 by inhibiting its phosphorylation by cdk5. *J. Cell. Biol.*, 203(3):521–535, 2013.

[54] M. J. Hubbard and P. Cohen. Regulation of protein phosphatase-1g from rabbit skeletal muscle. 2. catalytic subunit translocation is a mechanism for reversible inhibition of activity toward glycogen-bound substrates. *Eur. J. Biochem.*, 186:711–716, 1989.

[55] M. J. Hubbard and P. Cohen. On target with a new mechanism for the regulation of protein phosphorylatoin. *TIBS*, 93:172–177, 1993.

[56] T. Hunter. Protein kinases and phosphatases: The yin and yang of protein phosphorylation and signaling. *Cell*, 80(2):225–236, 1995.

[57] T. D. Hurley, J. Yang, L. Zhang, K. D. Goodwin, Q. Zou, M. Cortese, A. K. Dunker, and A. A. DePaoli-Roach. Structural basis for regulation of protein phosphatase 1 by inhibitor-2. *J. Biol. Chem.*, 282(39):28874–28883, 2007.

[58] A. Iosub-Amir and A. Friedler. Protein-protein interactions of aspp2: an emerging therapeutic target. *Med. Chem. Commun.*, 5:1435–1443, 2014.

[59] M. Ito, T. Nakano, F. Erdodi, and D. J. Hartshorne. Myosin phosphatase: strucutre, regulation and function. *Mol. Cell. Biochem.*, 259:197–209, 2004.

[60] K. Iwabuchi, P. L. Bartel, B. Li, R. Marraccino, and S. Fields. Two cellular proteins that bind to wild-type but not mutant p53. *Proc. Natl. Acad. Sci. USA*, 91:6098–6102, 1994.

[61] H. Jin, T. Sperka, P. Herrlich, and H. Morrison. Tumorigenic transformation by cpi-17 through inhibition of a merlin phosphatase. *Nature*, 442:576–579, 2006.

[62] Y. Jin, S. Fotso, Z. Yongtang, M. Sevvana, H. Laatsch, and W. Zhang. Halichondria sulfonic acid, a new hiv-1 inhibitory guanidino-sulfonic acid, and halistanol sulfate isolated from the marine sponge halichondria rugosa. *Nat. Prod. Res.*, 12:1129–35, 2006.

[63] A. C. Joerger and A. R. Fersht. Structure-function-rescue: the diverse nature of common p53 cancer mutants. *Oncogene*, 15(26):2226–2242, 2007.

[64] D. F. Johnson, G. Moorhead, F. B. Caudwell, P. Cohen, Y. H. Chen, M. X. Chen, and P. T. W. Cohen. Identification of protein phosphatase-1-binding domains on the glycogen and myofibrillar targeting subunits. *Eur. J. Biochem.*, 239:317–325, 1996.

[65] C. A. Jost, M. C. Marin, and WG. Jr. Kaelin. p73 is a simian [correction of human] p53-related protein that can induce apoptosis. *Nature*, 6647(389):191–194, 1997.

[66] K. M. Kampa, J. D. Acoba, D. Chen, J. Gay, H. Lee, K. Beemer, E. Padiernos, N. Boonmark, Z. Zhu, A. C. Fan, A. S. Bailey, W. H Fleming, C. Corless, D. W. Felsher, L. Naumovski, and C. D. Lopez. Apoptosis-stimulating protein of p53 (aspp2) heterozygous mice are tumor-prone and have attenuated cellular damage-response thresholds. *PNAS*, 106(11):4390–4395, 2009.

[67] A. Karsan, I. Pollet, L. Yu, K. C. Chan, T. P. Conrads, D. A. Lucas, R. Andersen, and T. Veenstra. Quantitative proteomic analysis of sokotrasterol sulfate-stimulated primary human endothelial cells. *Mol Cell Proteomics*, 4:191–204, 2005.

[68] M. S. Kelker, R. Page, and W. Peti. Crystal structures of protein phosphatase-1 bound to nodularin-r and tautomycin: a novel scaffold for structure-based drug design of serine/threonine phosphatase inhibitors. *J. Mol. Biol.*, 1(385):11–21, 2009.

[69] A. Khromov, N. Choudhury, A. S. Stevenson, A. V. Somlyo, and M. Eto. Phosphorylation-dependent autoinhibition of mysoin light chain phosphatase ac-

counts for ca2+ sensitization force of smooth muscle contraction. *J. Biol. Chem.*, 284(32):21569–21579, 2009.

[70] C. K. Kim, I. H. Song, H. Y. Park, Y. J. Lee, H. S. Lee, C. J. Sim, D. C. Oh, K. B. Oh, and J. Shin. Suvanine sesterterpenes and deacyl irciniasulfonic acids from a tropical coscinoderma sp sponge. *J. Nat. Prod.*, 6:1396–1406, 2014.

[71] J. Kimura, E. Ishizuka, Y. Nakao, W. Y. Yoshida, P. J. Scheuer, and M. Kelly-Borges. Isolation of 1-methylherbipoline salts of halisulfate-1 and of suvanine as serine protease inhibitors from a marine sponge, coscinoderma mathewsi. *J. Nat. Prod.*, 61:248–250, 1998.

[72] A. Kita, S. Matsunaga, A. Takai, H. Kataiwa, T. Wakimoto, N. Fusetani, M. Isobe, and K. Miki. Crystal structure of the complex between calyculin a and the catalytic subunit of protein phosphatase 1. *Structure*, 5:715–724, 2002.

[73] G. M. Konig, S. Kehraus, S. F. Seibert, A. Abdel-Lateff, and D. Muller. Natural products from marine organisms and their associated microbes. *Chembiochem.*, 2(7):229–238, 2006.

[74] E. G. Krebs and E. H. Fischer. The phosphorylase b to a converting enzyme of rabbit skeletal muscle. *Biochimica et Biophysica Acta*, 20:150 – 157, 1956.

[75] G. S. Kumar, E. Gokhan, S. De Munter, M. Bollen, P. Vagnarelli, W. Peti, and R. Page. The ki-67 and repoman mitotic phosphatases assemble via an identical, yet novel mechanism. *eLife*, 5:16539, 2016.

[76] R. Kumari, S. Kohli, and S. Das. p53 regulation upon genotoxic stress: intricacies and complexities. *Mol. Cell. Oncol.*, 3(1):e969653, 2014.

[77] P. H. Kussie, S. Gorina, V. Marechal, B. Elenbaas, J. Moreau, A. J. Levine, and N. P. Pavletich. Structure of the mdm2 oncoprotein bound to the p53 tumor suppressor transactivation domain. *Science*, 274(5289):948–953, 1996.

[78] J. W. Lee, H. S. Lee, J. Shin, J. S. Kang, J. Yun, H. J. Shin, J. S. Lee, and Y. J. Lee. Suvanine analogs from a coscinoderma sp. marine sponge and their

cytotoxicities against human cancer cell lines. *Arch. Pharm. Res.*, 6:1005–1010, 2015.

[79] R. Lei, M. Xue, L. Zhang, and Z. Q. Lin. Long noncoding rna malat1-regulation microrna 506 modulates ovarian cancer growth by targetin iaspp. *Onco. Targets. Ther.*, 10:35–46, 2017.

[80] G. Lettre, E. A. Kritikou, M. Jaeggi, A. Calixto, A. G. Fraser, R. S. Kamath, J. Ahringer, and M. O. Hengartner. Genome-wide rnai identifies p53-dependent and -independent regulators of germ cell apoptosis in c. elegans. *Cell Death Differ.*, 11:1198–1203, 2004.

[81] A. J. Levine. p53, the cellular gatekeeper for growth and division. *Cell*, 88:323–331, 1997.

[82] D. W-C. Li, J-P Liu, P. C. Schmid, R. Schlosser, H. Feng, W-B Liu, Q. Yan, L. Gong, S-M. Sun, M. Deng, and Y. Liu. Protein serine/threonine phosphatase-1 dephosphorylates p53 at ser-15 and ser-37 to modulate its transcriptional and apoptotic activities. *Oncogene*, 25:3006–3022, 2006.

[83] U. Lindequist. Marine-derived pharmaceutical - challenges and opportunites. *Biomol. Ther.*, 24(6):561–571, 2016.

[84] Z. J. Liu, X. Lu, Y. Zhang, S. Zhong, S. Z. Gu, X. B. Zhang, X. Yang, and H. M. Xin. Downregulated mrna expression of aspp and the hypermethylation of the 5'-untranslated region in cancer cell lines retaining wild-type p53. *FEBS J.*, 7(579):1587–1590, 2005.

[85] Z. J. Liu, Y. Zhang, X. B. Zhang, and X. Yang. Abnormal mrna expression of aspp members in leukemia cell lines. *Leukemia*, 4:880, 2004.

[86] S. Llanos, C. Royer, M. Lu, D. Bergamaschi, W. H. Lee, and X. Lu. Inhibitory member of the apoptosis-stimulating proteins of the p53 family (iaspp) interacts with protein phosphatase 1 via a noncanonical binding motif. *J. Biol. Chem.*, 286(50):43039–43044, 2011.

[87] A. Lopez-Girona, D. Mendy, T. Ito, K. Miller, A. K. Gandhi, J. Kang, S. Kara-sawa, G. Carmel, P. Jackson, M. Abbasian, A. Mahmoudi, B. Cathers, E. Rychak, S. Gaidarova, R. Chen, P. H. Schafer, H. Handa, T. O. Daniel, J. F. Evans, and R. Chopra. Cereblon is a direct protein target for immunomodulatory and antipro-liferative activities of lenalidomide and pomalidomide. *Leukemia*, 11(26):2326–2335, 2012.

[88] I. S. Lossos, Y. Natkunam, R. Levy, and C. D. Lopez. Apoptosis stimulating protein of p53 (aspp2) expression differs in diffuse large b-cell and follicular center lymphoma: correlation with clinical outcome. *Leuk. Lymphoma*, 12:2309–2317, 2002.

[89] J. Loughery, M. Cox, L. M. Smith, and D. W. Meek. Critical role for p53-serine 15 phosphorylation in stimulating transactivation at p53-responsive promoters. *Nucleic Acid Res.*, 42(12):7666–7680, 2014.

[90] M. Lu, H. Breyssens, V. Salter, S. Zhong, Y. Hu, C. Baer, I. Ratnayaka A. Sullivan, N. R. Brown, J. Endicott, S. Knapp, B. M. Kessler, M. R. Middleton, C. Siebold, E. Y. Jones, E. V. Sviderskaya, J. Cebon, T. John, O. L. Caballero, C. R. Goding, and X. Lu. Restoring p53 function in human melanoma cells by inhibiting mdm2 and cyclin b1/cdk1-phosphorylated nuclear iaspp. *Cancer Cell*, 23:618–633, 2013.

[91] C. Y. Lui, X. Lv, T. Li, Y. Xu, X. Zhou, S. Zhao, Y. Xiong, Q. Y. Lei, and K. L. Guan. Pp1 cooperates with aspp2 to dephosphorylate and activate taz. *J. Biol. Chem.*, 7(286):5558–5568, 2011.

[92] E. Lundberg, L. Fagerberg, D. Klevebring, I. Matic, T. Geiger, J. Cox, C. Algenas, J. Lundeberg, M. Mann, and M. Uhlen. Defining the transcriptome and proteome in three functionally different human cell lines. *Mol. Syst. Biol.*, 6:450, 2010.

[93] Y. Ma, K. Yakushijin, F. Miyake, and D. Horne. A concise synthesis of in-dolic enamides: coscinamide a, coscinamide b, and igzamide. *Tetrahedron Lett.*, 50:4343–4345, 2009.

[94] C. MacKintosh, K. A. Beattie, S. Klumpp, P. Cohen, and G. A. Codd. Cyanobacterial microcystin-lr is a potent and specific inhibitor of protein phosphatases 1 and 2a from both mammals and higher plants. *FEBS Lett.*, 264:187–192, 1990.

[95] C. MacKintosh, A. J. Garton, A. McDonnell, D. Barford, P. T. Cohen, N. K. Tonks, and P. Cohen. Further evidence that inhibitor-2 acts like a chaperone to fold pp1 into its native conformation. *FEBS Lett.*, 2-3(397):235–238, 1996.

[96] R. W. MacKintosh, K. N. Dalby, D. G. Campbell, P. T. Cohen, P. Cohen, and C. MacKintosh. The cyanobacterial toxin microcystin binds covalently to cysteine-273 on protein phosphatase 1. *FEBS Lett.*, 3(371):236–240, 1995.

[97] T. N. Makarieva, L. K. Shubina, A. I. Kalinovsky, V. A. Stonik, and G. B. Elyakov. Steroids in porifera ii. steroid derivatives from two sponges of the family halichondriiae. sokotrasterol sulfate, a marine steroid with a new pattern of side chain alkylation. *Steroids*, 42(3):267–281, 1983.

[98] H. Malve. Exploring the ocean for new drug developments: Marine pharmacology. *J. Pharm. Bioallied Sci.*, 8(2):83–91, 2016.

[99] L. V. Manes and P. Crews. Chemistry and revised structure of suvanine. *J. Org. Chem*, 53:570–575, 1988.

[100] G. Manning, G. D. Plowman, T. Hunter, and S. Sudarsanam. Evolution of protein kinase signaling from yeast to man. *Trends Biochem. Sci.*, 27(10):514–520, 2002.

[101] MarineLit. http://pubs.rsc.org/marinlit/, June 2017.

[102] P. R. Marinho, N. K. Simas, R. M. Kuster, R. S. Duarte, S. E. Fracalanzza, D. F. Feerreira, M. T. Tomanos, G. Muricy, M. Giambiagi-Demarval, and M. S. Laport. Antibacterial activity and cytotoxicity analysis of halistanol trisulphate from marine sponge petromica citrina. *J. Antimicrob. Chemother.*, 10:2396–2400, 2012.

[103] S. De Marino, C. Festa, M. V. D'Auria, M. Bourguet-Kondracki, S. Petek, C. Debitus, R. M. Andres, M. C. Terencio, M. Paya, and A. Zampella. Coscinolactams a

and b: new nitrogen-containing sesterterpenoids from the marine sponge coscinoderma mathewsi exerting anti-inflammatory properties. *Tetrahedron*, 65:2905–2909, 2009.

[104] J. T. Maynes, K. S. Bateman, M. M. Cherney, A. K. Das, H. A. Luu, C. F. Holmes, and M. N. James. Crystal structure of the tumor-promoter okadaic acid bound to protein phosphatase-1. *J. Biol. Chem.*, 47(276):44078–44082, 2001.

[105] J. T. Maynes, H. A. Luu, M. M. Cherney, R. J. Anderson, D. Williams, C. F. B. Holmes, and M. N. G. James. Crystal structure of protein phosphatse-1 bound to moturporin and dihydromicrocystin-la: Elucidation of the mechanism of enzyme inhibition by cyanobacterial toxins. *J. Mol. Biol*, 356:111–120, 2006.

[106] J. T. Maynes, K. R. Perreault, M. M. Cherney, H. A. Luu, M. N. James, and C. F. Holmes. Crystal structure and mutagenesis of a protein phosphatase-1 :calcineurin hybrid elucidate the role of the beta12-beta13 loop in inhibitor binding. *J. Biol. Chem.*, 41(279):43198–43206, 2004.

[107] T. L. McCready, B. F. Islam, F. J. Schmitz, H. A. Luu, J. F. Dawson, and C. F. Holmes. Inhibition of protein phosphatase-1 by clavosines a and b. novel members of the calyculin family of toxins. *J. Biol. Chem.*, 6(276):4192–4198, 2000.

[108] L. M. Miller-Jenkins, S. R. Durell, S. J. Mazur, and E. Appella. p53 n-terminal phosphorylation: a defining layer of complex regulation. *Carcinogenesis*, 33(8):1441–1449, 2012.

[109] A. Molchadsky and V. Rotter. p53 and its mutants on the slippery road from stemness to carcinogenesis. *Carcinogenesis*, 4(38):347–358, 2017.

[110] R. W. Moni, P. G. Parsons, R. J. Quinn, and R. J. Willis. Critical micelle concentration and hemolytic activity–a correlation suggested by the marine sterol, halistanol trisulfate. *Biochem. Biophys. Res. Commun.*, 1:115–120, 1992.

[111] G. Moorhead, R. W. MacKintosh, N. Morrice, T. Gallagher, and C. MacKintosh. Purification of type 1 protein (serine/threonine) phosphatases by microcystin-sepharose affinity chromatography. *FEBS Lett.*, 1(356):46–50, 1994.

134

[112] G. B. Moorhead, L. Trinkle-Mulcahy, M. Nimick, V. De Wever, D. G. Campbell, R. Gourlay, Y. M. Lam, and A. I. Lamond. Displacement affinity chromatography of protein phosphatase one (pp1) complexes. *BMC Biochem.*, 9:28, 2008.

[113] G. B. Moorhead, V. De Wever, G. Templeton, and D. Kerk. Evolution of protein phosphatases in plants and animals. *Biochem. J.*, 2(417):401–409, 2009.

[114] G. B. G. Moorhead, L. Trinkle-Mulcahy, and A. Ulke-Lemée. Emerging roles of nuclear protein phosphatases. *Nat. Rev. Mol. Cell. Biol.*, 8(3):234–244, 2007.

[115] S. Mori, G. Ito, N. Usami, H. Yoshioka, Y. Ueda, Y. Kodama, M. Takahashi, F. M. Fong, K. Shimokata, and Y. Sekido. p53 apoptotic pathway molecules are frequently and simultaneously altered in nonsmall cell lung carcinoma. *Cancer*, 8:1673–1682, 2004.

[116] T. Mori, H. Okamoto, N. Takhashi, R. Ueda, and T. Okamoto. Aberrant overexpression of 53bp2 mrna in lung cancer cell lines. *FEBS Lett.*, 2-3:124–128, 2000.

[117] M. H. G. Murno, J. W. Blunt, E. J. Dumdei, S. J. H. Hickford, R. E. Lill, S. Li, C. N. Battershill, and A. R. Duckworth. The discovery of development of marine compounds with pharmaceutical potential. *J. Biotechnol.*, 20:15–20, 1999.

[118] S. Murphy, B. Larrivee, I. Pollet, K. S. Craig, D. E. Williams, X. Huang, M. Abbott, F. Wong, C. Curtis, T. P. Conrads, T. Veenstra, M. Puri, Y. Hsiang, M. Roberge, R. J. Anderson, and A. Karsan. Identification of sokotrasterol sulfate as a novel proangiogenic steriod. *Circ. Res.*, 99:257–265, 2006.

[119] T. L. Nero, C. J. Morton, J. K. Holien, J. Wielens, and M. W. Parker. Oncogenic protein interfaces: small molecules, big challenges. *Nature*, 12:248–262, 2014.

[120] J. V. Olsen, B. Blagoev, F. Gnad, B. Macek, C. Kumar, P. Mortensen, and M. Mann. Global, in vivo, and site-specific phosphorylation dynamics in signaling networks. *Cell*, 3(127):635–648, 2006.

[121] J. V. Olsen, M. Vermeulen, A. Santamaria, C. Kumar, M. L. Miller, L. J. Jensen, F. Gnad, J. Cox, T. S. Jensen, E. A. Nigg, S. Brunak, and M. Mann. Quantitative

phosphoproteomics reveals widespread full phosphorylation site occupancy during mitosis. *Sci. Signal.*, 104(3):3, 2010.

[122] T. Oltersdorf, S. W. Elmore, A. R. Shoemaker, R. C. Armstrong, D. J. Augeri, B. A. Belli, M. Bruncko, T. L. Deckwerth, J. Dinges, P. J. Hajduk, M. K. Joseph, S. Kitada, S. J. Korsmeyer, A. R. Kunzer, A. Letai, C. Li, M. J. Mitten, D. G. Nettesheim, S. Ng, P. M. Nimmer, J. M. O'Connor, A. Oleksijew, A. M. Petros, J. C. Reed, W. Shen, S. K. Tahir, C. B. Thompson, K. J. Tomaselli, B. Wang, M. D. Wendt, H. Zhang, S. W. Fesik, and S. H. Rosenberg. An inhibitor of bcl-2 family proteins induces regression of solid tumours. *Nature*, 435:677–681, 2005.

[123] W. Peti, A. C. Nairn, and R. Page. Structural basis for protein phosphatase 1 regulation and specificity. *FEBS J.*, 280(2):596–611, 2013.

[124] PubChem. https://pubchem.ncbi.nlm.nih.gov/.

[125] M. J. Ragusa, B. Dancheck, D. A. Critton, A. C. Nairn, R. Page, and W. Peti. Spinophilin directs protein phosphatase 1 specificity by blocking substrate binding sites. *Nat. Struc. Mol. Biol.*, 17(4):459–464, 2010.

[126] J. Roman-Gomez, A. Jimenez-Velasco, X. Agirre, F. Prosper, A. Heiniger, and A. Torres. Lack of cpg island methylator phenotype defines a clinical subtype of t-cell acute lymphoblastic leukemia associated with good prognosis. *J. Clin. Oncol.*, 28(23):7043–7049, 2006.

[127] S. Rotem, C. Katz, H. Benyamini, M. Lebendiker, D. Veprintsev, S. Rudiger, T. Danieli, and A. Friedler. The structure and interactions of the proline-rich domain of aspp2. *J. Biol. Chem.*, 27(283):18990–18999, 2008.

[128] S. Rotem-Bamberger, C. Katz, and A. Friedler. Regulation of aspp2 interaction with p53 core domain by an intramolecular autoinibitory mechanism. *PLOS ONE*, 8(3):1–9, 2013.

[129] S. Sachdev, A. Hoffmann, and M. Hannink. Nuclear localization of ikappab alpha is mediated by the second ankyrin repeat: the ikappab alpha ankyrin repeats define

a novel class of cis-acting nuclear import sequences. *Mol. Cell. Biol.*, 5:2524–2534, 1998.

[130] Y. Samuels-Lev, D. J. O'Connor, D. Bergamaschi, G. Trigiante, J. Hsieh, T. Crook, and X. Lu. Aspp proteins specifically stimulate the apoptotic function of p53. *Mol. Cell.*, 8:781–794, 2001.

[131] M. Schumacher, M. Kelkel, M. Dicato, and M. Diederich. Gold from the sea: Marine compounds as inhibitors of the hallmarks of cancer. *Biotechnol. Adv.*, 29:531–547, 2011.

[132] E. Scotto-Lavino, M. Garcia-Diaz, G. Du, and M. A. Frohman. The basis for the isoform-specific interaction of myosin phosphatase subunits protein phosphatase 1c beta and myosin phosphatase targeting subunit 1. *J. Biol. Chem.*, 285(9):6419–6424, 2009.

[133] Y. Shi. Serine/threonine phosphatases: mechanism through structure. serine/threonine phosphatases: mechanism through structure. serine/threonine phosphatases: mechanism through structure. *Cell*, 139(3):468–484, 2009.

[134] S. Y. Shieh, M. Ikeda, Y. Taya, and C. Prives. Dna damage-induced phosphorylation of p53 alleviates inhibition by mdm2. *Cell*, 3(91):325–334, 1997.

[135] M. Shimada and M. Nakanishi. Response to dna damage: why do we need to focus on protein phosphatases. *Front. Oncol.*, 8(3):eCollection 2013, 2013.

[136] H. Shimizu, M. Ito, M. Miyahara, K. Ichikawa, S. Okubo, T. Konishi, M. Naka, T. Tanaka K. Hirano, D. J. Hartshorne, and T. Nakano. Characterization of the myosin-binding subunit of smooth muscle myosin phosphatase. *J. Biol. Chem.*, 269(48):30417–30411, 1994.

[137] M. J. Shopik. Molecular basis for regulation of protein phosphatase-1c by timap. *Masters Thesis, University of Alberta, Canada*, 2008.

[138] T. D. Skene-Arnold, H. A. Luu, R. G. Uhrig, V. De Wever, M. Nimick, J. Maynes, A. Fong, M. N. G. James, L .Trinkle-Mulcahy, G. B. Moorhead, and C. F. B.

Holmes. Molecular mechanisms underlying the interaction of protein phosphatase-1c with aspp proteins. *Biochem. J.*, 449:649–659, 2013.

[139] J. A. Skinner and A. R. Saltiel. Cloning and identification of mypt3: a prenylatable myosin targetting subunit of protein phosphatase 1. *Biochem. J.*, 356:257–267, 2001.

[140] A. P. Somlyo and A. V. Somlyo. Signal transduction and regulation in smooth muscle. *Nature*, 372:231–236, 1994.

[141] A. P. Somlyo and A. V. Somlyo. Signal transduction by g-proteins, rho-kinase and protein phosphatase to smooth muscle and non-muscle myosin ii. *J. Physiol.*, 522:177–185, 2000.

[142] J. Stanell, T. Stiewe, C. C. Theseling, M. Peter, and B. M. Putzer. Gene expression changes in response to e2f1 activation. *Nucleic Acid Res.*, 8(30):1859–1867, 2002.

[143] A. Sullivan and X. Lu. Aspp: a new family of oncogenes and tumour suppressor genes. *BJC*, 96:196–200, 2007.

[144] I. Tan, C. H. Ng, L. Lim, and T. Leung. Phosphorylation of a novel myosin binding subunit of protein phosphatase 1 reveals a conserved mechanism in the regulation of actin cytoskeleton. *J. Biol. Chem.*, 276(24):21209–21216, 2001.

[145] M. Terrak, F. Kerff, K. Langsetmo, T. Tao, and R. Dominguez. Structural basis of protein phosphatase 1 regulation. *Nature*, 429:780–784, 2004.

[146] R. S. Tibbetts, K. M. Brumbaugh, J. M. Williams, J. N. Sarkaria, W. A. Cliby, S. Y. Shieh, Y. Taya, C. Prives, and R. T. Abraham. A role for atr in the dna damage-induced phosphorylation of p53. *Genes Dev.*, 2(13):152–157, 1999.

[147] H. Tidow, A. Andreeva, T. J. Rutherford, and A. R. Fersht. Solution structure of aspp2 n-terminal domain (n-aspp2) reveal a ubiquitin-like fold. *J. Mol. Biol.*, 371(4):948–958, 2007.

[148] E. Townsend, R. Moni, R. Quinn, and P. G. Parsons. Reversible depigmentation of human melanoma cells by halistano trisulfate, a novel marine sterol. *Melanoma Res.*, 2:349–357, 1992.

[149] L. T. Vassilev, B. T. Vu, B. Graves, D. Carvajal, F. Podlaski, Z. Filipovic, N. Kong, U. Kammlott, C. Lukacs, C. Klien, N. Fotouhi, and E. A. Liu. In vivo activation of the p53 pathway by small-molecule antagonists of mdm2. *Science*, 303:844–848, 2004.

[150] I. Verbinnen, M. Ferreira, and M. Bollen. Biogenesis and activity regulation of protein phosphatase 1. *Biochem. Soc. Trans.*, 45:89–99, 2017.

[151] A. M. Vigneron, R. L. Ludwig, and K. H. Vousden. Cytoplasmic aspp1 inhibits apoptosis through the control of yap. *Genes Dev.*, 21(24):2430–2439, 2010.

[152] V. Vives, J. Su, S. Zhong, I. Ratnayaka, E. Slee, R. Goldin, and X. Lu. Aspp2 is a haploinsufficient tumor suppressor that cooperates with p53 to suppress tumor growth. *Genes Dev.*, 20:1262–1267, 2006.

[153] B. Vogelstein, D. Lane, and A. J. Levine. Surfing the p53 network. *Nature*, 6810(408):307–310, 2000.

[154] P. Wakula, M. Beullens, H. Ceulemans, W. Stalmans, and M. Bollen. Degeneracy and function of the ubiquitous rvxf motif that mediates binding to protein phosphatase-1. *J. Biol. Chem.*, 278(21):18817–18823, 2003.

[155] A. Yang, M. Kaghad, Y. Wang, E. Gillett, M. D. Fleming, V. Dotsch, N. C. Andrews, D. Caput, and F. McKeon. p63, a p53 homolog at 3q27-29, encodes multiple products with transactivating, death-inducing, and dominant-negative activities. *Mol. Cell.*, 3(2):305–316, 1998.

[156] J-P. Yang, M. Hori, T. Sanda, and T. Okamoto. Identification of a novel inhibitor of nuclear factor-kb, rela-associated inhibitor. *J. Biol. Chem.*, 274(22):15662–15670, 1999.

[157] J. Yong, I. Tan, L. Lim, and T. Leung. Phosphorylation of myosin phosphatase targeting subunit 3 (mypt3) and regulation of protein phosphatase 1 by protein kinase a. *J. Biol. Chem.*, 281(42):31202–31211, 2006.

[158] A. Zeke, M. Lukás, W. A. Lim, and A. Reményi. Scaffolds: interaction platforms for cellular signalling circuits. *Trends Cell Biol.*, 19(8):364–374, 2009.

[159] P. Zhang, Y. Zhang, K. Gao, Y. Wang, X. Jin, Y. Wei, H. Saiyin, D. Wang, J. Peng, J. Ma, Y. Tang, R. Wumaier, H. Yu, Y. Dong, H. Huang, L. Yu, and C. Wang. Aspp1/2-pp1 complexes are required for chromosome segregation and kinetochore-microtubule attachments. *Oncotarget*, 6(39):41550–41565, 2015.

[160] R. Zhang, H. Shi, F. Ren, H. Liu, M. Zhang, Y. Deng, and X. Li. Misregulation of polo-like protein kinase 1, p53 and p21waf1 in epithelial ovarian cancer suggests poor prognosis. *Oncol. Rep.*, 3(33):1235–1242, 2015.

[161] X. Zhang, M. Wang, C. Zhou, S. Chen, and J. Wang. The expression of iaspp in acute leukemias. *Leuk. Res.*, 2:179–183, 2005.

[162] Y. Zhang, Y. Wang, Y. Wei, J. Ma, J. Peng, R. Wumaier, S. Shen, P. Zhang, and L. Yu. The tumor suppressor proteins aspp1 and aspp2 interact with c-nap1 and regulate centrosome linker reassembly. *Biochem. Biophys. Res. Commun.*, 458:494–500, 2015.

[163] Z. Zhu, J. Ramos, K. Kampa, S. Adimoolam, M. Sirisawad, Z. Yu, D. Chen, L. Naumovski, and C. D. Lopez. Control of aspp2/(53bp2l) protein levels by proteasomal degradation modulates p53 apoptotic function. *J. Biol. Chem.*, 41(280):34473–34480, 2005.

Appendix

After the potency and specificity of Halistanol Sulfate, Sokotrasterol Sulfate, and Suvanine was tested, the compounds were then analyzed for their effect on the dephosphorylation of p53 by disrupting the multimeric complex between iASPP•PP-1cα•p53. It has been established that Ser15 on p53 is dephosphorylated by PP-1c [82] and that when iASPP is bound to PP-1c *in vitro*, p53 dephosphorylation is increased (Robyn Millott, unpublished data). Robyn Millott from the Holmes Lab, has been able to demonstrate increased dephosphorylation of Ser15 in the presence of PP-1cα•iASPP$_{608\text{-}828}$ compared to PP-1cα alone (unpublished data). In order to test if the identified compounds have an effect on the dephosphorylation of p53, I measured the levels of phosphorylation at Ser15 on p53 in the presence and absence of the compounds.

Preliminary analysis of p53 dephosphorylation in the presence of Suvanine is shown in Figure 6.2. PP-1cα was pre-incubated alone and with iASPP$_{608\text{-}828}$ and each was pre-incubated with or without 100 μM of Suvanine for 30 mins at 37 °C. This concentration of Suvanine was chosen because it is approximately double the DC$_{50}$ concentration of the iASPP•PP-1c disruption. These samples were added to p53 phosphorylated by DNA-PK and incubated for 90 mins at 37 °C. The membrane of the following Western Blot is shown in Figure 6.2. The results show that the iASPP•PP-1cα complex alone increases in Ser15 dephosphorylation, reconfirming unpublished data of Robyn Millott. As well, the dephosphorylation of Ser15 by the iASPP•PP-1cα complex increases further in the presence of Suvanine (100 μM). Interestingly, the percent of Ser15 dephosphorylation by PP-1cα alone increased by 5.37 % ($\pm$ 1.10 %) in the presence of Suvanine (100 μM) when compared the control. The percent of Ser15 dephosphorylation by iASPP$_{608\text{-}828}$•PP-1cα decreased by 8.36 % ($\pm$ 1.58 %) in the presence of Suvanine (100 μM) when compared to the control (Table 6.1). Although there seems to be an effect of the p53 Ser15 dephosphorylation by the presence of 100 μM Suvanine, this data is not significant enough to draw any conclusions.
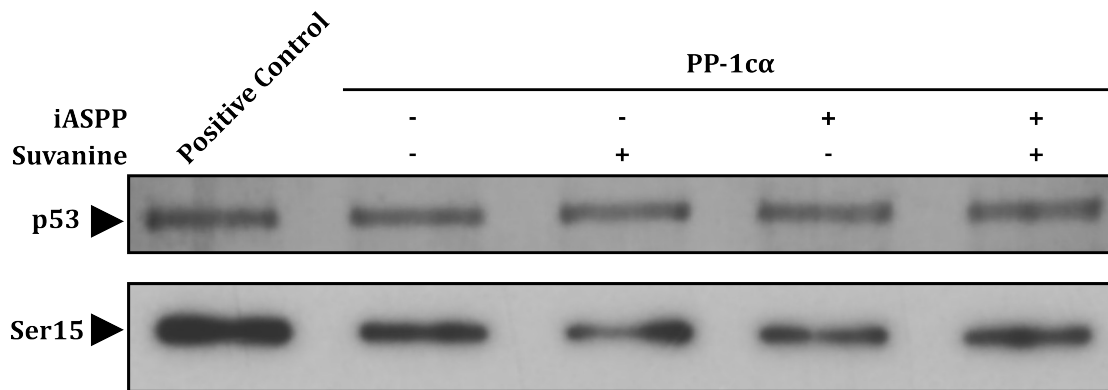
Figure 6.2: **Decreased Dephosphorylation of Serine 15 on p53 by PP-1cα in the Presence of iASPP$_{608-828}$ and Suvanine.** Phosphorylation of Ser15 on p53 was carried out by incubating p53 (0.125 μg) with DNA-PK (75 U) in phosphorylation Buffer for 90 mins at 30 °C per reaction. Phosphorylation reaction was stopped with 1 mM LY249002 inhibitor. PP-1cα (0.5 μg), iASPP$_{608-828}$ (0.5 μg), and Suvanine (100 μM) were pre-incubated for 30 mins at 30 °C per reaction. The phosphorylation reaction (5.5 μL) and the pre-incubation reaction (4.5 μL) were combined and incubated for 30 mins at 30 °C. Dephosphorylation reaction was stopped with 1X SDS-PAGE Buffer and samples were boiled for 5 mins at 100 °C and separated by a 12 % SDS-PAGE. Proteins were transferred to a nitrocellulose membrane at 75 V for 45 mins at 4 °C. Nitrocellulose membrane was incubated in Blocking Buffer for 90 mins at RT and 1:15,000 Ser 15 1 ° antibody over night, at 4 °C. Nitrocellulose membrane was washed for 10 mins with TBST Buffer, three times, and in 1:10,000 2 ° antibody for 1 hr at RT. Nitrocellulose membrane was developed with 20 % ECL Solution and the film exposed for 1 min. The assay was carried out in duplicate with a representative figure shown above.

Table 6.1: **Percent Change in Serine15 Dephosphorylation in the Presence of 100 μM Suvanine.**

Proteins	% Change in Ser15 Dephosphorylation	Std Dev
PP-1cα	+5.33	± 1.10
PP-1cα + iASPP$_{608-828}$	-8.36	± 1.58

The results shown in Figure 6.2 demonstrate that the iASPP•PP-1c•p53 protein complex does increase dephosphorylation of Ser15, confirming the unpublished data of Robyn Millott. This reconfirms that the mulitmeric complex is a viable and good to target. Secondly, there was a very preliminary effect on dephosphorylation caused by the

presence of Suvanine. When Suvanine (100 μM) was added, there was a slight increase in dephosphorylation caused by PP-1cα alone, but a slight decrease in dephosphorylation caused by the iASPP•PP-1cα complex. This decrease in dephosphorylation is the desired result, but currently the data is not significant enough to draw conclusions. The experiment needs to be further optimized to determine if Suvanine decrease dephosphorylation for certain. At the moment, the assay is set-up to have 1:1:1 binding of all three proteins, but this is not a true first-order kinetic assay. In future assays, the parameters could be changed to make a first-order kinetic assay by making the enzyme rate-limiting. As well, decreasing the amount of PP-1cα present may be the best way to see a more significant change in dephosphorylation in the presence of Suvanine. There may be too much PP-1cα present to demonstrate the effect of Suvanine because the excess PP-1cα can continue to dephosphorylate p53.